Analytical Techniques for the Analysis of Uranium Bearing Materials

A Dissertation Presented for the
Doctor of Philosophy
Degree
The University of Tennessee, Knoxville

Nathaniel D. Fletcher
December 2022

Acknowledgments

I would first like to thank my advisor Dr. Sheng Dai for his support over the last few years. His managing style allowed me to become a more independent scientist, and I believe this was exactly what I need to instill confidence in myself as a researcher. I would also like to thank my committee members Dr. Thanh Do, Dr. Konstantinos Vogiatzis, and Dr. Yanwen Zhang for taking the time to advise me. Acknowledgments also to both the Department of Chemistry at the University of Tennessee as well as Oak Ridge National Laboratory for providing the resources to make my research possible.

Also, I would like to thank my friends for their support was well as for being a necessary distraction at times. Special acknowledgments to my lab mates for always being willing to allow me to bounce ideas off them. I think best when explaining things to others and they were always willing to stop what they were doing and listen.

Next, I would like to acknowledge my family for their support. I am sure they would of liked to see me more often than they did over the last few years, but they never once complained. Special thanks to my parents for helping to teach me to always have high expectations for myself.

Lastly, a very special thank you to my wife Dr. Ashley Rice. Without her encouragement I do not know how I could have gotten to this point. Thank you for your support and for never letting me stay down on myself.

Abstract

The interest in the use of nuclear power has increased drastically in recent years. This is due to significantly increased efficiency at producing energy when compared to fossil fuels. With the increased use of nuclear power comes an increased need to monitor for uranium bearing materials outside of regulatory control. This dissertation covers four projects aimed at improving the analysis of these materials. The first project aims to develop a method that allows for the analysis of elements that exist in nature as anions by triple quadrupole ICP – MS. This would allow for the ability to measure more potential attributes of uranium bearing materials with the added benefits provided by ICP – MS such as lower limits of detection. The second project sought to apply this method to the analysis of a Springfield sample set of uranium ore concentrates, and to compare the results to that obtained by pyrohydrolysis with ion chromatography. The next project was the development of a separation method that would allow for the separation of the Hf-Lu, Rb- Sr, Nd-Sm, Pb and U systems with only one aliquot of sample used. This would be especially useful in cases where there is very little sample available. The final project involves another separation although this is a liquid-liquid extraction of Nd in ionic liquid. For this project potentiometric titrations were performed to determine the proton affinity distribution of various ligands to better understand their potential usefulness in the separation of rare earth elements from the nuclear fuel cycle. A spectrophotometric method was also validated in order to determine the stability constant of a complex formed between a ligand and Nd. Each of these projects aims towards providing analytical techniques for the analysis of

materials that could be collected or end up outside of regulatory control along certain points of the nuclear fuel cycle.

Table of Contents

Chapter 1 Introduction 1

1.1 Nuclear Forensics 2

1.1.1 Nuclear Fuel Cycle 2

1.2 Uranium Ore Concentrates 4

1.3 Inductively Coupled Plasma – Mass Spectrometry 6

1.4 Rare Earth Element Separations 10

1.5 Inductively Coupled Plasma – Optical Emission Spectroscopy 11

1.6 Ionic Liquids 12

1.7 Ultraviolet-Visible Spectroscopy 14

Chapter 2 Determining P, S, Br, and I Content in Uranium by Triple Quadrupole Inductively Coupled Plasma Mass Spectrometry 15

2.1 Abstract 16

2.2 Introduction 17

2.3 Experimental 20

2.3.1 Materials and Methods 20

2.3.2 Instrumentation 21

2.4 Results and Discussion 21

2.4.1 Reaction-Gas Determination and Interferences 21

2.4.2 Method Demonstration 27

2.4.3 Limit of Detection 31

2.4.4 CUP-2 Analysis 35
2.5 Conclusions 37
Chapter 3 Determination of Phosphorus and Sulfur in Uranium Ore Concentrates by Triple Quadrupole Inductively Coupled Plasma Mass Spectrometry 39
3.1 Abstract 40
3.2 Introduction 41
3.3 Experimental 44
3.3.1 Materials 44
3.3.2 Pyrohydrolysis Method 45
3.3.3 Triple Quadrupole Method 47
3.4 Results and Discussion 48
3.4.1 Quality Controls 48
3.4.2 UOC Samples 53
3.4.3 Uncertainty 58
3.5 Conclusions 59
Chapter 4 Method for the Separation of Hf-Lu, Rb-Sr, Nd-Sm, Pb and U 62
4.1 Introduction 63
4.2 Experimental 66
4.2.1 Materials and Reagents 66
4.2.2 Column 1: Ln Resin 67
4.2.3 Column 2: Ln Resin 67
4.2.4 Column 3: AG 50W-X12 Resin 69

4.2.5 Column 4: Ln Resin 69
4.2.6 Instrumentation 69
4.3 Results and Discussion 70
4.3.1 Optimization 70
4.3.1.1 Column 1 70
4.3.1.2 Column 2 73
4.3.1.3 Column 3 74
4.3.1.4 Column 4 75
4.3.2 Elution Profiles 75
4.3.3 Column Yields 78
4.4 Conclusions 80
Chapter 5 Titrations for the Determination of Stability Constants for the Extraction of Nd in Ionic Liquid using Various Ligands and the Determination of Proton Affinity Distributions of Ligands 81
5.1 Introduction 82
5.2 Experimental 85
5.2.1 Potentiometric Titrations 85
5.2.2 Spectrophotometric Titrations 86
5.3 Results and Discussion 88
5.3.1 Potentiometric Titrations 88
5.3.2 Spectrophotometric Titrations 94
5.4 Conclusions 95

Chapter 6 Summary and Conclusions 96

Bibliography 100

Appendix 137

Vita 142

List of Tables

Table 2.1 Optimized TQ ICP – MS parameters. 22

Table 2.2 Selected spectral interferences for all analytes. 26

Table 2.3 LOD for the analytes with IDL (ng mL^{-1}) and MDL (µg g U^{-1}). 34

Table 3.1 List of UOC samples and description of each 46

Table 3.2 Average concentrations and expected values of the QCs for P and S (µg g^{-1}). 49

Table 3.3 S concentrations as determined by TQ ICP–MS and pyrohydrolysis (µg^{-1}) 55

Table 3.4 Concentration of P in each sample as determined by the TQ ICP–MS (µg g^{-1})57

Table 4.1 Each element analyzed listed with the wavelength and m/z monitored. 71

Table 4.2 The optimized separation method. 72

List of Figures

Figure 1.1 Uranium ore concentrate samples with analysis described in chapter 3. 5

Figure 1.2 Diagram of a quadrupole. 9

Figure 1.3 A diagram demonstrating an electron multiplier including the ion path, indicated as the blue line, as well as the resulting electron cascade, indicated by the increasing thickness of the blue lines. 9

Figure 2.1 A diagram demonstrating the difference between on-mass and off-mass analysis using the TQ ICP - MS. Depicts spectral interferences passing through Q1 but not Q3 while the desired ion passes through to the detector. This is a pictorial display of both modes of operation, these modes can be performed sequentially. ... 24

Figure 2.2 Average daily concentration of P with three analysis per day. Solid line denotes known concentration and the dashed lines indicate uncertainty in the QC. 28

Figure 2.3 Average daily concentration of S with three analysis per day. Solid line denotes known concentration and the dashed lines indicate uncertainty in the QC. 30

Figure 2.4 Average daily concentration of Br with three analysis per day. Solid line denotes known concentration and the dotted lines indicate uncertainty in the QC. . 30

Figure 2.5 Average daily concentration of I with three analysis per day. Solid line denotes known concentration and the dotted lines indicate uncertainty in the QC. 32

Figure 2.6 Cup-2 data for P, S, and Br with a line indicating the recommended value ... 36

Figure 3.1 Concentrations of CUP-2 for P and S over a period of 18 days with a line indicating expected value. 49

Figure 3.2 Concentration of P and S in two aliquots of Feldspath over 18 days with a solid line indicating certified value and dashed line indicating uncertainty given by the CRM. 50
Figure 3.3 Concentration of P in two aliquots of Viognier with a solid line indicating certified value and dashed lines indicating uncertainty given by the CRM 52
Figure 3.4 Variable contributions to the uncertainties in South Alligator of P (left) and S (right). 60
Figure 4.1 Flow chart demonstrating the developed separation method. 68
Figure 4.2 Elution profiles for each of the four columns with a-d representing columns 1-4, respectively. Step numbers from Table 4.2 are listed. 77
Figure 4.3 Column yields shown for each of the four columns with a-d representing columns 1-4 respectively. 79
Figure 5.1 Development of HypSpec model demonstrating the initial setup. 89
Figure 5.2 Image demonstrating the manual curve fitting in HypSpec. The diamonds indicate experimental values while the red dotted line is calculated result. 90
Figure 5.3 Isotherm (left) and pKa distribution (right) of citric acid. Bottom is pKa distribution of citric acid as determined by Jagiello et al.[219] 92
Figure 5.4 Isotherm (left) and pKa distribution (right) of the carboxy-HOPO ligand. 93
Figure 5.5 Isotherm (left) and pKa distribution (right) of the octyl-HOPO ligand. 93

Chapter 1
Introduction

1.1 Nuclear Forensics

Much of the work described in this dissertation falls under the umbrella of nuclear forensics, and so it is worth discussing what nuclear forensics is and how it is applied. Nuclear forensics rose in prominence in the 1990s as the first cases of smuggling of nuclear material were reported.[1] This required the development of analytical techniques for the analysis of the nuclear material in order to determine information such as the original location, age, intended use, or production method of the material.[2, 3] This is done by analyzing various aspects of the material referred to as signatures or attributes.[4] One example is the use of isotope ratios for chronometry (age dating) such as the $^{230}Th/^{234}U$ ratios.[5, 6] While some isotope ratios can be used to determine age, ratios such as the Pb and Sr isotope ratios can also be utilized to determine geolocation of the material as the ratios can vary based on region.[7-10] While attributes can originate from the mined material, others are introduced during the nuclear fuel cycle. Thus, it is important to have a basic understanding of the nuclear fuel cycle in order to determine if the attributes being analyzed are impacted by the nuclear fuel cycle or point directly to the mine source.[11]

1.1.1 Nuclear Fuel Cycle

In recent years the interest in nuclear power has increased drastically due to the high efficiency as well as potential for mitigating climate change.[12, 13] With this increase in use comes an increase in the need for nuclear forensic techniques for the analysis of potentially illicit materials.[14, 15] There also comes an increased need to understand how potential attributes of the nuclear materials may be impacted by various steps of the nuclear fuel cycle.[16, 17]

The nuclear fuel cycle is pictured as a cycle as it refers to the use of nuclear material from the first mining of the U until the spent fuel is sent to a waste disposal facility where it is either sent to waste or recycled and entered back into the nuclear fuel cycle.[18, 19] The first step in the nuclear fuel cycle is the actual mining of the material. From there, the ore is transported to a near by milling facility where it is then crushed. The next step involves a leaching process where the uranium is separated from the rock. This solution is then precipitated to form a uranium ore concentrate (UOC).[20, 21] The UOCs are then shipped to a uranium conversion facility. At this facility the UOCs are dissolved so that the U can be purified through liquid-liquid extraction and precipitated. This can then be transferred to a furnace where it is converted to UO_3 through calcination and then reduced by H_2 gas to form UO_2. Once the UO_2 is formed the material can be transported to an enrichment facility for the next steps in the nuclear fuel cycle.[11]

There are many different types of enrichment processes that can be used depending on the level of enrichment necessary as well as capabilities of the facility. The enrichment level required for a nuclear power plant is 3-5% while the level required for nuclear weapons is 90%, and natural levels of ^{235}U are at 0.7%.[22-24] One common form of enrichment for material useful in nuclear power plants involves the use as UF_6 as a feed material. The lighter $^{235}UF_6$ molecules can be separated during collection to allow for gradual enrichment. The UF_6 is then reduced to UF_4 so that it can be converted into UO_2.[11, 25] From there the material undergoes fuel fabrication before use in a nuclear reactor. After use in the reactor, the irradiated fuel can be transported to a waste facility where the spent fuel can be disposed of. The material could also be reprocessed and continue on the nuclear

fuel cycle to again undergo fuel fabrication and be utilized in a nuclear reactor. While understanding the nuclear fuel cycle is important in determining how potential attributes of uranium bearing materials can be impacted by the steps within it. The real U bearing materials studied in this work were UOCs and so special attention will be paid to them.

1.2 Uranium Ore Concentrates

Uranium ore concentrates are often referred to as yellow cake (figure 1.1) as they generally appear yellow. However, UOCs can also appear black. This color will depend on the type of U present (uranium oxide versus uranium amides).[26] As mentioned previously, the formation of the UOC is among the first steps of the nuclear fuel cycle. The first step in the formation of a UOC is the ore is crushed and ground. Once the ore is homogenized the U is leached followed by an ion exchange reaction in an effort to remove some of the impurities. The solution is then precipitated and dried. This final product is what is referred to as the UOC.[27-29] Chapter 3 will focus on the analysis of certain anions as attributes specifically of UOCs. In order to understand if these can be used as a geolocator it is important to understand if the leaching process has an impact on the attributes as this would indicate that the attributes are indicative of the leaching process used to form the UOC and not the geology of the area that was mined.

The ore can either be leached of U on site, or the U can be leached at a milling facility. The leaching procedure used can have an impact on certain attributes of the UOC such as sulfate concentration.[30, 31] Beyond anions other attributes such as rare earth element

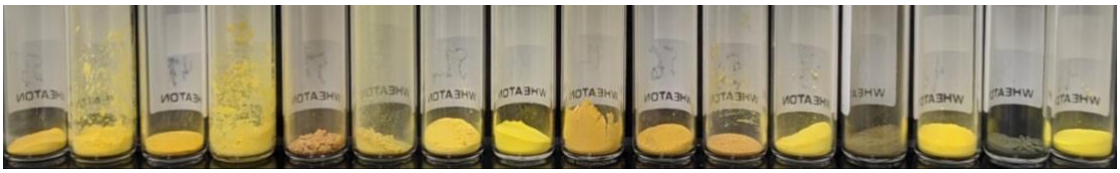


Figure 1.1 Uranium ore concentrate samples with analysis described in chapter 3.

patterns have been analyzed to determine the origin of the UOC.[32] One common form of leaching is the use of sulfuric acid to leach uranium from the ore.[33, 34] Another form of leaching involves the use of microorganisms to release the U from the ore. This process is referred to as bioleaching.[35] When sulfuric acid is used as the leachate the amount will vary. Sometimes multiple rounds of sulfuric acid leaching is used while other times the sulfuric acid leaching will be followed up with other forms of U striping such as NaCl stripping followed by a precipitation using NH_3. The method for production of the UOC will vary depending on the minerology present.[36, 37] All analysis of UOC samples examined in chapter 3 were performed utilizing inductively coupled plasma – mass spectrometry (ICP – MS).

1.3 Inductively Coupled Plasma – Mass Spectrometry

Inductively coupled plasma – mass spectrometry was first introduced as a method for the analysis of trace elements in 1980 by Houk et al.[38] Since the inception of the ICP – MS it has become an incredibly powerful and versatile tool in analytical chemistry.[39-42] The ICP – MS is made up of three parts. The ion source is the plasma.[43] The mass analyzer is where the analyte of interest is separated out based on certain characteristics such as size or mass to charge ratio, depending on type of mass analyzer used. Common forms of mass analyzers include time of flight, quadrupoles, and double focusing magnetic sectors.[44-46] The magnetic sector is especially useful in determining isotopic ratios.[47] The first ICP – MS utilized a quadrupole as the mass analyzer.[38] The last part of the ICP – MS is the detector. The two main types of detectors are electron multipliers and faraday cups.[48] The specific ICP – MS used in this work was a Thermo Scientific iCAP triple quadrupole (TQ)

and RQ ICP – MS. The TQ ICP – MS is discussed in detail in chapter 2, but the general quadruple ICP – MS will be discussed further here.

The ICP – MS used in this work involved a probe connected to an auto sampler that pumped sample to the sample introduction system using a peristaltic pump. The first part of the sample introduction system is the nebulizer where the aerosol is created.[49] From the nebulizer, the aerosol is then sprayed into a quartz cyclonic spray chamber that is peltier cooled. The spray chamber allows for the removal of large droplets while the peltier cooling provides multiple benefits. The cooling first allows for the removal of extra solvent to reduce interference from oxides. Also, by keeping the spray chamber at a constant temperature signal drift from temperature change can be reduced.[50-52] From the spray chamber, the aerosol then enters the torch where the plasma is generated. The plasma has a temperature ranging from 10,000 K, at the source, to 6000 K at the outskirts. Given this high level of energy from the plasma, the aerosol undergoes desolvation, and the electron is stripped from the atom to create a cationic species of the elements present.[53]

After the ions exit the plasma they are pulled into a high vacuum area (10^{-5} torr) where they enter the mass analyzer, a quadrupole in this case.[54] The quadrupole was first proposed in 1953 by Paul and Steinwegen.[55] The quadrupole consists of four circular rods that are parallel to each other (Figure 1.2). These operate by placing both and alternating and direct current on each of the four parallel rods. The current applied to these rods can be adjusted until the ratio of alternating and direct current allows for ions of a specific mass to pass through. All ions of a different mass are ejected from the quadrupole. This is why the quadruple is described as sorting based on a mass to charge ratio.[56-58] The current

applied to the quadrupole can also be adjusted so that multiple analytes can be measured in succession on one sample. One downfall of the quadrupole is that it is simply sorting by mass to charge ratio, which means that anything of a specific mass to charge ratio will be allowed to the detector and measured as the specific analyte of interest. These species that have the same mass to charge ratio but are not the analyte of interest are referred to as interferences. These must be removed either during the wet chemistry or through the use of a reaction cell in TQ analysis as described in chapter 2.[59-61]

After the desired ion passes through the quadrupole it flows to the detector where the instrument response can be converted to concentration using a calibration curve.[62] The detector utilized in the ICP – MS from the work presented in this dissertation included an electron multiplier. When the ion of interest first makes contact with the cone of the electron multiplier a secondary electron is emitted. Then, as they travel farther down the multiplier the secondary electrons make contact with the multiplier walls resulting in the ejection of multitudes of secondary electrons. This eventually results in a cascade of electrons that can be measured as a pulse by the detector (Figure 1.3).[63, 64] This pulse is measured by a preamplifier and can be amplified more than one million times. It is important to allow for dead time between analytes so the preamplifier can measure the results from the previous analyte before continuing to the next. This efficiency of the detector plays a major role in the overall sensitivity of the instrument.[65]



Figure 1.2 Diagram of a quadrupole.

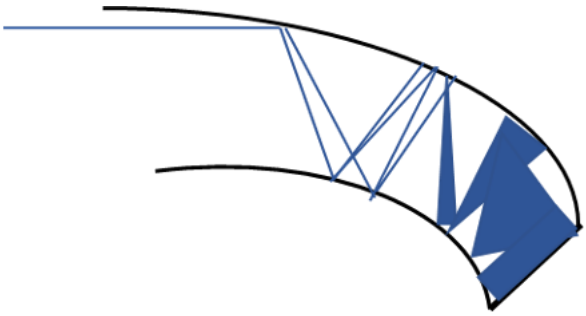


Figure 1.3 A diagram demonstrating an electron multiplier including the ion path, indicated as the blue line, as well as the resulting electron cascade, indicated by the increasing thickness of the blue lines.

1.4 Rare Earth Element Separations

The rare earth elements are a vital group for the determination of attributes of U bearing materials. It is necessary to understand the importance of the separation of these rare earth elements for analysis, as well as what information this analysis can provide about a sample. The rare earth elements consist of a group of elements from lanthanum to lutetium and scandium to yttrium. There is a pattern to the abundance of the rare earth elements in the earth's crust that can be utilized it order to determine provenance of a sample.[66, 67] The isotope ratios of various rare earth elements can be determined in an effort to geolocate the sample. This can be done because isotope ratios will vary slightly depending on location of the rock. This often is due to varying ages of the crust and so it is important to acquire samples from similar depths.[68-70] Some of the isotope ratios of interest for geolocating a sample are the Sr, Nd, and Hf ratios.

While the goal is to measure the isotope ratios of these various rare earth elements, this cannot be done without first running separations. This is because it is necessary to measure specific isotopes of each element. This is usually performed using a double focusing magnetic sector multi collector ICP – MS so that multiple isotopes can be measured simultaneously.[71-73] While the multi collector is an excellent tool, the instrument will only report the instrument response at each mass regardless of what the isotope of interest is. For example, the Hf isotope ratio used for fingerprinting samples is $^{176}Hf/^{177}Hf$, however; Lu also has an isotope at 176. This is why separations are necessary prior to the analysis of specific isotope ratios.[74-76] In each case it is important that the fraction be

completely clean as often the variations in isotopic ratios are only in the fourth or even fifth decimal place.[77, 78]

1.5 Inductively Coupled Plasma – Optical Emission Spectroscopy

Inductively coupled plasma – optical emission spectroscopy (ICP – OES) was utilized during optimization of the rare earth element separation method. The idea behind plasma as a spectral source was first introduced in 1956 by Badarau et al.[79] Greenfield et al were then the first to report the use of ICP – OES for analytical purposes in 1964.[80] Since the inception of ICP – OES it has become an incredibly versatile tool in analytical chemistry. The ICP – OES has been utilized in a wide variety of fields including chemistry, geology, pharmaceuticals, and food analysis.[81-83] This wide spread use is due to the ability of the ICP – OES to handle a wide range of sample matrices while keeping detection times low. The ICP -OES is able to measure multitudes of elements simultaneously while maintaining accuracy.[84] The speed of detection as well as robust ability to handle sample matrices made the ICP – OES ideal for analysis of samples during optimization of the rare earth element separation method due to the higher concentrations used (10 μg ml^{-1}).

The ICP – OES used in this study was an Agilent Technologies 5110. Similarly to the ICP – MS, a quartz cyclonic spray chamber was utilized during introduction of the sample. Unlike the ICP – MS, the ICP – OES can be broken down into only two parts, the ICP and the optical spectrometer. The plasma is generated in the same manner as when utilized during ICP – MS. Argon is passed through the torch while an RF signal is applied to coils surrounding the torch. A brief discharge is then created using a spark to begin the process of ionization that results in ignition of the plasma.[85] The oscillating magnetic field

generated by the RF coil along with a continuous gas flow then allows for a stable flow of the plasma.[86] Once the plasma is generated, an aerosol of sample can be passed through the injector into the plasma where the ions are formed for analysis.[87, 88]

While in ICP – MS, where the mass analyzer was a quadrupole, the mass to charge ratio was utilized to identify specific analytes and the intensity of the mass could be measured quantitatively. In the case of ICP – OES, analytes are identified based on the characteristic wavelengths emitted during ionization. These wavelengths are emitted during relaxation after the ions enter an excited state due to collisions with other particles.[85] This energy difference between excited and ground state is what is characteristic to specific elements. The intensity of this wavelength is also directly proportional to the concentration of the element.[89] An optical spectrometer is utilized to differentiate between wavelengths as well as to measure the intensity of the light.[90] The ICP – OES utilized in this study included a charge-coupled detector (CCD). This CCD includes multitudes of detector elements on one small chip. This allows for the simultaneous identification of several elements while also measuring the intensity. The intensity can then be converted to concentration of the element using a calibration curve.[91, 92]

1.6 Ionic Liquids

The definition of the term ionic liquid is rather broad and can vary depending on the researcher. This speaks to the versatility of ionic liquids as they can maintain a wide variety of properties. Ionic liquids generally refer to any solution that consists entirely of ions, meaning no water is present. This usually is specified to include the stipulation that the ionic liquid be liquid at room temperature although that is not always a necessity.[93]

When disregarding this stipulation even molten salts could be considered and ionic liquid. There is a long list of common cations for ionic liquids, but some of these common cations for ionic liquids include alkylmethylimidazolium $[C_nmim]^+$ and 1-butyl-3mythylimidasolium $[BMIM]^+$. While common anions utilized in ionic liquids includes triflate $[OTf]^-$ and bis(trifluoromethanesulfonyl)imide $[NTf_2]^-$.[94-96] There are many advantages to the use of ionic liquids including the ability to use them at temperatures above 100 ℃.[97]

Research interest in ionic liquids has skyrocketed due to multitude of advantages and uses they can provide.[98-101] Some of the most important and exploitable advantages of ionic liquids are that they have thermal stability, electrochemical stability, tunable structures, and a low melting point. This low melting point has led to interest in ionic liquids as pharmaceutical salts.[102, 103] Also the electrochemical stability allows for the use of ionic liquids in electrochemical devises such as water splitting.[104, 105] Ionic liquids also maintain such structural variability including ionic liquids with good thermal stability and low vapor pressure, which makes them ideal for use in energetic materials.[106, 107] This nonvolatility can also be advantageous for use in sensors. In this case, the ionic liquid is generally used to alter the surface of the electrode.[108-110] The fact that these liquids are ionic also allows for the solvation environments to be varied which can be exploited in extractions.[111-113] The ionic nature as well as electrochemical stability make them especially suited for the processing of rare earth elements.[114-117] The work displayed in chapter five in part describes the extraction of Nd using various ligands in ionic liquid.

1.7 Ultraviolet-Visible Spectroscopy

Ultraviolet-visible spectroscopy (UV – Vis) was based off the principles in Beer's law which was founded in 1852. Beer's law states that the absorbance of sample is equal to the molar absorptivity multiplied by the path length and the concentration of the sample.[118] This indicates there is a linear relationship between the concentration and absorbance of sample. The only requirement is that the sample absorbs light in the UV or visible light range. The instrument can calculate absorbance based on the transmittance of light before and after sample was added in the same sample matrix.[119] This simplicity as well as the low cost has allowed for the use of UV – Vis spectroscopy in a wide variety of disciplines.[120-122]

The UV – Vis can be broken down into three basic parts. These include the light source, wavelength selector, and detector.[122] Common light sources to cover the UV – Vis range are a combination of tungsten lamp for the visible region and deuterium lamp for the UV region.[118] The particular UV-Vis used in this study employed a diffraction grating in a monochromator to select each wavelength to monitor.[123] This was done by collimating the light and reflecting to a mirror that focused light on the detector so that the intensity of the light at each particular wavelength could be determined.[124, 125] The detector used was again a CCD detector similar to that used on the ICP – OES. The intensity response from the detector can then be converted to absorbance and a spectrum of absorbance vs wavelength can be obtained. The work performed using the UV-Vis is discussed in chapter 5.

Chapter 2

Determining P, S, Br, and I Content in Uranium by Triple Quadrupole Inductively Coupled Plasma Mass Spectrometry

This chapter was originally published in the Journal of Radioanalytical and Nuclear Chemistry as shown below and is reproduced here with permission.

Fletcher, N. D.; Manard, B. T.; Metzger, S. C.; Ticknor, B. W.; Bostick, D. A.; Hexel, C. R. Determining P, S, Br, and I content in uranium by triple quadrupole inductively coupled plasma mass spectrometry. Journal of Radioanalytical and Nuclear Chemistry 2020, 324 (1), 395-402, Article. DOI: 10.1007/s10967-020-07057-0.

All experimental work and data analysis was performed by myself. experimental design as well as editing was performed by myself as well as Benjamin Manard, Shalina Metzger, Brian Ticknor, Debra Bostick, and Cole Hexel.

2.1 Abstract

The trace impurities of a uranium ore concentrate (UOC) can be examined to determine mine source, methods of production, and quality. This study presents a method to determine the concentration of halides and main group elements, specifically P, S, Br and I, utilizing triple quadrupole inductively coupled plasma - mass spectrometry. These analytes were measured in a uranium matrix to simulate a UOC sample. The concentrations determined with this method showed agreement with known values. Solutions with and without uranium were compared. A UOC certified reference material, CUP-2, was analyzed to further demonstrate the effectiveness of the method.

2.2 Introduction

Nuclear reactors supply over ten percent of the world's energy needs [129]. Most nuclear reactors use uranium as the fissile material. One of the initial steps in the uranium nuclear fuel cycle is the production of a uranium ore concentrate (UOC) from various deposits (e.g. sandstone, lignite, and vein). Extraction of uranium from the mined material often results in high amounts of impurities within the final product, and analysis of these UOC impurities can be used in forensic and safeguard applications.

UOCs are produced by adding acids to mined and milled ore to leach out and concentrate uranium. The extraction method will vary depending on the type of mineral [3]. The impurities present in the UOC are dependent on both the production method and the geographic area from which the ore was mined [130]. The geological location of the mined ore is important as different locations may have varying degrees of impurities present. Quantification of these impurities can help identify the original source of the UOC. The specific chemical and elemental signatures found in nuclear materials can provide information regarding the production history of the material through region specific trace element patterns, including rare earth elements and anions [2, 36, 131]. Several studies have demonstrated that analysis of these can be used to identify a UOC to a specific origin [37, 130, 132].

No single signature has been shown to uniquely determine the source of a given material, so it is often necessary to analyze multiple signatures as part of complete forensic analysis [37]. The measurement of halides and main group elements, often present in UOCs

as anions, can provide information regarding the process history [133]. For example, Badaut *et. al.* found clear differences in anion concentrations when analyzing UOC samples from different geographical locations. The authors were able to determine which sample set originated in Beverley Mine (Australia) based on a low sulfate concentration, 15 μg mL^{-1} versus 100 to 900 μg mL^{-1} at other locations, as only one location in the study involved a process history that did not use large amounts of sulfate [36]. Anion content was determined using ion chromatography (IC) with conductivity detection.

Several techniques have been used to measure the composition of UOCs [134]. Handheld Raman spectrometers can be used as a screening method during the initial production. These systems determine the chemical form of uranium oxides as well as impurities with minimal sample preparation [135]. This method suffers in sensitivity. Fourier-transform infrared spectrometry (FTIR) has also been demonstrated for UOC analysis, identifying uranium oxides and some anionic species that fall in the mid IR range [136]. For example, sulfates and nitrates are often analyzed via FTIR due to their prominent bands at 1120 cm^{-1} and 1384 cm^{-1}, respectively [3]. One drawback to FTIR is the reliance on a peak in the IR range which limits the applicability of the measurement. The most common methods for determining a multitude of trace elements in a UOC include inductively coupled plasma - mass spectrometry (ICP - MS) [137, 138] and inductively coupled plasma – optical emission spectroscopy [139, 140]. ICP – MS is a method of choice for many studies because it can analyze a wide range of elements at very low concentrations (ng mL^{-1}) [37, 130, 137, 141, 142]. Although halides are generally present in UOCs as salts or anions, they may be analyzed by ICP - MS if the ionization energy of the plasma is sufficient. In the case of sulphate and

phosphate, the ICP - MS only detects S and P, but it is assumed that they originated as sulphate and phosphate ions.

The halides and some main group elements like F, Cl, P, S, Br, and I, typically present as anionic species, have unique properties that must be addressed for accurate or precise measurement when analyzing by ICP - MS. These elements are prone to volatility, spectral interferences, and sample carry-over effects. Some studies have minimized these issues by using a pyrohydrolysis method to extract the anions, IC to separate them, and conductivity detection for analysis [37, 143-145]. This method has been shown to be effective, but the detection limits are generally orders of magnitude lower when employing an ICP - MS. For example, Balcone-Boissard *et. al.* found that Br and I concentrations fell below detection limits when analyzing by conductivity detection but were measurable by ICP - MS [143]. If utilizing this instrument, carry-over can be addressed by washing through a base such as tetra-methyl ammonium hydroxide (TMAH). TMAH can also address volatility issues by keeping the anion in solution [146, 147].

This paper demonstrates a method to determine the content of specific halide and main group elements in a uranium matrix using a triple quadrupole (TQ) ICP - MS. The TQ removes spectral interferences by employing a reaction gas in the second quadrupole and eliminating the interference in the third quadrupole. Using this methodology individual analyte separation, such as IC, is not needed before analysis. Additionally, a hazardous alkaline solution like TMAH was not required when using extended wash times to minimize carry-over effects.

2.3 Experimental

2.3.1 Materials and Methods

All standards and samples were prepared in 2% nitric acid (HNO_3), diluted from a concentrated stock of Fisher Optima grade (Pittsburgh, PA, USA) using ASTM Type I water (18.2 MΩ·cm) produced by a Thermo Scientific Barnstead GenPure xCAD Plus Ultra-Pure water purification system (Waltham, MA, USA). Trace amounts of Fisher Optima grade hydrofluoric acid (HF) was used in the preparation of CUP-2 reference material.

Standards were prepared volumetrically by serial dilution from single element stocks (10 µg mL^{-1}) purchased from High Purity Standards (Charleston, SC, USA). Solutions were prepared fresh in HDPE containers. Quality control (QC) solutions were also prepared by serial dilution from a single element stock of iodide (100 µg mL^{-1} I) and a multi-element stock containing P, S, and Br (100 µg mL^{-1} PO_4, SO_4, and Br) (Multi Element IC Std 1 Solution A) purchased from High Purity Standards. External calibration was utilized for quantification with a 4-point calibration curve. P, Br and I had concentrations of 0, 1, 5, and 10 ng mL^{-1} while S had concentrations of 0, 50, 75, and 100 ng mL^{-1}. The QC solution contained concentrations of 5 ng mL^{-1} Br and I, 1.6 ng mL^{-1} P, and 50 ng mL^{-1} S. All solutions in the uranium matrix runs, including the blank, were analyzed in a uranium matrix of 50 µg mL^{-1} that was prepared from a stock solution of uranium (High Purity Standards). Extended wash times of at least 10 minutes were performed with 2% HNO_3. Solutions were analyzed immediately after preparation to minimize losses due to volatility.

CUP-2 was prepared by weighing a 200 mg fraction of the dried UOC powder and adding 8M HNO_3 - 0.05M HF. The sample was microwave digested using a CEM (Mathews, NC, USA) Discover SP-D microwave. The dissolved UOC was diluted gravimetrically to approximately 10 mg UOC g solution^{-1}. The uranium concentration was determined using Davies-Gray titration, and the sample was subsequently diluted to a uranium concentration of 50 µg mL^{-1} in 2% HNO_3 - 1 mM HF.

2.3.2 Instrumentation

A Thermo Scientific (Bremen, Germany) iCAP TQ ICP - MS was used for analyte measurement. The TQ has the ability to utilize ultrahigh purity (99.994%) gases within the reaction cell. Available reaction gases include oxygen, hydrogen, ammonia, and nitrogen (Airgas, Radnor, Pennsylvania). The optimized instrument parameters are listed in Table 2.1. A Peltier cooled quartz cyclonic spray chamber was used with a self-aspirating PFA 50 µL min^{-1} nebulizer (ESI, Omaha, Nebraska, USA). The cyclonic spray chamber removes larger droplets from the aerosol, and the Peltier cooling system reduces the amount of solvent that enters the plasma, leading to reduction of interferences such as oxides and hydroxides. The constant temperature also helps reduce signal drift associated with environmental temperature changes [43].

2.4 Results and Discussion

2.4.1 Reaction-Gas Determination and Interferences

The analytes begin as anions in solution, but when they enter the plasma, the ionization energy is high enough to remove electrons converting them to cations despite

Table 2.1 Optimized TQ ICP – MS parameters.

Plasma power (W)	1550
Reaction gas flow (mL min^{-1})	0.338
Nebulizer gas flow (L min^{-1})	1.10
Cool gas flow (L min^{-1})	14.0
Spray chamber temperature (°C)	2.70
CR entry lens (V)	-100
CR exit lens (V)	-160
D1 lens (V)	-200
D2 lens (V)	-83.9
Deflection entry lens (V)	-30.0
Extraction lens 2 (V)	-135
Focus lens (V)	20.3
Pole bias	-1
Q1 entry lens (V)	-99
Q1 focus lens (V)	0.76
Quad entry lens (V)	-25.2

their high electronegativities. Fluorine and chlorine were investigated, but their ionization potentials limited the formation of cations in the plasma. The difficulty in measuring these elements by ICP – MS with a sufficient detection limit has been demonstrated in another study [137]. No further analysis of F or Cl was performed. The TQ ICP - MS can be used for on-mass or off-mass analysis as shown in Figure 2.1. On-mass analysis is when the mass detected is the same as the analyte mass set to pass through Q1, and the spectral interferences react with the collision cell gas so that Q3 will filter them out. For the case of off-mass analysis the analyte itself reacts with the gas in the collision cell so that the mass is shifted away from the spectral interferences, and Q3 filters out any mass other than that of the combined mass of the selected gas and the original analyte (Fig. 2.1). On-mass analysis was employed for $^{127}I^{+}$ and off-mass analysis was employed for $^{31}P^{16}O^{+}$, $^{32}S^{16}O^{+}$, and $^{79}Br^{16}O^{+}$.

The TQ ICP - MS utilized for this study incorporated four different reaction gases (hydrogen, helium, ammonia, and oxygen) employed as operating modes. Additionally, the kinetic energy discrimination (KED) mode uses a small amount of He in the collision cell to filter out unwanted spectral interferences based on their collision cross section. This requires a difference in size between the analyte and spectral interference rather than a difference in reactivity. The choice of collision cell gas for each ion depends on the thermochemistry and kinetics of the collisions that occur in the cell. For each ion, an ion exchange reaction with each gas can be proposed. For these reactions to occur, the enthalpy of formation of the reactants must be greater than that of the products. If this is not the case, then additional energy will be necessary for the reaction to proceed. This energy can

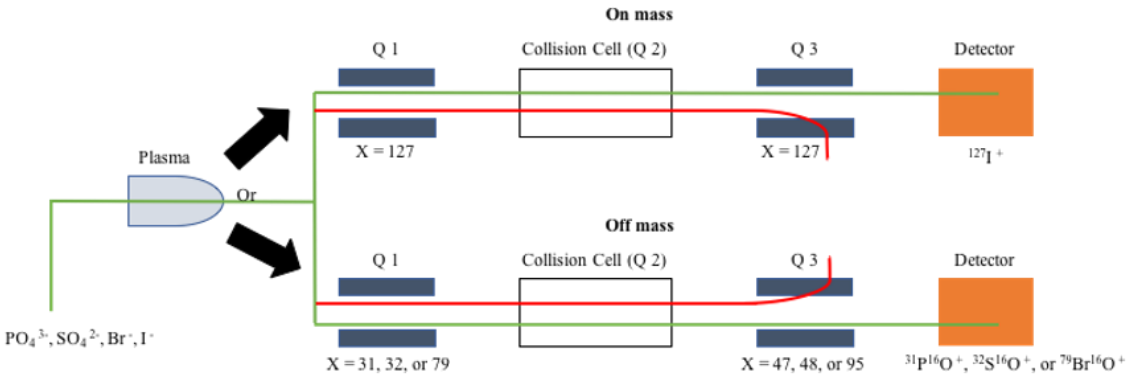


Figure 2.1 A diagram demonstrating the difference between on-mass and off-mass analysis using the TQ ICP - MS. Depicts spectral interferences passing through Q1 but not Q3 while the desired ion passes through to the detector. This is a pictorial display of both modes of operation, these modes can be performed sequentially.

originate from collisions that occur in the cell or by radio frequency [148]. If there is not enough energy to create a favorable reaction, then that reaction gas is not suitable for use with that ion. The best mode for each of the analytes was experimentally determined before method demonstration. Each species was analyzed via all modes, at 100 ng mL^{-1} to determine ion transmission with the reaction gas. Single element solutions of the interfering ions were then injected at µg mL^{-1} levels to determine spectral interference removal.

Phosphorus showed favorable response by either oxygen or KED mode. Both modes removed the spectral interferences listed in Table 2.2. The oxygen mode was chosen for P because it showed greater sensitivity (60x) than KED mode. For S, oxygen mode was the only mode that demonstrated the ability to resolve the spectral interferences by an off-mass shift (Table 2.2). Both oxygen and KED modes were evaluated for Br and showed favorable results. Upon analysis of single element interferences KED mode showed elevated Br counts due to an unresolved interference from Gd and Dy. For I, KED, oxygen, and helium were all investigated, all were able to eliminate spectral interferences (Table 2.2). The ion transmission was limited with KED having the least and helium having the greatest sensitivity. Oxygen provided half the sensitivity of helium for I analysis, but the number of counts were sufficient to make the measurements. Ultimately, oxygen mode was chosen for I as well. In this way all analytes studied utilized oxygen as the reaction gas in the collision cell. Using oxygen mode only kept analysis times down by limiting reaction gas equilibration times. These results were similar to the method developed by Balcaen *et. al.* which used oxygen as a reaction gas for off-mass analysis in organic matrices containing

Table 2.2 Selected spectral interferences for all analytes.

Element	Interferences					
^{31}P	$^{1}H^{16}O^{14}N$	$^{16}O^{15}N$	$^{3}H^{16}O^{12}C$	$^{2}H^{17}O^{12}C$	$^{1}H^{18}O^{12}C$	$^{12}C^{19}F$
	$^{63}Cu^{++}$	$^{62}Ni^{++}$	$^{1}H^{30}Si$			
^{32}S	$^{16}O^{16}O$	$^{1}H^{16}O^{15}N$	$^{18}O^{14}N$	$^{1}H^{31}P$	$^{12}C^{20}Ne$	$^{13}C^{19}F$
	$^{65}Cu^{++}$	$^{64}Ni^{++}$	$^{64}Zn^{++}$			
^{79}Br	$^{40}Ar^{39}K$	$^{16}O^{63}Cu$	$^{14}N^{65}Cu$	$^{1}H^{78}Se$	$^{12}C^{67}Zn$	$^{1}H^{62}Ni^{16}O$
	$^{66}Zn^{13}C$	$^{64}Zn^{15}N$	$^{158}Gd^{++}$	$^{157}Gd^{++}$	$^{158}Dy^{++}$	$^{1}H^{78}Kr$
^{127}I	$^{115}In^{12}C$	$^{87}Rb^{40}Ar$	$^{126}Te^{1}H$	$^{1}H^{110}Pd^{16}O$	$^{111}Cd^{16}O$	$^{1}H^{110}Cd^{16}O$
	$^{87}Sr^{40}Ar$	$^{113}In^{14}N$	$^{115}Sn^{12}C$	$^{114}Cd^{13}C$	$^{238}U^{16}O^{++}$	$^{113}Cd^{14}N$

P and S, but Br and I were analyzed using charge transfer reactions instead of on-mass or off-mass analysis [149]. Oxygen mode was used for the remainder of the experiment.

2.4.2 Method Demonstration

For method demonstration the method was run on three separate days to determine accuracy and reproducibility. On each day the P, S, Br, and I were analyzed with and without a uranium matrix (50 µg mL^{-1}), three times per day, to investigate the magnitude of uranium ion count suppression. The High Purity Standards IC solutions were used as a quality control to demonstrate the effectiveness of the method. All reported uncertainties are represented as 2σ as determined from the triplicate daily data points from each experiment. The reported uncertainties for the 3 day average concentrations are expanded uncertainties calculated using the sum of the square. The components in the uncertainty model were the slope of the calibration curve, the concentration of the stock standards, and the measurement variability. All RSDs were calculated by multiplying the standard deviation by 100 and dividing by the average concentration of the analyte.

It was necessary to use a weighted average of the matrix blank to correct for change in sensitivity across the run. The matrix blank was analyzed before and after a run, and a linear correction was applied to the sample. Signal sensitivity in the QCs decreased by an average of 20% during the run. After the corrections were applied, the daily average concentrations of P showed reproducibility across the 3 days of experiments, ~ 2.7% RSD without a uranium matrix and ~ 2.9% with a uranium matrix (Fig. 2.2). The average concentration of P among the three days was 1.74 ± 0.18 ng mL^{-1} when not in a uranium matrix and 1.64 ± 0.15 ng mL^{-1} in a uranium matrix. In both cases the uncertainties overlap

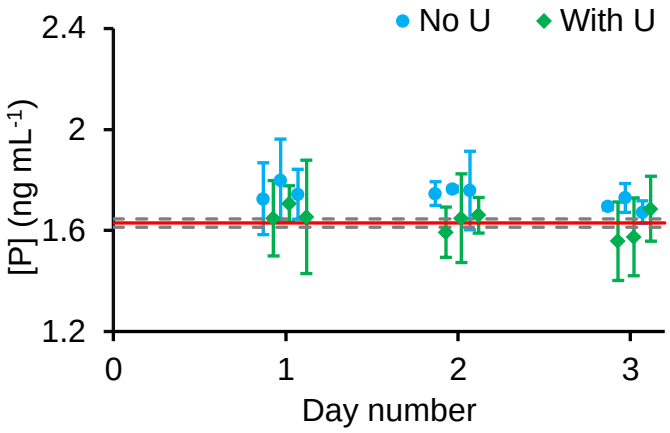


Figure 2.2 Average daily concentration of P with three analysis per day. Solid line denotes known concentration and the dashed lines indicate uncertainty in the QC.

with the known value of 1.630 ± 0.016 ng mL^{-1}. The values for the three-day average concentrations show agreement with each other.

Runs with and without a uranium matrix proved reproducible over three days with an average concentration of S measured at 50.1 ± 2.5 ng mL^{-1} (~ 1.7% RSD) with no matrix and 47.4 ± 3.3 ng mL^{-1} (~ 1.6% RSD) in a uranium matrix (Fig. 2.3). Both measured values show good recovery of the known concentration of 50.00 ± 0.50 ng mL^{-1} within the uncertainty of the measurement at a 0.14% difference when not in a uranium matrix and a 5.4% difference in a matrix (Fig. 2.3). While there is a difference between solutions with and without a uranium matrix on the third day, this could be attributed to run to run variability of the method. The solutions show agreement with each other as the average concentrations fall within the uncertainties.

For Br, the method demonstrated run to run reproducibility for solutions both with (~ 2.2% RSD) and without (~ 2.6% RSD) a uranium matrix. (Fig. 2.4). The three day average concentrations were 5.30 ± 0.30 and 5.15 ± 0.35 ng mL^{-1}, respectively. These values showed agreement with the known concentration of 5.00 ± 0.10 ng mL^{-1} for both solutions not in a uranium matrix (3.0% different) and in a uranium matrix (5.7% different) as well as with each other. The agreement between the three day average concentrations indicates the method may be useful for the determination of Br in a uranium matrix.

Iodine was more difficult to analyze than the other species due to the carry-over and volatility effects. Initial 3 minute washout times were extended to 10 minutes to eliminate any carry-over effects from I. Issues with I carry-over has been previously

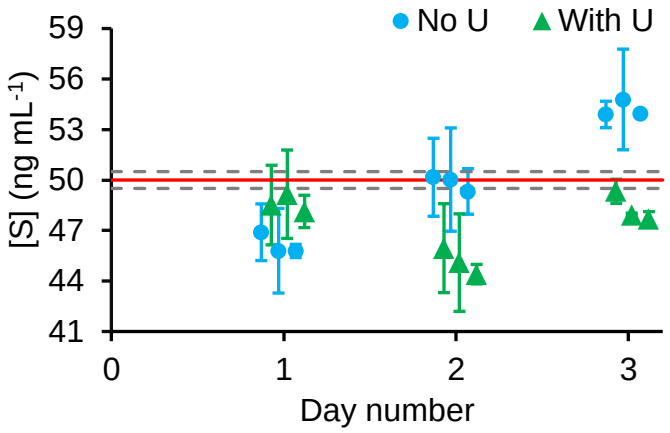


Figure 2.3 Average daily concentration of S with three analysis per day. Solid line denotes known concentration and the dashed lines indicate uncertainty in the QC.

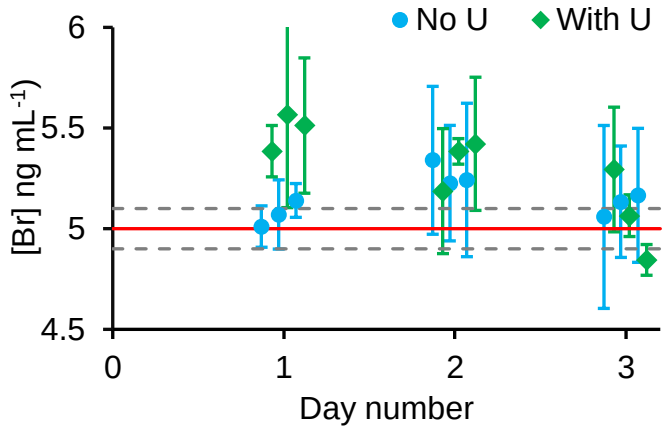


Figure 2.4 Average daily concentration of Br with three analysis per day. Solid line denotes known concentration and the dotted lines indicate uncertainty in the QC.

reported [150]. While in an acid matrix it was necessary to run the sample immediately after preparation to avoid losing I to volatilization [151]. Since samples were analyzed within 10 minutes, more study is necessary to determine if I can be measured after microwave digestion. TMAH can be used to help keep iodine in solution, but at a pH above 8, uranium will precipitate out of solution [37, 152]. In the current method, the only added sample preparation for I is the addition of uranium to the blank and standards. This matrix matching step allows for the counts from the UO^{++} interference at 127 amu to be accounted for, leaving only I^{+} counts.

After performing a blank subtraction, the method showed agreement with the known value of 5.00 ± 0.10 ng mL^{-1} for average concentration of I both with (1.3% difference) and without (2.7% difference) a uranium matrix (Fig. 2.5). The method demonstrated run to run reproducibility with an RSD of ~ 2.2% when not in a uranium matrix and ~ 2.7% in a uranium matrix. An average three day concentration of 4.9 ± 1.1 ng mL^{-1} for solutions with no matrix and 4.9 ± 1.4 ng mL^{-1} with a uranium matrix was determined. The small difference between results with and without the matrix suggests that the method is suitable for analyzing I in UOCs with little sample preparation. Additionally, the method does not require the use of TMAH or other alkaline materials used in many other ICP - MS studies [153].

2.4.3 Limit of Detection

The limit of detection for each analyte was calculated as both an instrument detection limit (IDL) and a method detection limit (MDL). The IDL was used to compare the results

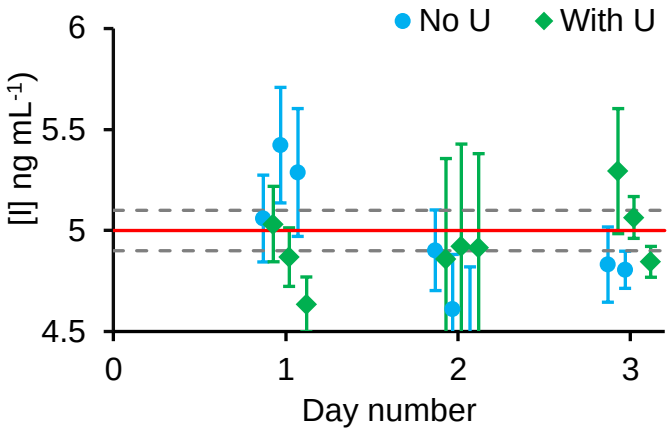


Figure 2.5 Average daily concentration of I with three analysis per day. Solid line denotes known concentration and the dotted lines indicate uncertainty in the QC.

of the method with and without a uranium matrix while the MDL shows the effectiveness of the method for each species. The IDL was calculated using Eq. (1) where σ_B is the standard deviation of the blank and m is the slope of the external calibration curve. The MDL was determined by propagating the IDL through the method preparation steps such that the uranium concentration was 50 µg mL^{-1}.

$$IDL = \frac{3\sigma_B}{m} \quad (1)$$

The IDLs of P, S, and Br were nearly identical whether the uranium matrix was present or not (Table 2.3). This supports the assertion that these analytes can be analyzed in a uranium matrix with little impact on the limit of quantification. The IDL of I was higher in a uranium matrix which would be expected due to the presence of the UO^{++} interference (Table 2.2). While the IDL for I was higher than the other analytes, the method still demonstrated the ability to detect I in a uranium matrix at the concentrations utilized in this study (Fig. 2.5). The IDL for S was similar to that found in another study while the P and Br IDLs were two to three orders of magnitude lower than those found in the same study using IC and conductivity detection [36].

The MDLs for P, Br, and I were similar while S was about one order of magnitude higher in concentration (Table 2.3). Sulfur had a higher MDL than the other analytes due to the higher background (50x counts) in the blank solutions. Sulfur values vary depending on the process in the formation of UOCs, and this element is a more valuable process indicator [154]. Thus a high S blank, with the associated higher MDL, does not preclude a useful measurement of this species in UOC materials. Also, the higher MDL for S should

Table 2.3 LOD for the analytes with IDL (ng mL^{-1}) and MDL (µg g U^{-1}).

	P	S	Br	I
No U IDL	0.164	1.71	0.0736	0.00311
U IDL	0.160	1.50	0.0640	0.235
U MDL	3.20	30.0	1.28	4.70

not be an issue in analysis due to the generally high values of SO_4^{2-} in UOC [36]. This is consistent with the results of an interlaboratory study, primarily utilizing sector field ICP - MS, where the average level of reported S in a UOC was nearly 6000 µg gU^{-1} [137]. The MDLs for P and S in the present work were similar to reported values from the interlaboratory study [137]. No participants reported values for Br or Cl due to the difficulty in quantifying them by ICP – MS. This method was successful in quantifying Br and had a MDL that was the lowest of all analytes studied (Table 2.3).

2.4.4 CUP-2 Analysis

A certified reference material (CRM), CUP-2, was analyzed for anion content and the results were compared to the recommended values. CUP-2 is a UOC CRM that was jointly produced by the Canadian Certified Reference Materials Project and the Canadian Uranium Producers Metallurgical Committee. The CRM solution was diluted to a concentration of 50 µg U mL^{-1}, consistent with the uranium content used during method demonstration. The calibration standards were matrix matched in the same manner as was performed previously. CUP-2 was evaluated three times on three separate days so an average concentration value could be reported, and the reproducibility of the method for the CRM could be investigated. The CRM was analyzed for P, S, Br, and I, although there is no recommended value for Br or I.

The average P and S concentrations determined using the method described in this study show agreement with the provisionally recommended values for the CUP-2 CRM (Fig. 2.6). The average three day P concentration (410 ±45 µg g U^{-1}) was within 3.1% of

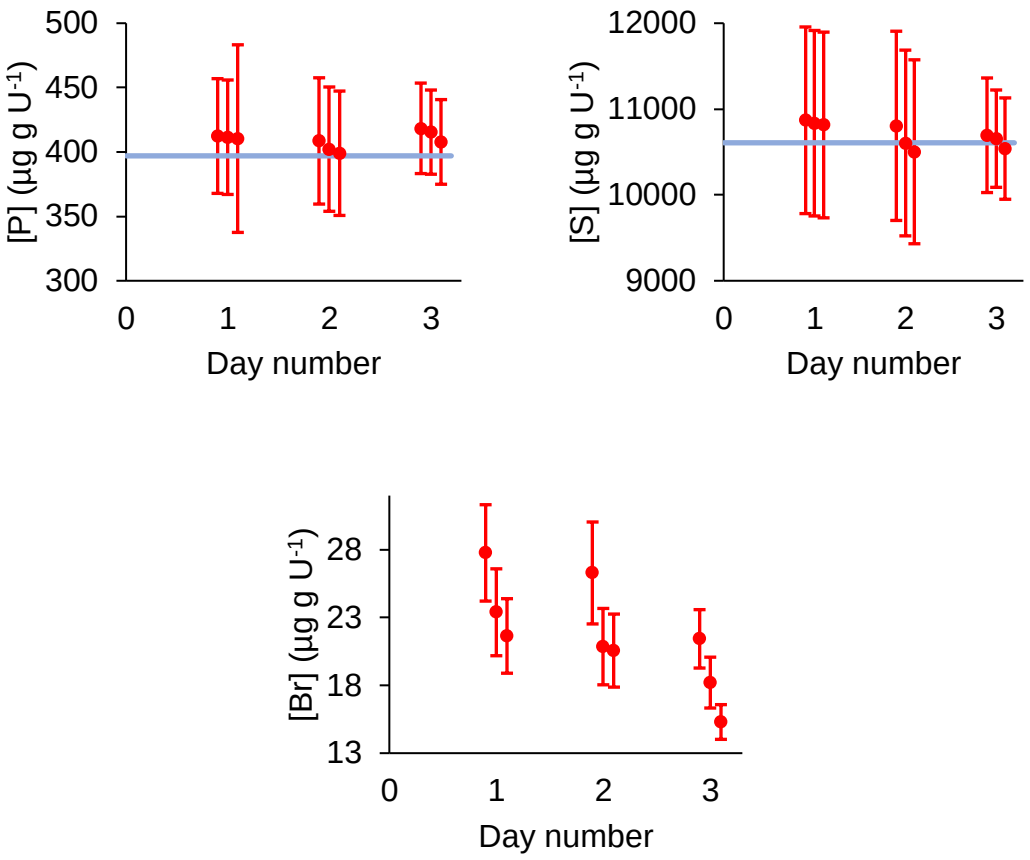


Figure 2.6 Cup-2 data for P, S, and Br with a line indicating the recommended value

the recommended value (397 µg g U^{-1}), and the S concentration (10700 ± 900 µg g U^{-1}) was within 0.89% of the recommended value (10607 µg g U^{-1}) (Fig. 2.6). This agreement suggests that the TQ ICP - MS method is suitable for detection of P and S in UOC materials. As mentioned previously, Br and I values are not available for CUP-2, because of the challenge of measuring the halides in material such as UOCs, but they were analyzed using the method developed in this study. No I was detected in CUP-2, nor has it been previously reported. This may be due several factors (e.g. extended storage time, volatility, and sample preparation). Further studies are required to determine if I could be detected in CUP-2 immediately after the sample was prepared. Bromine was detected utilizing this method with a three day average concentration of 21.7 ± 2.6 µg g U^{-1}. While there is no recommended value to compare this result to, the determined concentration is above the MDL of this study (Table 2.3). The use of the TQ and the method developed here may open the door for more routine analysis of these analytes in the future, allowing an evaluation of their value as signatures of the UOC source.

2.5 Conclusions

A method for analyzing P, S, Br, and I in a uranium matrix using a TQ ICP - MS is presented here. The instrument removed interferences that are common for the analytes in this study, and the results showed agreement between runs with and without a 50 µg mL^{-1} uranium matrix for P, S, Br, and I. While the method may sacrifice precision on a multiple day analysis and stability issues in the acid matrix were observed for I, the average concentrations for all analytes agreed with known values. When analyzing the data for possible matrix effects, a comparison of the results with and without uranium shows that

this method is suitable for accurate quantification of P, S, Br, and I when using matrix matching standards. When analyzing CUP-2, the experimentally determined concentrations for P and S agreed with the recommended values. This suggests that the method may be useful for those species and allows the possibility of Br and I analysis which have not traditionally been undertaken by ICP - MS in UOC materials in the past. The method allows for faster analysis times with less sample preparation, bypassing the use of chemical separations and alkaline washes.

Chapter 3

Determination of Phosphorus and Sulfur in Uranium Ore Concentrates by Triple Quadrupole Inductively Coupled Plasma Mass Spectrometry

This chapter was originally published in Talanta as shown below and is reproduced here with permission.

Fletcher, N. D.; Manard, B. T.; Bostick, D. A.; Bostick, W. D.; Metzger, S. C.; Ticknor, B. W.; Rogers, K. T.; Hexel, C. R. Determination of phosphorus and sulfur in uranium ore concentrates by triple quadrupole inductively coupled plasma mass spectrometry. *Talanta* **2021**, *221*. DOI: 10.1016/j.talanta.2020.121573.

All experimental work and data analysis in this chapter was performed by myself. All expermintal design and editing was performed by myself as well as Benjamin Manard, Debra Bostick, William Bostick, Shalina Metzger, Brian Ticknor, Kayron Rogers, and Cole Hexel.

3.1 Abstract

The analysis of impurities in a uranium ore concentrate (UOC) could provide information regarding the source, production history, and potential intended use of the UOC. This study involves the analysis of UOC samples for phosphorus and sulfur. Concentrations were determined by triple quadrupole inductively coupled plasma – mass spectrometry and compared with results from a pyrohydrolysis method and previously reported results. The sulfur and phosphorus concentrations, determined by the mass spectrometer, were used to identify possible trends in the data, and the uncertainties were calculated using the Guide to Uncertainty Measurements workbench software. The triple quadrupole inductively coupled plasma - mass spectrometer method allows for the removal of interferences in the analysis of species that begin as anions. This method could not be performed with a

traditional quadrupole instrument as the interferences could not be resolved. The newly developed method also allows for a high sample throughput as more than 25 samples were analyzed in every run.

3.2 Introduction

One of the first steps in the nuclear fuel cycle is the production of a uranium ore concentrate (UOC).[2] UOCs are generated at a milling facility after the ore is mined, pulverized, and subsequentially leached of its uranium with acids. A solvent extraction method is then utilized to separate the uranium from the leachate prior to precipitation.[134] The solid UOC can then be utilized for its intended purpose (e.g. production of material used as fuel for nuclear reactors or feed for enrichment processes). A wide range of processing methods, depending on the type of mineral, can be implemented to develop UOCs.[3, 134, 155] The produced UOCs will contain impurities that are present from the mine or that were introduced during the processing of the ore. A thorough analysis of these trace element impurities can provide indications about the source, process history, and quality of the material.[36, 131] The analysis of UOCs is commonly performed by inductively coupled plasma mass spectrometry or optical emission spectroscopy (ICP-MS/OES) due to the wide range of trace elements that can be determined at lower concentrations (ng mL^{-1}).[138, 139, 142] Studies have demonstrated that the analysis of trace element patterns such as rare earth elements or anions can provide information on the processing history or the region the UOC originated in.[37, 132] Halides and some main group elements are usually present as anions in UOCs, and the anion content can provide information about the production history of the material.[133] Sulfate is especially common as many processing methods

involve the use of sulfuric acid during leaching, resulting in high concentrations of sulfate.[36, 137] The $^{34}S/^{32}S$ ratio has also been demonstrated as a viable signature for the identification of the source of the material, particularly if specific reagents (H_2SO_4) were used in the extraction and/or leaching processes.[154] The isotopic signature of sulfur can be perturbed depending on the processing steps. Krajko *et. al.* demonstrated that leaching was the processing step that significantly impacted the sulfur values (^{34}S) by analyzing samples before and after leaching.[154]

One method for the determination of anions in a uranium matrix is total reflection X-ray fluorescence spectrometry.[156] This is a popular method because of the low sample amount requirement and the ability of the method to measure nonmetal and metals, but it is unable to measure some analytes such as phosphorus. Combustion IR has also been used to determine sulfate and other anion levels. This has been demonstrated in UOCs as wells as nuclear fuel.[157, 158] Another method that has been widely applied for the analysis of anions in UOCs involves the use of pyrohydrolysis to extract the anions, ion chromatography (IC) for separation, and conductivity for detection.[36, 143, 144] This extraction method has been previously reported for the separation of various anions, such as fluorine and chlorine, from nuclear material.[159]

While pyrohydrolysis can be effective, it has been shown to be limited in the recovery of analytes such as sulfur or sulfate.[145] Other studies have utilized ICP–MS to analyze trace elements including halides and main group elements due to the lower limits of detection provided for some analytes.[146, 151] This was demonstrated by Balcone-Boissard *et. al.* when they determined that bromine and iodine levels in geochemical reference

materials were below detection limits when measuring by IC with conductivity detection, but detection was possible by ICP–MS.[143] While IC with conductivity detection actually measures anions, it should be noted that in ICP–MS the plasma has enough ionization energy to remove electrons from the anions so they are measured as cations.[148] In another study, Keegan *et. al.* developed a water leach method where a pulverized UOC sample was soaked in deionized water for 24 hours. The resulting solution was then filtered and the soluble anions were analyzed by IC and high resolution ICP–MS and sulfate was determined to be the predominate anion impurtity.[37] As the processing history of those samples was known, the authors suggest the sulfate was linked to the production history.[37]

Halide and main group elements like phosphorus, sulfur, bromine, and iodine can be measured by ICP–MS, but they have properties that can make analysis difficult, such as volatility and spectral interferences. One study demonstrated the possibility of analyzing anions using high resolution ICP–MS to resolve the spectral interferences.[160] This study illustrated that at high mass resolution ($m\ \Delta m^{-1}$ 4000) the spectral interferences of S can be better resolved in comparison with a quadrupole that has a resolution of 300-400. In the case of the quadrupole the accuracy of the measurement was much lower due to unresolved interferences. They found that they could resolve ^{32}S from isobaric interferences $^{16}O^{16}O$ and $^{14}N^{18}O$ in uranium material with a limit of detection of 2 μg g U^{-1}.[160]

Another possible method for the analysis of anions with spectral interferences is the use of a triple quadrupole (TQ) ICP–MS, as interferences can be removed prior to detection through the use of reaction gases in a collision cell.[149, 161] While analysis of elements such as sulfur has shown to be unreliable using a single quadrupole ICP–MS, the

TQ ICP–MS allows for the analysis to be performed on a quadrupole after the mass of the interferences or analyte has been shifted. This may provide a more rapid and cost effective form of analysis when compared to high resolution ICP–MS. In this study, 17 UOC samples from various mines around the world were analyzed. The sample series originated in locations where other samples have been collected and analyzed previously. Results from this study were compared to previously reported results when available. The UOC samples were analyzed using a TQ ICP–MS with a previously developed method to determine phosphorus, sulfur, bromine, and iodine content.[161] Concentrations determined by the TQ ICP–MS were compared to data obtained using a pyrohydrolysis extraction method and IC with conductivity detection. The phosphorus and sulfur content obtained by TQ ICP–MS was then used to identify possible trends in the data. Analysis of the uncertainties was performed to determine what aspects of the TQ ICP–MS method had the greatest impact on the overall uncertainties.

3.3 Experimental

3.3.1 Materials

Standards and samples were prepared using Fisher Optima grade (Pittsburgh, PA, USA) nitric acid (HNO_3). The HNO_3 was diluted from a stock with ASTM type 1 water (18.2 MΩ cm) from a Thermo Scientific Barnstead GenPure xCAD Plus Ultra-Pure water purification system (Waltham, MA, USA). Trace amounts of Fisher Optima grade hydrofluoric acid (HF) were utilized to aid in the dissolution of the samples. The Viognier and Feldspath certified reference materials (CRMs) were purchased from the Commission d'ETAblissement des Méthode d'Analyses (CETAMA). Feldspath is a UOC CRM with

certified values determined for SO_4 and PO_4, and Viognier is a synthetic CRM with a certified value listed for P. CUP-2 is a reference material that was jointly produced by the Analytical Subcommittee of the Canadian Uranium Producers Metallurgical Committee and the Canadian Certified Reference Materials Project, and has recommended values for P and S. Viognier and Feldspath were analyzed by both the pyrohydrolysis and TQ ICP–MS methods while CUP-2 was analyzed by only the TQ ICP–MS method. All samples indicated in Table 3.1 were analyzed along with the CRMs.

3.3.2 Pyrohydrolysis Method

The samples indicated in Table 2.1 were first weighed out, along with the Viognier and Feldspath QCs, in aliquots $\leq$ 0.5 g due to the small amount of sample available. The pyrohydrolysis system utilized for the extraction did not involve accelerants. Moisture saturated oxygen was passed over the sample in a furnace tube and the tube was heated to 800ºC. This extracts the anions as a volatile gas, which is then trapped and condensed into a distillate solution. The system utilized two gas scrubbers to trap the anions to ensure as much analyte as possible was recovered. Each trap contained 20 mL of a diluted carbonate buffer that can also be used as the eluent for IC. The stock was purchased from Thermo Fisher Scientific (Waltham, MA, USA) and diluted such that the solution contained 4.5 mM Na_2CO_3 and 0.8 mM $NaHCO_3$ at a pH of about 10.5. Each scrubber trap was held at ice water temperature.

The recovered distillate was analyzed by IC with conductivity detection using a Thermo Scientific IC System (Dionex ICS-1100). The separation column used was Dionex

Table 3.1 List of UOC samples and description of each

Sample	Country	Region	Phase
Mary Kathleen	Australia	Queensland	U_3O_8 Uranium Oxide
Radium Hill	Australia	South Australia	$Na((UO_2)4O_2(OH)_5)(H_2O)_5$ Metaschoepite-Na
Ranger Mine	Australia	Northern Territory	$Na_{0.35}UO_{2.95}$; $Na_6U_7O_{24}$ Sodium Uranium Oxide
South Alligator	Australia	Northern Territory	$(UO2)_4O(OH)_6(H_2O)_5$ Metaschoepite
Blind River	Canada	Elliot Lake, Ontario	$Na_2U_3O_9$ Sodium Uranium Oxide
Denison	Canada	Elliot Lake, Ontario	$Na_2(UO_2)_2(Si_2O_5)_3 \cdot 4H_2O$ Sodium Uranyl Silicate Hydrate
Dyno Mine	Canada	Bancroft, Ontario	$NH_3U_2O_6 \cdot 3H_2O$ Ammonium Uranium Oxide Hydrate
Eldorado Uranium	Canada	Beaverlodge area Saskatchewan	$(NH_4)_3((UO_2)_{10}O_{10}(OH))((UO_4)(H_2O)_2)(H_2O)_2$ Ammonium Uranium Oxide Hydroxide Hydrate
Rabbit Lake	Canada	Saskatchewan	$UO_4 \cdot 2H_2O$ Metastudite
Faraday	Canada	Bancroft, Ontario	$2UO_3 \cdot NH_3 \cdot 3H_2O$ Uranium Oxide Ammonia Hydrate
Madawaska Mine	Canada	Bancroft, Ontario	$Na_6U_7O_{24}$; $Na_2O(UO_3H_2O)$; $Na((UO_2)O(OH))$ Sodium Uranium Oxides
Milliken Lake	Canada	Elliot Lake, Ontario	$U_2(NH_3)O_6 \cdot 3H_2O$ Uranium Amine Oxide Hydrate
North Span	Canada	Elliot Lake, Ontario	$(UO_2)_4O(OH)_6(H_2O)_5$ Metaschoepite
Rio Algom	Canada	Elliot Lake, Ontario	$(NH_4)_{2(}(UO_2)_2(SO_4)O_2)$ Zippeite
Stanleigh	Canada	Elliot Lake, Ontario	$U_3(NH_3)O_9 \cdot 5H_2O$ Uranium Amine Oxide Hydrate
Gunnar Mine	Canada	Beaverlodge area, Saskatchewan	$U_3(NH_3)O_9 \cdot 4H_2O$ Uranium Amine Oxide Hydrate
ESI USA	USA	Florida	$U_3(NH_3)O_9 \cdot 4H_2O$ Uranium Amine Oxide Hydrate

IonPac AS23. All standards were diluted from stocks purchased from Thermo Fisher Scientific. Solution ICC-200 was used for PO_4 and SO_4.

3.3.3 Triple Quadrupole Method

All samples were prepared by weighing out 300 mg of UOC powder. The CRMs analyzed in this study were UOC CRMs Viognier, Feldspath, and CUP-2. Samples and CRMs were dissolved in 8M HNO_3 at 120°C. Samples that were not dissolved after one week were digested using a CEM (Mathews, NC, USA) Discover SP-D microwave. The microwave was ramped to 225°C and held for 20 minutes at 260 PSI. Uranium content of the UOC samples and QCs was determined using a Thermo Scientific (Bremen, Germany) inductively coupled plasma – optical emission spectrometer (ICP-OES). The solutions were then diluted gravimetrically with 2% HNO_3 - 1 mM HF to 50 μg U mL^{-1} solution.

The solutions were initially screened and then measured for P, S, Br, and I content periodically over a period of about three weeks to determine stability of the sample once in solution. Concentrations of the analytes were determined using a Thermo Scientific iCap TQ ICP–MS. All standards were prepared fresh daily, gravimetrically, using single elements stocks (10 μg mL^{-1}) purchased from High Purity Standards (Charleston, SC, USA). The calibration standards of P ranged from 5 to 700 ng g^{-1}, S ranged from 250 to 1600 ng g^{-1}, and Br and I ranged from 0.5 to 40 ng g^{-1}. Standards were matrix matched to the samples to have a uranium concentration of 50 μg g^{-1} using a single element uranium standard (High Purity Standards, 1000 μg mL^{-1}). The method allowed for the analysis of more than 25 samples in a single run.

3.4 Results and Discussion

3.4.1 Quality Controls

The CRMs Feldspath, Viognier, and CUP-2 were analyzed as QCs by the TQ ICP–MS method in order to determine the accuracy of the method. The CRMs were also analyzed once by pyrohydrolysis. For the TQ ICP–MS method, since the QCs were dissolved multiple analysis, 9 times over a period of 18 days, of the same aliquot was performed. CUP-2 was analyzed to ensure the accuracy of the instrument as determination of P and S concentrations in CUP-2 has already been demonstrated.[161] Concentrations determined for P and S by TQ ICP–MS suggested the method was accurate as the expected value was generally within the uncertainty of the measurement (Fig. 3.1). The average concentration over the 18 days was close to the expected value with < 1% difference (Table 3.2).

Duplicate analysis of Feldspath by the TQ ICP–MS was performed to demonstrate sample preparation reproducibility. Two aliquots were prepared for analysis in the same manner as the samples. The Br and I concentrations were both unreliable and varied greatly depending on the day. While the certified Feldspath value was for PO_4, this was converted to P by multiplying by the percentage of P in PO_4 so the certified value could be compared to results obtained by TQ ICP–MS. The duplicate analysis of Feldspath for P suggests that the method was reproducible among separate QC aliquots (Fig. 3.2). Given the demonstrated reproducibility among the two aliquots of QC, the average across all measurements was calculated and compared to the certified value for P (Table 3.2). The average P concentration

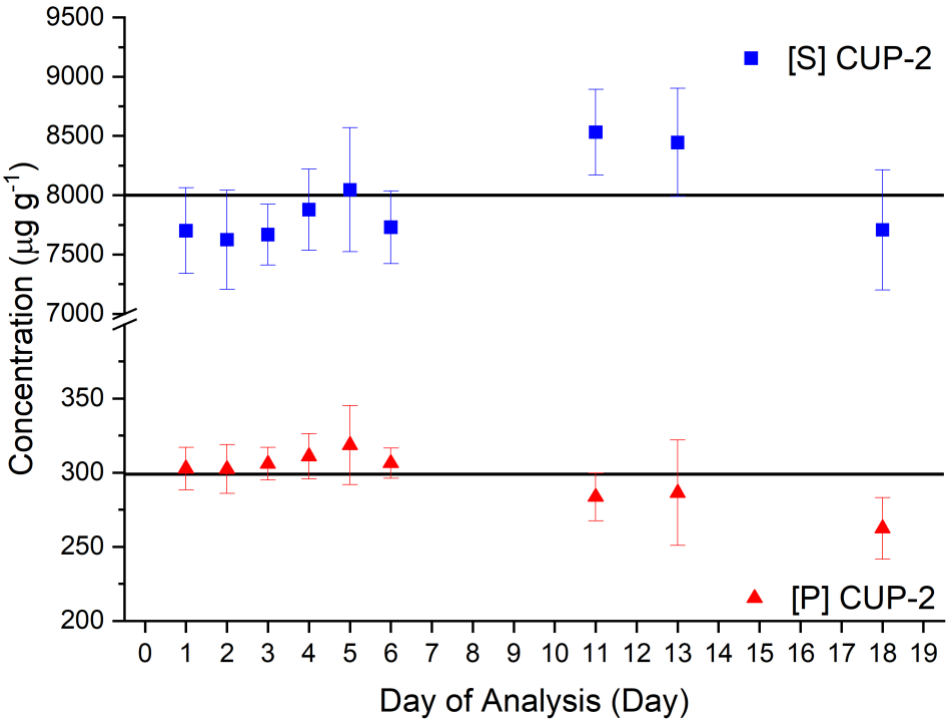


Figure 3.1 Concentrations of CUP-2 for P and S over a period of 18 days with a line indicating expected value.

Table 3.2 Average concentrations and expected values of the QCs for P and S (µg g^{-1})

	P (µg g^{-1})		S (µg g^{-1})	
	Expected	**TQ ICP–MS**	**Expected**	**TQ ICP–MS**
Feldspath	51 ± 5.2	53 ± 4.2	5340 ± 330	4840 ± 340
Viognier	43 ± 1.8	46 ± 4.1	NA	ND
CUP-2	299	298 ± 23	8000	7930 ± 570

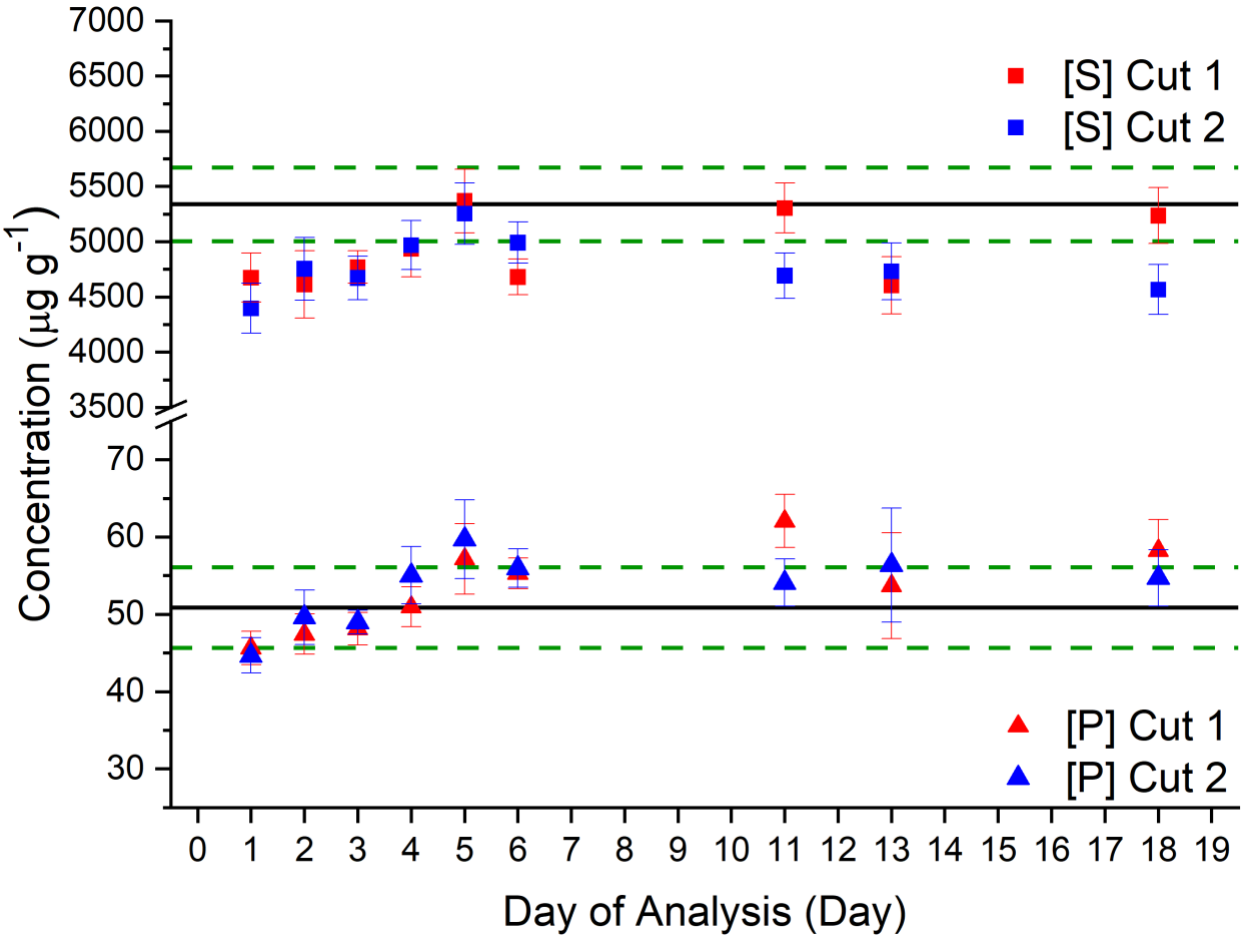


Figure 3.2 Concentration of P and S in two aliquots of Feldspath over 18 days with a solid line indicating certified value and dashed line indicating uncertainty given by the CRM.

showed good agreement with the expected value as it was within the uncertainty of the certificate with a 3.9% difference.

For the analysis of S in Feldspath a conversion of the certified SO_4 to S was performed by multiplying the value by the percentage of S in the molar mass of SO_4 so that a comparison between the certified value and values obtained by TQ ICP–MS could be made. Analysis of Feldspath for S also showed good reproducibility (Fig. 3.2). While the determined concentration on some days seemed to reach the expected value of 5340 $\mu g\ g^{-1}$ the data suggests the concentration in solution is less than the certified value (Fig. 3.2). Given the similarity among the separate aliquots, the average of all runs was again used to compare with the expected value. This resulted in a 9.4% difference (Table 3.2). The difference is not attributed to low ion transmission through the instrument due to the excellent agreement between the actual and certified values for S in the QC check CUP-2 (Table 3.2). One possible explanation for the lower than expected concentrations of S determined in Feldspath by TQ ICP–MS is a loss of S during dissolution of the sample. This could potentially be mitigated by performing the dissolution of the sample at a lower temperature to lessen the volatility.

Viognier showed similar results to the Feldspath in that the Br results were unreliable. The ICP–MS method did not detect any S, but this was expected as no S was added to the synthetic CRM. As was demonstrated in the Feldspath QC (Fig. 3.1) there is a slight increase in the P concentrations over the first 4 days, although this is less pronounced in Viognier 2 (Fig. 3.3). All the concentration values from the two aliquots

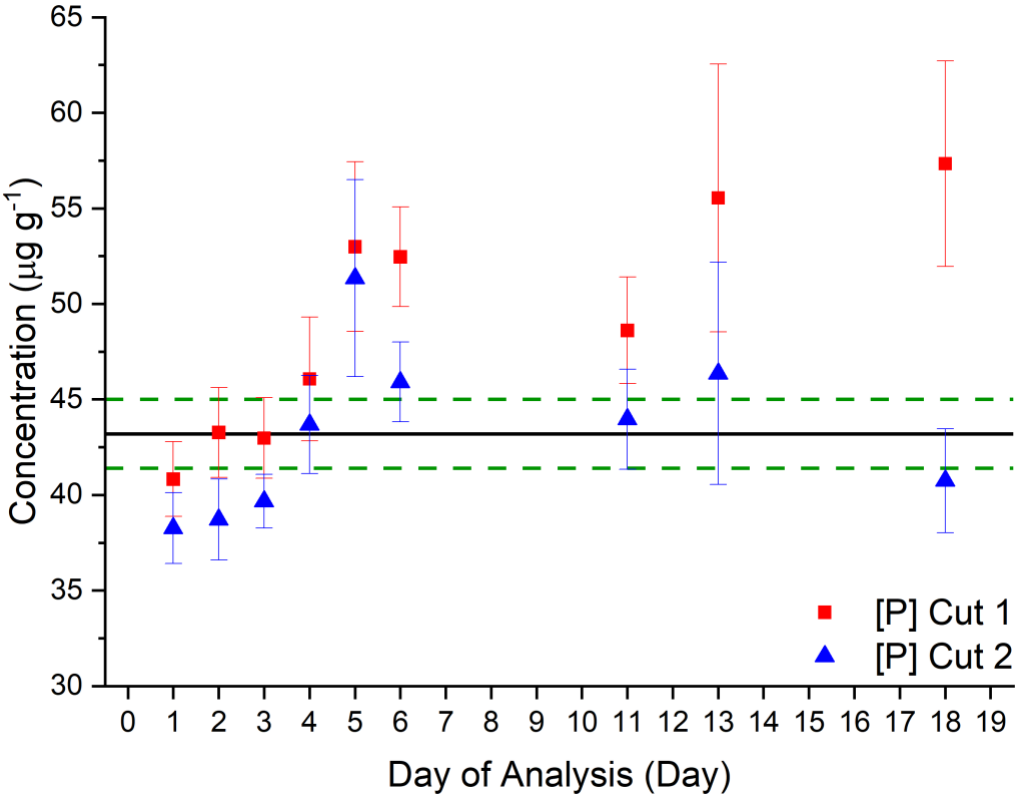


Figure 3.3 Concentration of P in two aliquots of Viognier with a solid line indicating certified value and dashed lines indicating uncertainty given by the CRM

were averaged, and a 7.0% difference from the expected value was determined (Table 3.2). The uncertainty of the average concentration of P contained the expected concentration which suggests accurate measurement of P in Viognier.

The pyrohydrolysis method was only able to detect SO_4 and concentrations were converted to S for comparison to the TQ ICP–MS method. The pyrohydrolysis technique determined a S concentration in the Feldspath QC of 1644 µg g^{-1}. This was much lower than the certified concentration of 5340 µg g^{-1}, and results in a 69% difference. For SO_4, poor recovery may be due to the conversion to the more volatile gasses. When examining the chromatograms, a peak attributed to SO_3 and SO_2 was identified. The SO_3 peak was also identified by IC after pyrohydrolysis on rock samples in a study performed by Shimizu *et al.*[145] The increased volatility of the gases, especially SO_2, may result in an inability for the scrubbers to capture all of the S. This second peak was factored in to the reported S concentration. While the pyrohydrolysis method resulted in the detection of a portion of the SO_4, no PO_4 was detected. The lack of PO_4 recovery may have been due the formation of a uranium phosphate during processing.

3.4.2 UOC Samples

All samples were analyzed in the same manner as the QCs. The measured concentrations were compared to previously reported data. One of these studies was an interlaboratory report that analyzed the Springfields sample collection of UOCs for trace elements, including P and S for some of the samples analyzed in the study.[158] The ultimate goal of the interlaboratory study was to assist the International Atomic Energy Agency in developing the ability to determine the origin of UOCs from trace elements. Participating

laboratories included the Los Alamos National Laboratory Atomic Weapons Establishment, , Lawrence Livermore National Laboratory, and the European Commission Karlsrhue. The Atomic Weapons Establishment reported P and S concentrations for some of the samples analyzed in the paper. They determined P concentrations by ICP–MS while S concentrations were determined by combustion IR. The S concentrations in this report were generally higher than what was determined in the pyrohydrolysis experiment, but lower than what was reported using the TQ ICP–MS method (Table 3.3). This may be due to a loss of S during the combustion of the sample in combustion IR.

Both the TQ ICP–MS and pyrohydrolysis methods were able to detect S in the UOC samples. As was demonstrated in the analysis of the CRM Feldspath, the recoveries using the TQ ICP–MS method were higher than the pyrohydrolysis method. The differences in S levels between the two methods varied greatly depending on the sample. For some samples the pyrohydrolysis method determined a S concentration that was 70% of what was determined by TQ ICP–MS, and for other samples the TQ ICP–MS determined a concentration that was over double what was determined by the pyrohydrolysis method (Table 3.3). This variability and lower S concentrations suggests that the pyrohydrolysis method was less effective in measuring S when compared to the TQ ICP–MS method. When comparing the TQ ICP–MS to results obtained in other studies there is little consensus on the S concentrations. In some cases, such as Ranger Mine, the concertation determined by the TQ ICP–MS was within the uncertainty of what was reported in another study, but the results were again generally higher from the TQ ICP–MS method (Table 3.3). The S concentration in Feldspath determined by the TQ ICP–MS were much closer

Table 3.3 S concentrations as determined by TQ ICP–MS and pyrohydrolysis (μg^{-1})

Sample	TQ ICP–MS	Pyrohydrolysis*	Other references
Mary Kathleen	17700 ± 1140	10093	
Radium Hill	2300 ± 150	1396.2	
¥Ranger Mine	2030 ± 180	810.74	1052 ± 572[130]
South Alligator	5060 ± 290	1172.8	3344 ± 148[158]
Blind River	4790 ± 290	1234.8	
Denison	12600 ± 700	762.58	
Dyno Mine	958 ± 110	575.26	564[162*]
Eldorado Uranium	7370 ± 490	2852.3	5427[162*]
Rabbit Lake	1570 ± 120	1085.5	1165[162*]
Faraday	1810 ± 130	2644.4	
Madawaska Mine	2020 ± 150	1553.6	1636[162*]
Milliken Lake	10600 ± 730	3257.7	
North Span	12200 ± 750	2448.0	
Rio Algom	10900 ± 660	4131.9	6190 ± 1598[158]
Stanleigh	14900 ± 860	8795.9	
Gunnar Mine	1070 ± 96	682.43	705[162*]
ESI USA	21000 ± 1200	11823	

¥ indicates that concentrations were converted to µg g U^{-1}* indicates that a value was originally reported as a concentration of SO_4 but was converted to a S concentration to compare with the TQ ICP–MS data.

to the certified value than the value reported by pyrohydrolysis. Given the result is closer to the expected value, the TQ ICP–MS data was utilized to identify any possible trends in S concentrations.

There were several trends or observations that could be identified when analyzing the TQ ICP–MS data for S. As mentioned previously, the TQ ICP–MS method did not detect any S in the Viognier QC which was expected as there was no S added to this CRM. Another observation was that Rio Algom had one of the higher S concentrations at 10900 ± 660 µg g^{-1} (Table 3.3). This was expected as the phase of this UOC contained SO_4 (Table 1), although it is still much lower in concentration than some of the other samples. There are some samples that had much higher levels of S including ESI USA (19677 µg g^{-1}) and Mary Kathleen (17670 µg g^{-1}) (Table 3.3). This demonstrates that S has been shown to be more valuable as a process indicator. While Rio Algom contained S in the phase, other samples with no S in the phase had higher levels.[154] This suggests that of the samples with higher levels of S, the analyte most likely originated from the leaching process, through the use of H_2SO_4 in the production of the UOC instead of the ore itself.

Similar to the S data, there was a wide range in P concentrations as determined by the TQ ICP–MS with values ranging from 23 ± 3.0 µg g^{-1} (Mary Kathleen) to 4230 ± 250 µg g^{-1} (Madawaska Mine). The ESI USA sample was much higher in P than the other samples with a concentration of 11600 ± 660 µg g^{-1}. Samples with higher levels of P are Dyno Mine, Faraday, and Madawska Mine which have a range of concentrations from 1202 ± 71 µg g^{-1} to 4230 ± 250 µg g^{-1} (Table 3.4) which originate in Bancroft, Ontario in Canada (Table 3.1). This region has been shown to have higher levels of P than other are

Table 3.4 Concentration of P in each sample as determined by the TQ ICP–MS (μg g^{-1})

Sample	TQ ICP–MS	Other references
Mary Kathleen	23 ± 3.0	
Radium Hill	201 ± 12	
Ranger Mine	119 ± 8.2	
South Alligator	533 ± 30	589 ± 29[158*]
Blind River	611 ± 38	
Denison	414 ± 23	
Dyno Mine	1202 ± 71	1140 ± 140[37]; 1046 ± 22[158*]
Eldorado Uranium	346 ± 22	
Rabbit Lake	87 ± 5.5	
Faraday	2050 ± 120	2190 ± 260[37]; 1600 ± 150[158*]
Madawaska Mine	4230 ± 250	4980 ± 600[37]; 3970 ± 254[158*]
Milliken Lake	265 ± 19	
North Span	244 ± 34	
Rio Algom	412 ± 24	488 ± 34[158*]
Stanleigh	556 ± 31	
Gunnar Mine	1100 ± 77	977 ± 15[158*]
ESI USA	11600 ± 660	

*Indicates that the original data was converted from μg g U^{-1} to μg g $sample^{-1}$ using the percentage of U in the sample.

in Canada (Elliot Lake or Saskatchewn).[37] The average P concentrations for the Eliot Lake samples are within the uncertainties previously reported, and all P concentrations reported by *Keegan et. al.* were determined by IC after a water leach extraction method.[37] It is difficult to separate impacts from phase and location of the sample on P content. There seems to be little impact from morphology alone as Milliken Lake, Stanleigh, Gunnar Mine, and ESI USA were all uranium amine oxide hydrates, but their P concentrations varied from 265 ± 19 μg g^{-1} to 11600 ± 660 μg g^{-1}. While the phase was the same, the locations of the samples varied, suggesting morphology may play a lesser role in contributing to the P content (Table 3.1 and 3.4). This method showed agreement with results obtained in other studies as the concentrations determined by TQ ICP–MS are similar to results obtained in other studies (table 3.4).

3.4.3 Uncertainty

The Guide to the Expression of Uncertainty in Measurement (GUM) Workbench software was utilized to calculate the contributions of each step in the TQ ICP–MS method to the overall uncertainty using a representative sample, South Alligator. The GUM Workbench is commercial software that performs Taylor expansions to calculate the percentage of the uncertainty contributed by each variable. For both P and S, the main contribution to the uncertainty was from the slope of the calibration curve and the second highest contributing factor was the variability in the measurements (Fig. 3.4). The uncertainty of the slope was determined by calculating the relative standard error (RSE) of the calibration using equation 1 where x_c = calculated concentration of the standard, x_i = measured concentration of the standard, n = number of points in the calibration, and p =

the number of values in the fitting equation. For future measurements of P and S the uncertainty could be improved through a more accurate calibration curve. Once the samples were in solution, this study aimed to keep sample preparation analysis times down as much as possible. If preparation time were less of a concern isotope dilution mass spectrometry could be used instead of an external calibration to reduce uncertainties.[138] The uncertainty in I concentrations came almost entirely from the variability in the measurements. This points to the unreliability of the I measurements. The Br data was also unreliable. This was most likely due to the use of acid washed labware in the method. The acid washed materials resulted in matrix blanks that were unusually high when compared to blanks analyzed using non-acid washed materials. In future Br analysis it may be necessary to use separate unleached materials.

$$\mathrm{RSE} = 100 \times \sqrt{\left(\sum_{i=1}^{n}\left[\frac{x_c - x_i}{x_i}\right]^2\right)/(n-p)} \quad (1)$$

3.5 Conclusions

The TQ ICP–MS and pyrohyrdolysis methods both allowed for the detection of S, but only the TQ ICP–MS allowed for the reliable detection of P in UOCs. The TQ ICP–MS method also allowed for much better recoveries of S than the pyrohydrolysis method as was demonstrated by both the Feldspath and UOC sample results. Both methods allow for the interference free detection of S, while the TQ ICP–MS method also allowed for interference free detection of P. More study is necessary to determine if Br or I can be detected in UOCs by these methods. The better recoveries and ability to measure P using the TQ ICP–MS method indicate this method performed better than pyrohydrolysis for the

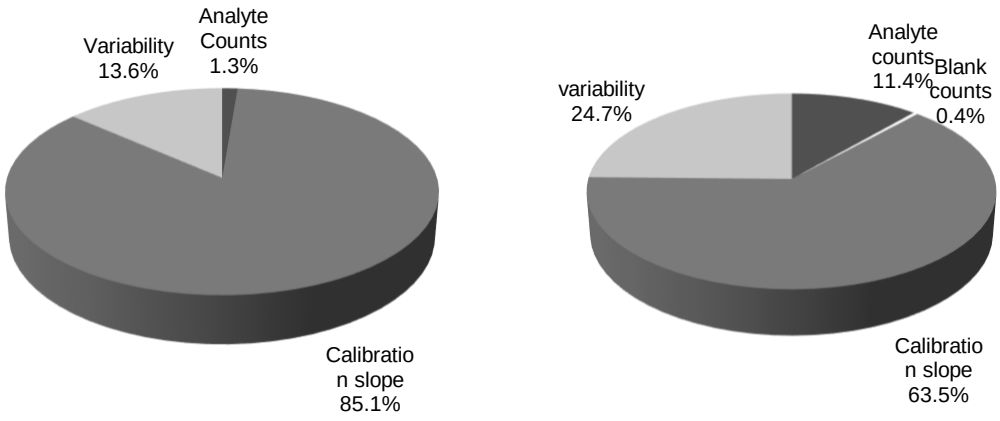


Figure 3.4 Variable contributions to the uncertainties in South Alligator of P (left) and S (right).

desired analytes. The concentrations of P and S determined by the TQ ICP–MS methods described here were in agreement with previously reported values providing an alternative method with shorter sample preparation times once they are in solution. The method also provides high sample throughput as more than 25 samples could be analyzed in a single run, and provides the ability to measure P and S by a quadrupole instead of high resolution ICP–MS.

Chapter 4

Method for the Separation of Hf-Lu, Rb-Sr, Nd-Sm, Pb and U

All experimental work and data analysis was performed by myself. All experimental design and editing was performed by myself as well as Alex Zirakpirav, Benjamin Manard, and Cole Hexel.

4.1 Introduction

Radiogenic isotope ratio systems are commonly utlized in the fields of both geochemistry and nuclear forensics. These systems have been applied to geologic material for use as a radiogenic tracer as well as in geochronology.[2, 163] Geochronolgy takes advantage of the relationship between parent and daughter atoms to determine an age of the material using the isotope ratio between the parent isotope and an isotope of the daughter.[164] Some systems of interst in geochronology are the isotope ratios of $^{176}Lu/^{177}Hf$, $^{87}Rb/^{86}Sr$, and $^{147}Sm/^{144}Nd$ and how they relate to isotope ratios of the daughter such as $^{176}Hf/^{177}Hf$, $^{87}Sr/^{86}Sr$ and $^{143}Nd/^{144}Nd$ respectively.[165] While these systems can be used to determine age when related to the daughter , other isotope ratios, like the daughter isotope ratios mentioned previously, can be used as tracers by comparing to region specific ratios.[163, 166, 167] Other systems include isotope ratios of individual elements such as Sm and Pb.[168-170] These systems for radiogenic tracing have been applied to a wide array of geologic materials, and they have also been applied to nuclear material such as uranium ore concentrates (UOCs).

Regarding the Nd isotopic system in UOCs, Krajko et al. determined the ratio of $^{143}Nd/^{144}Nd$ by multicollector - inductively coupled plasma - mass spectromotry (MC-ICP-MS), and compared these results determine any trends in the data. They found that the $^{143}Nd/^{144}Nd$ isotope ratio varies widely in UOCs, but some deposit types, such as intrusive

or quartz pebble conglomerate, have more specific ratios while other deposit types have greater variation.[168] Another study examined both the Pb and Sr isotope ratio systems in UOCs and found that there was extreme variation in the Pb isotope ratios.[171] This variation was most likely due to the inhomogeneity of the ore, as well as the contribution of natural Pb during the milling process. The $^{87}Sr/^{86}Sr$ ratio was found to vary less between replicate samples and demonstrated a relationship with the deposit type in some cases.[171] This study and others all demonstrate the need for analyzing multiple isotpic systems in the same sample to gain a better picture of the sample.[172]

Before these isotope ratios can be determined, separations must be performed to isolate them from potential isoabaric interferences.[173] As such, it is important to separate Lu-Hf, Rb-Sr, and Sm-Nd, since each of these isotopic systems contains isobaric interferences such as ^{176}Hf and ^{176}Lu. Lead must be isolated from Hg due to isobaric interference at ^{204}Pb and from Tl so that the $^{205}Tl/^{203}Tl$ can be used as an internal mass bias correction during analysis.[174] Separation of U from the other elements is necessary because the great excess of U in UOCs would have a negative impact on transmission of the other analytes.[175] The U content could also be used in U-Pb dating as well as to determine the grade (%U) of a UOC.[167, 169] There have been many separation methods developed for the systems of interest mentioned previously, but few of these methods are concerned with the ability to analyze all of these elements in one sample.[76, 176, 177]

One such study concerned only with the separation of Hf and Lu utilized a cation resin, AG50W-x8, to isolate Lu and TEVA spec resin to separate Hf from the rare earth elements (REE).[76] The study also determined that the REE cut could be retained for

separation of Nd and Sm using a di-(2-ethylhexyl)phophoric acid (HDEHP) extractant.[76] Another study developed a separation method that involved all elements of interest in this study, in addition to La, Ce and Th.[178] While this method does account for the elements of interest, it requires a multitude of columns and resins as well as the coupling and decoupling of some. Furthermore, it also requires complex solutions such as ascorbic acid. A simpler method was introduced by Yang et al. to separate Hf-Lu, Rb-Sr, and Nd-Sm. The HDEHP extractant Ln spec resin was first utilized to separate Hf and Lu. The other elements of interest for the study passed through this column and were loaded onto the cation exchange resin AG50W-X12 in order to separate Rb and Sr while the rest of the eluted matrix was loaded onto another Ln spec resin column to separate Nd and Sm.[179] While the method developed in the study was less complex, it did not include Pb or U, which are both elements of interest in the method proposed by the study described below.

The goal of this study was to develop a combined separation method for Hf, Lu, Rb, Sr, Nd, Sm, Pb and U. This was performed by adapting the Yang et al. separation method so that a similarly simple method could be implemented to include the separation of Pb and U along with Hf-Lu, Rb-Sr, and Nd-Sm using 2 mL polypropylene columns. Ideally, there would be few columns and the separation would be sequential with no aliquots taken for other columns to keep recoveries high. This can be especially important for cases such as Hf where the content in the UOC may be sample limiting.[180] After development and optimization of the method, elution profiles and column yields for each of the elements of interest were produced to determine the validity of the method.

4.2 Experimental

4.2.1 Materials and Reagents

All stock acid solutions were diluted using ASTM type I water (18.2 MΩ cm) from a Thermo Scientific (Waltham, MA, USA) Barnstead GenPure xCAD Plus Ultra-Pure water purification system. Samples and standards were prepared in 2% nitric acid (HNO_3) that was diluted from a Fisher chemical (Hampton, NH, USA) Optima grade stock. Various concentrations of hydrochloric acid (HCl) solutions were used as eluents in the columns all diluted from a Fisher ACS plus grade stock. Diluted solutions of Fisher Optima grade hydrofluoric acid (HF) and hydrogen peroxide (H_2O_2) were also utilized in the separation. Columns 1, 2 and 4 utilized individual prepacked polypropylene columns with 2 mL Ln spec resin and a 100-150 μm particle size purchased from Eichrom (Lisle, IL, USA). Column 3 used 2 mL of analytical grade Biorad (Hercules, CA, USA) AG 50W-X12 resin with a mesh size of 200-400 in a polypropylene column.

All samples and standards were prepared volumetrically from 1000 μg mL^{-1} single element stocks of Hf, Lu, Pb, U, Ti, Zr, Yb, Nd, Sm, Rb, and Sr purchased from High Purity Standards (Charleston, SC, USA). Simulated samples were prepared such that they could be loaded onto column 1 with a 10 μg mL^{-1} concentration for each analyte except for U, which was 50 μg mL^{-1} to simulate a nuclear material sample. All acids were stored in teflon containers, and separation cuts were collected in polypropylene beakers. Each cut was dried down on a hot plate at 115 °C to remove the matrix and diluted with 2% HNO_3 for analysis, or with the solution required to load on the next column in the sequence. In addition to Hf, Lu, Ti, Rb, Sr, Nd, and Sm, Yb and Zr were also included in this study to

ensure the method performed as expected during the optimization of this procedure. Adjustments were made to account for the specific circumstances of this study including differing sample load concentration, columns, and the additional separation of Pb and U.

4.2.2 Column 1: Ln Resin

After the preconditioning of column 1 the sample was loaded in 1.5 M HCl to allow for the immediate elution of Pb, Rb, Sr, Sm and Nd. Additional 1.5 M HCl was then passed through the column to remove the desired analytes from the column. The Pb, Rb, Sr, Sm and Nd cut was evaporated on a hotplate and brought up in 1.5 mL of 2.5 M HCl to be loaded onto column 3 (Fig. 4.1). The U, Hf, Zr, and Ti fraction was then stripped from the column using 2 M HF and dried down to be brought up in 4 M HCl + 0.5% H_2O_2 for column 2 (Fig. 4.1). The remaining fraction of Yb-Lu was first eluted using 4 M HCl, but 6 M HCl was utilized as well to ensure complete removal from column 1. The Yb-Lu cut was dried down and diluted with 2% HNO_3 for analysis.

4.2.3 Column 2: Ln Resin

After the conditioning of column 2, the Ti, Hf, Zr, and U fraction obtained from column 1 was loaded onto the column in 4 M HCl + 0.5% H_2O_2 (Fig 4.1). Titanium was eluted immediately and additional 4 M HCl + 0.5% H_2O_2 was added to completely strip Ti from the resin. This was evaporated and brought up in 2% HNO_3 for analysis. Titanium was separated to eliminate possible impacts on the transmission of Hf during analysis.[176] The Hf-Zr fraction was then removed from the resin using 0.1 M HCl-0.29 M HF. The Hf-Zr cut was eluted with enough volume to allow for the stripping of Hf-Zr while the U

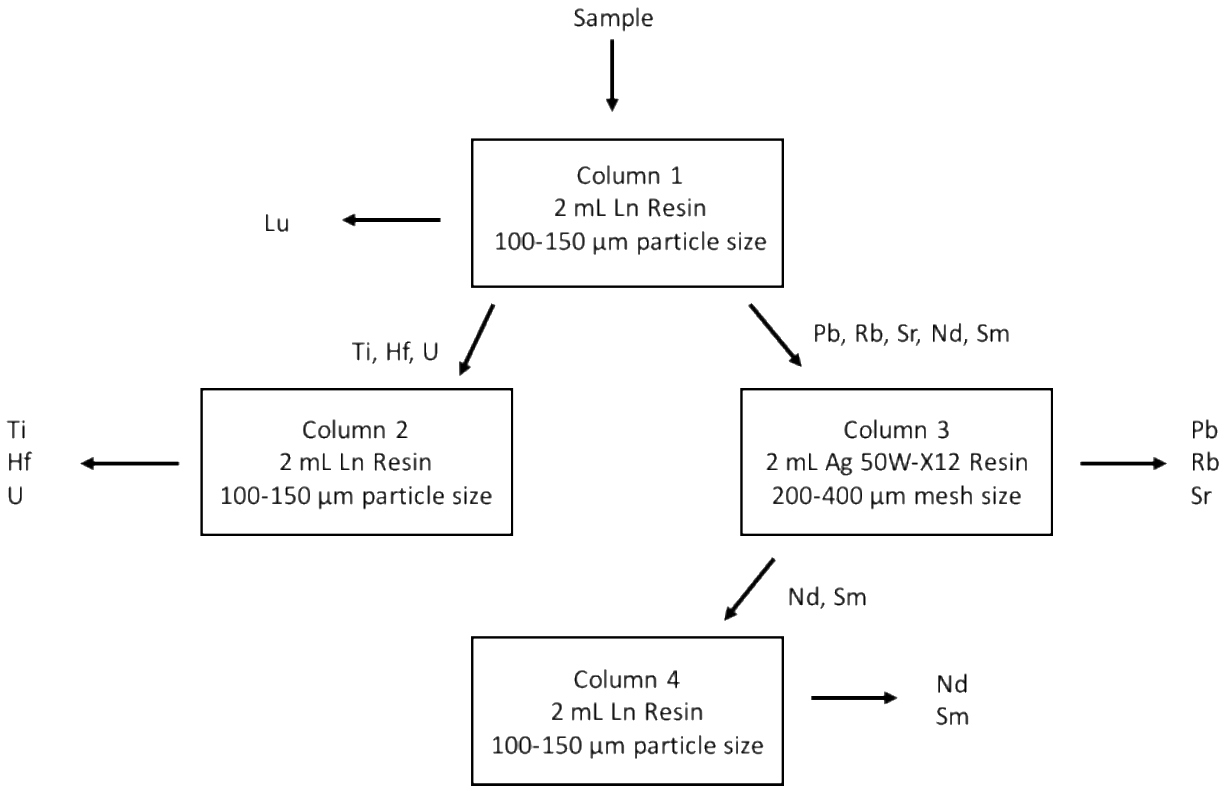


Figure 4.1 Flow chart demonstrating the developed separation method.

fraction remained on the column. The U could then be eluted using 2 M HF. Both the Hf-Zr and U fractions were dried down and diluted with 2% HNO_3 for analysis.

4.2.4 Column 3: AG 50W-X12 Resin

After the conditioning of Column 3 with 2.5 M HCl, the Pb, Rb, Sr, Nd and Sm fraction that was collected in column 1 was loaded onto the column in 2.5 M HCl (Fig. 4.1). This allowed for the immediate elution of Pb, and additional 2.5 M HCl was passed through the column to removal of any residual Pb. This was then evaporated and brought up in 2% HNO_3 for analysis. After the 2.5 M HCl, 5 M HCl was added to remove Rb and Sr sequentially. Each of these fractions were dried down and diluted in 2% HNO_3 for analysis. Following elution of Sr, the Nd and Sm fraction was eluted utilizing 6 M HCl. This was dried down and diluted with 0.14 M HCl for loading onto column 4 (Fig. 4.1).

4.2.5 Column 4: Ln Resin

After conditioning the Ln spec resin with 0.14 M HCl, the Nd and Sm fraction collected from column 3 was loaded onto the column in 1.5 mL of 0.14 M HCl. No Nd or Sm was eluted upon addition. The concentration of the acid passed through the column was then increased to 0.2 M HCl to elute the Nd fraction. Samarium was then stripped from the column with 0.4 M HCl. Each of these fractions were evaporated and brought up in 2% HNO_3 for analysis.

4.2.6 Instrumentation

All results for the optimization, elution profiles, and column yields were obtained through external calibration. An Agilent Technologies 5110 inductively coupled plasma optical emission spectrometer (ICP-OES) (Santa Clara, CA, USA) was utilized during

optimization of the method to quantify each analyte at the μg mL^{-1} level. The ICP-OES used a quartz nebulizer and cyclonic spray chamber, and the wavelength at which each element was measured is listed in Table 4.1. A Thermo Scientific iCAP RQ-ICP-MS (Bremen, Germany) was then used to determine column yields and elution profiles for each analyte. The RQ-ICP-MS utilized a quartz cyclonic spray chamber with peltier cooling, and a PFA nebulizer to aid in the measurement of each m/z listed in Table 4.1.

4.3 Results and Discussion

4.3.1 Optimization

4.3.1.1 Column 1

Initially, column 1 was utilized to attempt to elute Pb, Ti, Lu-Yb, Hf-Zr, and U in individual cuts while eluting Rb, Sr, Sm, and Nd in another cut to be loaded onto the next column. This would have allowed for the separation to remain at only three columns and similar to the Yang et al. method. The first attempt to isolate Pb in column 1 in 1.5 M HCl showed 94 ± 0.93% recovery, but the Rb, Sr, Nd and Sm also eluted in this fraction. Since Pb eluted with the other analytes that were loaded onto column 3 in step 17 of the separation, adjustments to the column 3 procedure were required to account for the Pb separation (Table 4.2). The issue that required the most significant changes during the optimization of this method involved the separation of U, Hf, and Ti.

One study suggested utilizing dilute HCl-HF media to elute Hf in HDEHP such as Ln resin.[178] This did allow for the elution of Hf in the desired fraction, but 94 ± 0.52% of Ti was also recovered in this fraction. Lutetium eluted after this, but 17 ± 0.60% of the U was also recovered in this fraction which could have an impact on transmission when

Table 4.1 Each element analyzed listed with the wavelength and m/z monitored.

	ICP-OES	RQ-ICP-MS
Element	Wavelength (nm)	m/z
Hf	277.336	178
Pb	220.353	208
Sr	216.596	88
Nd	378.425	142
Sm	442.434	152
U	294.192	238
Lu	261.541	175
Rb	780.026	85
Ti	308.804	48
Yb	211.667	172
Zr	267.865	90

Table 4.2 The optimized separation method.

Step	Description	Acid	Volume (mL)	Collect
		Column 1		
1	Prepare	6 M HCl + 0.2 M HF	60	matrix
2	Precondition	1.5 M HCl	20	matrix
3	Load sample	1.5 M HCl	5	Pb, Rb, Sr, Nd, Sm
4	Elute	1.5 M HCl	20	Pb, Rb, Sr, Nd, Sm
5	Elute	2 M HF	20	U, Hf Zr, Ti
6	Elute	4 M HCl	20	Yb-Lu
7	Elute	6 M HCl	20	Residual Yb-Lu
		Column 2		
8	Prepare	6 M HCl + 0.2 M HF	60	matrix
9	Precondition	4 M HCl + 0.21 M H_2O_2	10	matrix
10	Load sample	4 M HCl + 0.21 M H_2O_2	5	Ti
11	Elute	4 M HCl + 0.21 M H_2O_2	20	Ti
12	Elute	0.1 M HCl-0.29 M HF	15	Hf-Zr
13	Elute	2 M HF	20	U
		Column 3		
14	Prepare	6 M HCl	25	matrix
15	Wash	H_2O	5	matrix
16	Precondition	2.5 M HCl	4	matrix
17	Load sample	2.5 M HCl	1.5	Pb
18	Elute	2.5 M HCl	5	Pb
19	Elute	5 M HCl	3	Rb
20	Elute	5 M HCl	5.5	Sr
21	Elute	6 M HCl	20	Nd, Sm
		Column 4		
22	Prepare	6 M HCl	10	matrix
23	Wash	H_2O	15	matrix
24	Precondition	0.14 M HCl	15	matrix
25	Load sample	0.14 M HCl	1.5	matrix
26	Elute	0.14 M HCl	10	matrix
27	Elute	0.2 M HCl	28	Nd
28	Elute	0.4 M HCl	16	Sm

measured my ICP-MS. Given the difficulty in separating Hf from U and Ti without impacting the other elements, column 1 was split into two columns as is seen in Table 4.2. This allowed for the isolation of what was to be loaded on column 3, as well as separation of Lu from Hf and U. To start, only 5 mL of 2 M HF was utilized in step 5, but this resulted in poor separation of U as 88 ± 0.76% of Hf was recovered in the correct fraction, but 66 ± 0.56% of the U was in the Lu fraction (Table 4.2). This was addressed by increasing the volume of 2 M HF to 20 mL, resulting in a recovery of the U, Ti, and Hf in the desired fraction (step 5) which could be loaded onto Column 2.

4.3.1.2 Column 2

Given that the optimization of column 1 had already demonstrated Ti and Hf will elute together in dilute HCl-HF, and U, Hf and Ti will all elute in more concentrated HF. Titanium was first eluted using 4 M HCl with dilute H_2O_2. This allowed for the method to avoid the use of a more complex solution in the Ti separation such as ascorbic acid. The Hf could then be eluted separate from U using the 0.1 M HCl-0.29 M HF solution. Originally 10 mL was used to elute Hf. While no Hf was seen in other aliquots, only 89 ± 0.76% was recovered so this elution volume was adjusted to 15 mL to improve recovery. This resulted in a recovery of 94 ± 1.06%. The original volume used to elute U in step 13 was 5 mL, but this resulted in only a 5.6 ± 0.036% recovery. No U was seen in other fractions, indicating the remainder of the U was on the column. The volume in step 13 was then increased to 10 mL and 20 mL to demonstrate that U could be removed from the column. This resulted in a 7.4 ± 0.041% and 96 ± 0.58% recovery, respectively.

4.3.1.3 Column 3

After the optimization of column 1 it was clear that Pb would need to be loaded onto column 3 in addition to Rb, Sr, Nd and Sm. The first run of column 3 demonstrated that Pb could be eluted on the AG 50W-X12 resin using 2.5 M HCl. To ensure recovery of the Pb 9.5 mL of 2.5 M HCl was originally used to elute Pb including the sample load volume. While this did result in recovery of the Pb, 19 ± 0.38% of the Rb was also recovered in the Pb fraction. The amount of 2.5 M HCl used to elute Pb was adjusted to improve recoveries in the Rb fraction. Lowering the elution volume of the 2.5 M HCl to 6.5 mL allowed for recovery of Pb while also resulting in no recovery of Rb. Once the Pb recovery was established changes were also required to optimize the separation of Rb and Sr on the resin while also recovering enough Nd and Sm to load on the next column.

Initially, 4 mL of 5 M HCl was used in step 19 followed by 7 mL of 5 M HCl in step 20 (Table 4.2), but this led to many issues as about 3.5 ± 0.16% of the Sr was recovered in the Rb fraction. Also, about 25 ± 0.63% and 25 ± 0.17% of the Nd and Sm was recovered in the Sr fraction. While this does not result in any isobaric interferences, losing that level of Nd and Sm before loading on column 4 could have an impact on the ability to make reliable measurements in any sample with low levels of Nd and Sm. The volumes were adjusted to 3.5 mL and 5 mL for steps 19 and 20 respectively. This improved the separation between Sr and Nd-Sm as only 13 ± 0.32% of the Sr was found in the Nd-Sm fraction, but 11 ± 0.14% of the Rb was found in the Sr fraction. The volumes were then modified to 3 mL and 5.5 mL. This allowed for separation of Rb and Sr while minimizing the loss of Sr

in the Nd-Sm cut to only 10 ± 0.64%, and the loss of Nd-Sm in the Sr cut to 2.6 ± 0.86% and 3.7 ± 0.83%, respectively.

4.3.1.4 Column 4

The optimization of column 4 was unique in that the most drastic changes made came in the conditioning and matrix eluting steps and not in the separation itself. Initially, the column was preconditioned with 4 mL of 0.25 M HCl. No matter what followed this step about 75% of the Nd and Sm would elute in the fraction after the sample was loaded. This was occurring because the 4 mL of preconditioning was not enough to adequately condition the column. To address this, the preconditioning and sample load concentrations were decreased to 0.14 M HCl and the volume of the preconditioning step was increased to 15 mL. This allowed for better conditioning of the column, and allowed for neither Nd or Sm to come off the column when the sample was loaded on. The volume of 0.2 M HCl used to elute Nd was also increased from 24 mL to 28 mL because 7.0 ± 0.062% of the Nd was eluting in the Sm fraction before this adjustment.

4.3.2 Elution Profiles

After initial optimization of the separation method using the ICP-OES, an ICP-MS was then used to aide in the development of elution profiles. The ICP-MS was necessary due to the heightened sensitivity to determine smaller differences in the amount of analyte eluted in each fraction. The elution profiles allowed for a better picture of the performance of the separation method. They were developed by collecting smaller repeated aliquots from each fraction. Each fraction was broken up into 2 mL cuts for columns 1, 2, and 4 while fractions for column 3 were broken up into 1 mL aliquots, except for the elution of

Nd and Sm which was broken up into 2 mL cuts (Fig. 4.1). The aliquots were then dried down and brought up in 2% HNO_3, such that the maximum concentration in any aliquot could by 20 ng mL^{-1}, for analysis by ICP-MS. The elution profiles were then produced by relating the percent recovery of each aliquot to the total volume passed through the column at that point.

The elution profile for column 1 (Fig. 4.2a) demonstrated good separation in all the desired steps. While Lu is similar to Nd and Sm in that they are both trivalent, the elution profile indicates the Lu is bound much more tightly to the resin (Fig. 4.2a). This is because the binding strength is inversely proportional to the size of element.[181] Since the rare earth elements undergo contraction across the periodic table, Lu would be much smaller than Nd and Sm and therefore much more tightly bound to the resin.[182, 183] In step 5, it appears that the Hf and U are almost separated if collection is stopped after 30 mL. While only about 3% of the U was found in the same aliquot as one with Hf the scale is important. For any UOC sample, about 1 mg of U will be loaded on the column and Hf in that sample will be at the ng level per gram of U. This indicates that even with only 3% of the U in this fraction, U will still be in significant excess over the Hf and further separation is necessary.

The elution profile of column 2 (Fig. 4.2b) demonstrated clear separation among analytes of interest. Zirconium and Hf were expected to elute in the same fraction, and Zr should have no impact on the measurement of Hf.[179] As in column 2, the elution profile of column 3 (Fig. 2c) demonstrated separation of elements that impact the measurement of

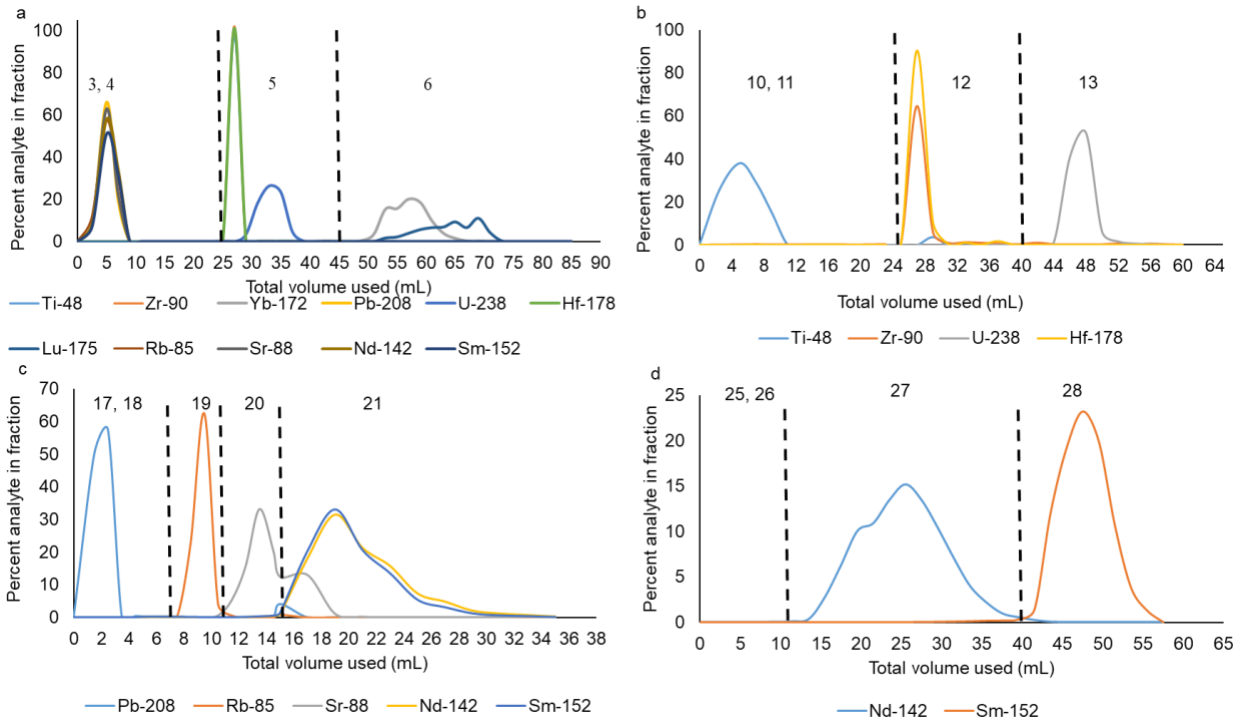


Figure 4.2 Elution profiles for each of the four columns with a-d representing columns 1-4, respectively. Step numbers from Table 4.2 are listed.

the desired analyte. About 12% of the Sr does elute in the Nd-Sm fraction (Fig. 4.2c). This should have no impact on the measurement of isotope ratios for Sr, Nd, or Sm. If a concentration for Sr is needed, then a cleaner separation of Sr and Nd-Sm may be necessary. The elution profile for column 4 (Fig. 4.2d) indicated a clear separation of Nd and Sm. No Nd or Sm eluted before step 27 where Nd was the desired analyte (Table 4.2).

4.3.3 Column Yields

After the elution profiles were developed, column yields were obtained by running the complete separation method without breaking up each fraction into separate aliquots. This was repeated three times so that the column yields could be obtained in triplicate. Each fraction was dried down and diluted in 2% HNO_3 such that the concentration for each analyte should be 5 ng mL^{-1}. The yield was determined by dividing the actual amount of analyte eluted in ng by the expected amount of analyte.

The column yield for each element was determined to further validate the separation method (Fig. 4.3). Separations were performed in triplicate to analyze the reproducibility of the method as well. The yields for column 1 (Fig. 4.3a) were all between 90 and 100% except Zr which was between 80 and 90%. Column 1 also demonstrated reproducibility as all three runs for each analyte were withing 10%. The yields for column 2 (Fig. 4.3b) were excellent as well as all elements of interest were between 90 and 100%. This also showed excellent reproducibility with all runs for each analyte falling within 10%. Column 3 (Fig. 4.3c) demonstrated yields again between 90 and 100% for Pb, Nd, and Sm. While those recoveries were all excellent, the recoveries for Rb and Sr were lower, 65-80% for Rb and 75-85% for Sr (Fig. 4.3c). This is lower than the yields for the other

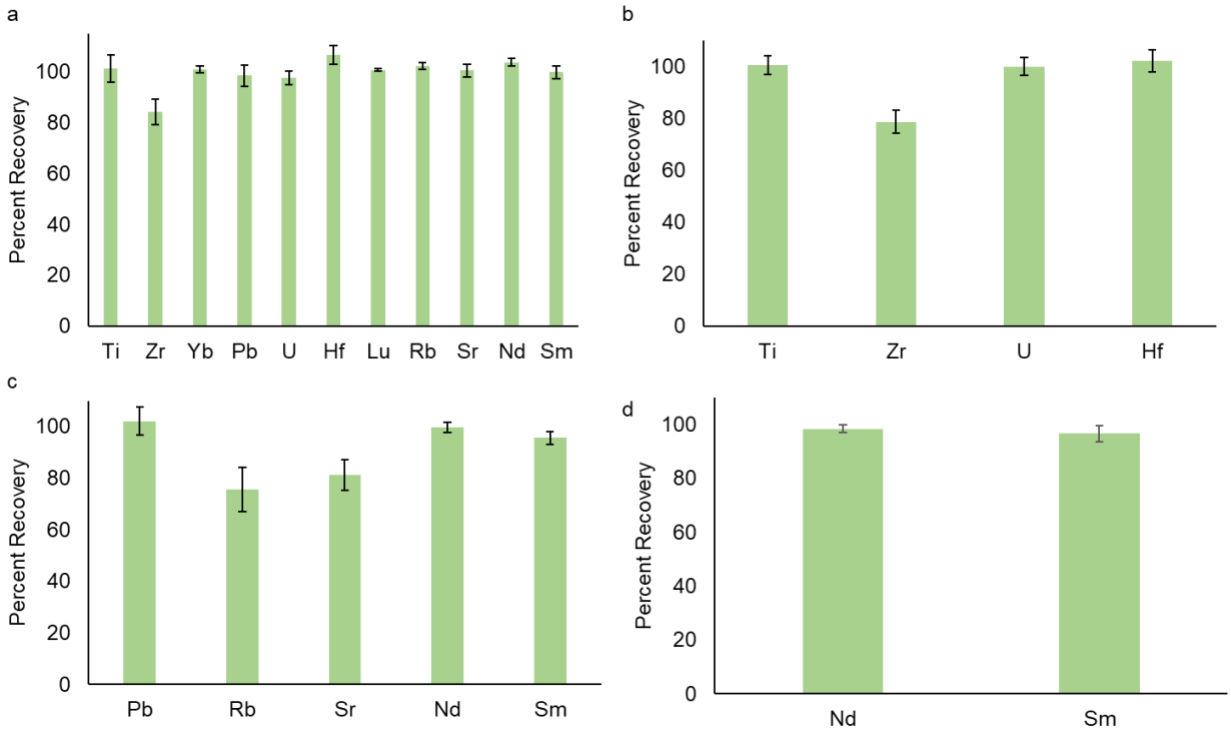


Figure 4.3 Column yields shown for each of the four columns with a-d representing columns 1-4 respectively.

analytes of interest, but this yield should be more than substantial for measuring isotope ratios of Sr. The reproducibility of column 3 varied slightly more than that of columns 1 or 2 as Rb ranged in recoveries by 17%. All other elements for column 3 fell in the 10% range. Column 4 (Fig. 4.3b) demonstrated higher recoveries than column 3 did for Rb and Sr as the yields for Nd and Sm were both between 90 and 100%. The reproducibility of column 4 was excellent as Nd recoveries varied by only 3% while Sm varied by only 6%.

4.4 Conclusions

Efficient separation techniques are required to accurately determine isotope ratios free of isobaric interferences that could result in inaccurate interference corrections. The developed separation method allows for the separation of Hf-Lu, Rb-Sr, Nd-Sm, Pb and U. Titanium was also separated from Hf as Ti may negatively impact the measurement of Hf by MC-ICP-MS. Separation is achieved through sequential application of Ln an AG resin. The separation uses a limited variety of acids and avoids the use of complex acids such as ascorbic acid or HCl or HNO_3 on their own. The optimized separation method demonstrated removal of isobaric interferences, and the determined column yields were high. A dissolved UOC CRM (CUP-2) was analyzed using the separation to determine the applicability of this method to high U samples. Uranium was included in this separation due to the impact the excess U can have on the measurement.

Chapter 5

Titrations for the Determination of Stability Constants for the Extraction of Nd in Ionic Liquid using Various Ligands and the Determination of Proton Affinity Distributions of Ligands

All experimental work described in this chapter was performed by myself. The stability constant determinations were also performed by myself. Calculation of the proton affinity distributions was performed by Bishnu Thapaliya. Synthesis of everything but the $Nd(NTf_2)_3$ was performed by Chi-Linh Do-Thanh. All experimental design was performed by myself and Sheng Dai.

5.1 Introduction

The research interest in ionic liquids has continued to rise in recent years due to the numerous exploitable advantages they provide. Some of these advantages include thermal and electrochemical stability, as well as a tunable structure.[184-186] This electrochemical stability and thermal stability has allowed for ionic liquids to be increasingly used in the development of electrochemical devices as well as sensors.[187-190] Ionic liquids are also extremely tunable in that the physicochemical properties can be altered by adjusting what cation is paired with what anion. Often, the physicochemical properties of these ionic liquids can be predicted using computational properties before they are even synthesized.[191, 192] It is this electrochemical and thermal stability along with the versatility of adjusting both cation and anion in the design of ionic liquids that makes them an ideal solvent in the liquid-liquid extraction of metals.[193-195]

One aspect that makes ionic liquids ideal for the liquid-liquid extractions of metal is their ability to dissolve ligands that are not soluble in water. They also are thermally stable which means there is no loss of solvent which can eliminate some safety concerns due that otherwise would be present due to the volatilization of traditional organic solvents.[196, 197] These properties have also allowed ionic liquids to gain prominence as a

possible use for solvent extraction of rare earth elements in the nuclear fuel cycle.[198] Specific ionic liquids can be developed that will successfully dissolve rare earth oxides.[199] Once dissolved in ionic liquids, a ligand could be added to extract specific rare earth elements.[200, 201]

The extraction of metals, especially rare earths, in ionic liquids using ligands has grown in popularity in recent years. There are many different combinations of ionic liquid and ligand that can be utilized in the extraction of the same metal.[202-204] For example, one study was able to extract Nd from an aqueous acidic phase using various ionic liquids where the anion was always octylphosphite but the cations used included 1-octyl-1-methyl piperidinium, morpholinium and pyrrolidinium.[205] While another study by Freiderich et al determined they were able to dissolve the Nd in the ionic liquid 1-butyl-3-methylimidazlium bis(trifluoromethylsulfonyl)imide ($BMIM^{+}NTf_2$) and perform a liquid-liquid extraction with the ligand N, N-dimethylacetamide (DMA).[206] In both cases the liquid-liquid extractions were succeful. When determining which ionic liquid or ligand to use it may come down to what extraction is desired as well the other elements present.[207, 208] When determining which ligand to use in a certain ionic liquid to extract a specific metal one useful tool to differentiate between the possible methods is through the calculation of the stability constant between the ligand and the metal.

The calculation of stability constants for metal-ligand systems has been performed for many years. The stability constant is important as it indicates the strength of the reaction between the metal and the ligand. Also, the stability constant can be utilized in determining the speciation of the metal-ligand system as well as the concentration of each species at

equilibrium.[209-211] The stability constant can be calculated using the equilibrium concentrations of the metal and ligand, as well as the equilibrium concentration of the metal-ligand complex as is demonstrated in equation 5.1.[212]

$$\log\beta_n = \frac{[M(L)_n]}{[M][L]^n} \tag{5.1}$$

When measuring these complexes by UV-Vis spectroscopy the equilibrium concentration of the metal-ligand complex can be calculated by question 5.2 where A is the absorbance, $\in$ is the molar absorptivity, and *l* is the path length of the cell.

$$A = \in l\ [M(L)_n] \tag{5.2}$$

Unfortunately, the equilibrium concentration of the metal and ligand are both unknown. For this reason, more advanced calculations are necessary. The stability constant could be calculated by hand if several assumptions are made that will negatively impact the results. Instead, curve fitting software can be used on spectra collected during a spectrophotometric titration to calculate the stability constant of the complexes by non-linear least square regression.[213-216]

In addition to the calculation of the stability constant, the determination of the proton affinity distribution of the ligand can also be a useful tool in the determination of proper experimental conditions for the use of the specific ligand in a liquid-liquid extraction.[217, 218] By understanding the distribution of proton affinities the experimental conditions could potentially be altered so that at a certain pH the ligand could bind to a metal while releasing that metal if the pH is adjusted. This would require an understanding of the important pKas of a ligand.[219] At higher pKas the proton is more tightly bound to the ligand. If the proton is more tightly bound then the metal being extracted would be

more tightly bound as well. Then by understanding the pKa distribution the pH could be lowered to deprotonate the ligand or strip the metal from the ligand.[220-222] In order to calculate the proton affinity distribution of the ligand a potentiometric titration is necessary. This requires the collection of pH and titrant volumes that can be converted into an isotherm before calculating the proton affinity distribution from curve fitting the isotherm.[223]

This work aimed to use both potentiometric and spectrophotometric titrations to better understand certain ligands as well as their interactions with Nd^{3+} in $BMIM^{+}NTf_2^{-}$. This was done by developing methods for the potentiometric and spectrophotometric titrations. Models were then developed and utilized for the calculation of the proton affinity distributions using potentiometric titrations as well as the stability constants of the metal-ligand complexes using the spectrophotometric titrations. The proton affinity distributions and metal-ligand complexes involving specific ligands were examined together when possible.

5.2 Experimental

5.2.1 Potentiometric Titrations

An aqueous solution of 0.001 M sodium nitrate ($NaNO_3$) was first prepared using deionized water. This was used as the electrolyte solution in each titration. The first titration was of citric acid as this has been performed before.[219] So validation of the method could be achieved. A 0.0164 M citric acid solution was prepared in 50 mL of sodium nitrate. In each subsequent titration the goal concentration of the species being titrated was 0.015 M This was titrated with 0.1 M standardized sodium hydroxide (NaOH) solution

purchased from Fischer Scientific. The titration was performed using a Mettler Toledo G20 compact auto titrator. Each titrations was carried out over a pH range of 2-12 because outside of this range the buffer capacity of water begins to fail. Increments of titrant added varied from 1 µL to 200 µL. Data points collected included both the pH and the volume of titrant added, and the amounted of data points collected ranged from 400-550.

In addition to the citric acid titration, a titration following the same procedure listed above was performed using a 6-carboxyl-1, 2-hydroxypyridinone (HOPO) ligand. In this case the carboxyl HOPO ligand was again dissolved in 50 mL of the 0.001 M $NaNO_3$ solution for a concentration, and the ligand solution was titrated with the NaOH solution. A potentiometric titration was also performed on 1-hydroxy-6-N-octylcarboxamido-2(1H)-pyridinone (octyl-HOPO). Since this ligand is not soluble in water, it was first dissolved in 10 mL of the ionic liquid $BMIM^+NTf_2^-$. After being dissolved in ionic liquid, 40 mL of the 0.001 M $NaNO_3$ solution was added to bring the total volume to 50 mL. This was again titrated with the standardized 0.1 M NaOH solution. After each of these titrations the isotherms were calculated as demonstrated by Contescu et al.[223] These isotherms were then loaded onto a model developed in MATLAB which applies curve fitting to the isotherm to determine the pKa distribution of the ligand.

5.2.2 Spectrophotometric Titrations

All titrations were performed with an Ocean Optics USB2000+ spectrometer connected to a DH-mini Ocean Optics light source containing both a deuterium and halogen lamp. All titrations were performed at 120 ℃ by using a hotplate and sand bath to maintain temperature of vessel. In each case the vessel was pumped in and out of the

cuvette using a peristaltic pump. This pumping allowed for each titration measurement to be collected at a specific temperature rather simply taking aliquots from the heated titration vessel and placing them in a room temperature cuvette. Pumping of the solution was paused before each collection of a spectra to avoid the presence of air bubbles impacting the spectra. In each case the goal of the titration was to perform a liquid-liquid extraction of Nd with the ligand.

The spectrophotometric titration method was developed using the ligand DMA because stability constants for this ligand in $BMIM^{+}NTf_2^{-}$ have already been determined by Freiderich et al.[206] This allowed for a validation of the method prior to use on other less studied ligands for the extraction of Nd^{3+}. For each titration $Nd(NTf_2)_3$ dissolved in $BMIM^{+}NTf_2^{-}$ was titrated with the various ligands. In the case of DMA the ligand was diluted in the ionic liquid so that the concentration was 6.904 M. The Nd^{3+} concentration used was 0.1287 M. Additions of DMA were made to the Nd^{3+} so that the ratio of Nd^{3+}:DMA increased by 0.25 after each addition, starting with a 1:0 ratio. After each addition of DMA a UV-Vis Spectra was collected. A 10 minute equilibration time was allowed before the collection of the spectra to allow for the ensure the reaction was finished. A titration was judged to be complete when there was no change in the spectra after enough addition in increase the ratio by 2. For example, moving from a 1:5 ratio to a 1:7 ratio.

After each titration the spectra were utilized to calculate the stability constants of the metal-ligand complexes using non-linear least-square regression by building models in the software HypSpec2014.[224] In HypSpec you can indicate the reactants and what products

you believe they will form as indicated in figure 5.1. You are then required to estimate a stability constant for each of the proposed products and indicate the initial concentration of both the Nd^{3+} as well as the titrant (Fig. 5.1). The spectra can then be uploaded. For both DMA and Octyl HOPO the wavelength range of interest was 725 nm -775 nm, but for TODGA the range used was 550 nm – 600 nm. This is because a lower concentration of Nd^{3+} was used for this titration and as such the absorbance measured at the 725 nm -775 nm range was too low.

After the spectra are uploaded to HypSpec the model can utilize the estimates you provide of the stability constants to determine what the spectra for each of the concentration levels should look like. You can then manually adjust these calculated curves until they match the spectra that were collected experimentally as demonstrated in figure 5.2. As the curves are adjusted this also changes the stability constant to better reflect the actual results. Once the curve fitting is satisfactory the software refines the stability constant utilizing a shift cutting method.[224]

5.3 Results and Discussion

5.3.1 Potentiometric Titrations

As mentioned previously, all potentiometric titrations were performed in 0.001 M $NaNO_3$ solution. This was to introduce a proton so the pH could be measured. The pH could not be measured in a solution that was 100% ionic liquid. The first titration was a titration of citric acid with NaOH to validate the method. From there the potentiometric titration was performed on a carboxy-HOPO ligand that could be dissolved in a 0.001 M

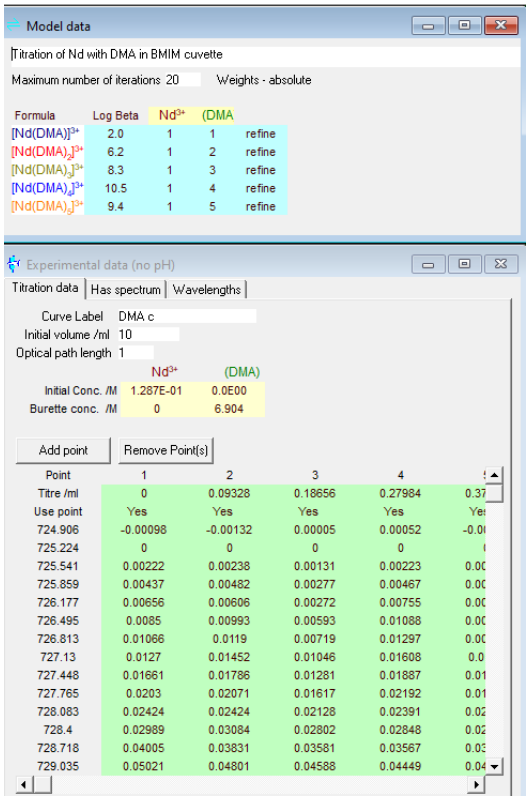


Figure 5.1 Development of HypSpec model demonstrating the initial setup.

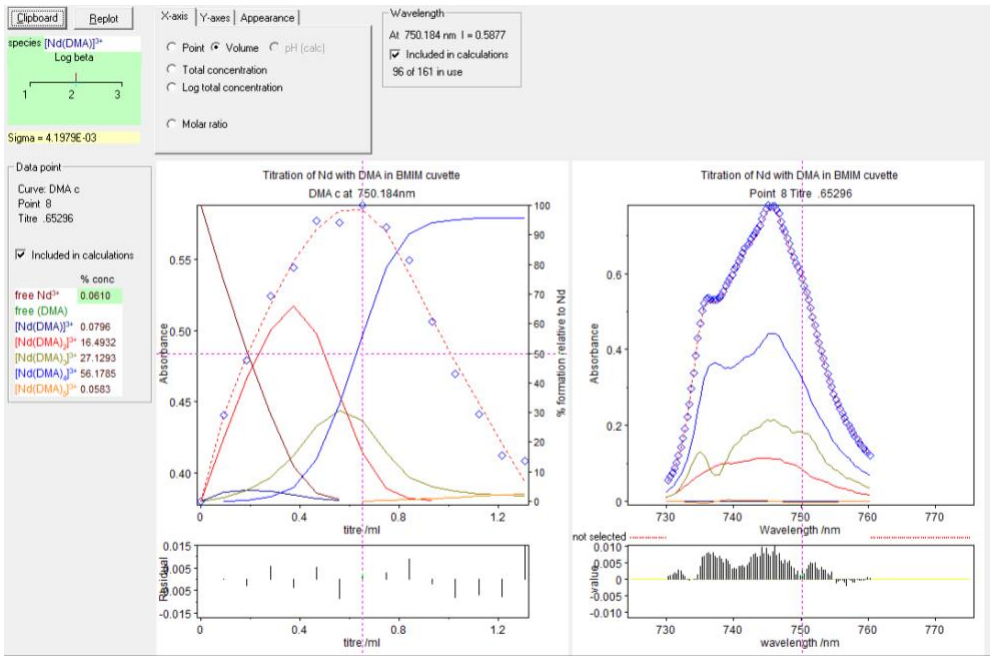


Figure 5.2 Image demonstrating the manual curve fitting in HypSpec. The diamonds indicate experimental values while the red dotted line is calculated result.

$NaNO_3$ solution and an octyl-HOPO ligand that required some ionic liquid in order to go into solution.

The calculated pKa distribution as well as the isotherm utilized in performing this calculation is displayed in figure 5.3. This figure also demonstrates that the calculated pKa distribution is similar to that which was determined by Jagiello et al.[219] In each case three narrow peaks are observed. The first ranging from 2.4 to 3.2, second from 3.8 to 4.7, and third from 5.4 to 6.2 (Fig. 5.3). Also, the relative intensities are similar. These three peaks are easily resolved which signals that this method can be utilized for both quantitative and qualitative purposes.

The isotherm for the carboxy-HOPO ligand resulted in one large peak for the pKa distribution (Fig. 5.4). This peak begins at a pKa of about 4.2 and ends at a pKa of 13. This indicates can indicate one of two possibilities. The first is that the method was unable to resolve the peaks present between the pKa values of 4 and 13. Given the excellent resolution demonstrated by the citric acid titration. The more likely scenario is that an ever increasing level of proton-binding occurs until the pKa of about 8.6 is reach where it begins to drop until no more proton binding occurs after the pKa of 13. This ligand could prove versatile right around the pH of 4 as the proton binding could be started or stopped by simply slightly adjusting the pH of the aqueous solution containing the carboxy-HOPO ligand.

The isotherm of the octyl-HOPO ligand indicates that the majority of activity is occurring between a pH of 6 and 10 (Fig. 5.5) This is the case with the exception of the narrow peak in the pKa distribution which is centered around 11(Fig. 5.5). The first two

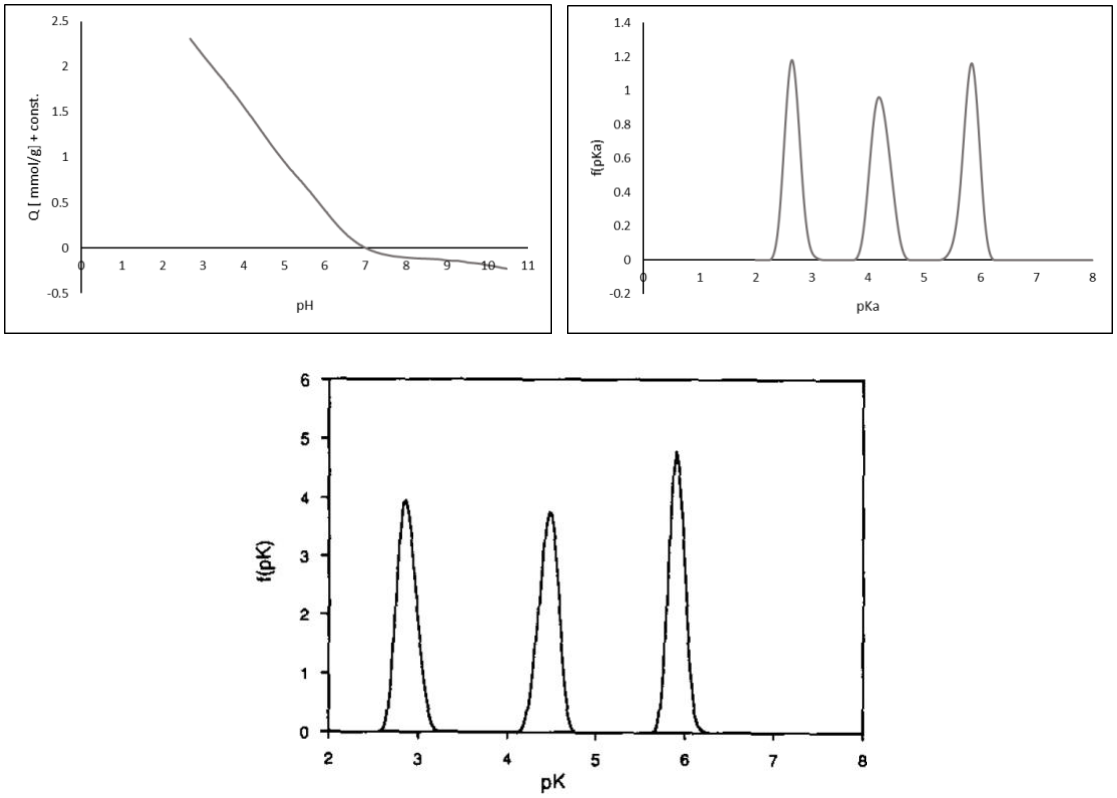


Figure 5.3 Isotherm (left) and pKa distribution (right) of citric acid. Bottom is pKa distribution of citric acid as determined by Jagiello et al.[219]

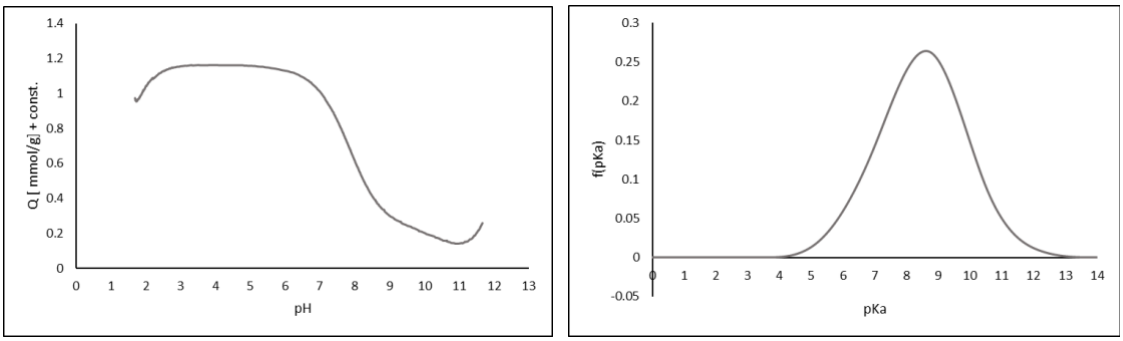


Figure 5.4 Isotherm (left) and pKa distribution (right) of the carboxy-HOPO ligand.

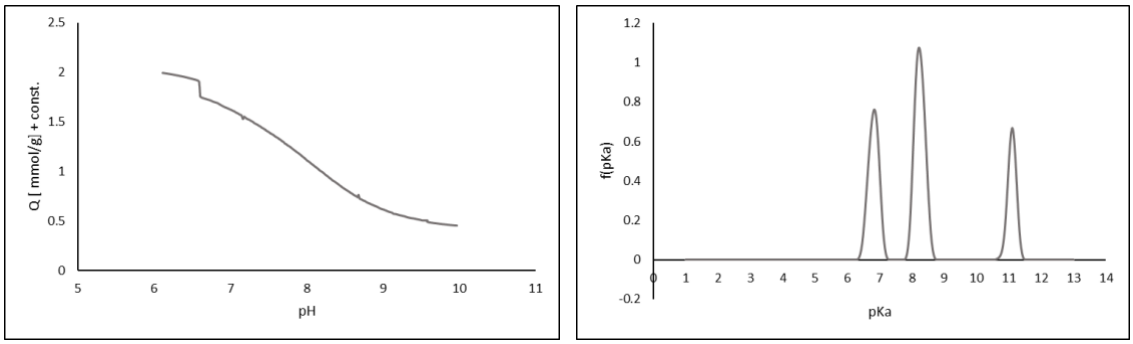


Figure 5.5 Isotherm (left) and pKa distribution (right) of the octyl-HOPO ligand.

peaks are separated by only 0.5 pKa units. This indicates the resolution of this method is at least as low as 0.5 pKa units as these two peaks are clearly completely resolved. Event though both the carboxy and octyl ligands are both HOPO ligands, it is clear that the proton binding of the two behaves very differently. The octlyl-HOPO ligand could prove especially useful in separations as the two peaks in the middle are centered around a pH of 7. This is ideal as maintain a pH closer to 7 allows for simpler adjustments when altering the pH of the solution. By simply adjusting the pH 1 unit the proton binding structure could potentially be adjusted twice.

5.3.2 Spectrophotometric Titrations

The spectrophotometric titration methods were developed utilizing the ligand DMA and extracting Nd. The goal of these titrations was to monitor the change in UV-Vis spectra as more DMA was added. This is because the change in spectra could be attributed to the binding of Nd with DMA. All spectra collected in the titration are shown in figure 5.3 of the appendix. There are five stability constands for Nd-DMA complexes. The five complexes formed are $Nd(DMA)_1$, $Nd(DMA)_2$, $Nd(DMA)_3$, $Nd(DMA)_4$, and $Nd(DMA)_5$. The accepted values of for these stability constants are $\log \beta = 2.12 \pm 0.05$, 6.72 ± 0.05, 8.76 ± 0.05, 10.72 ± 0.05 9.70 ± 0.05 respectively. The values for the complexes calculated in this study are 2.4334 ± 0.493, 6.07 ± 0.1712, 8.1197 ± 0.2429, 10.2376 ± 0.2468, and 9.7079 ± 0.27079. These values agree well with values determined in Freiderich et al.[180] This method can then be applied to other metal ligand complexes in order to determine the stability constants of each

5.4 Conclusions

This work demonstrated a method for the calculation of proton affinity distribution by potentiometric titration using an auto titrator. The method was successfully validated by a citric acid titration. The potentiometric titration also demonstrated excellent resolution as peaks as little as 0.5 pKa units apart were 100% resolved. The proton affinity distribution of a carboxy-HOPO and octyl-HOPO ligand were then identified. The octyl-HOPO ligand demonstrated an especially useful proton affinity distribution as there were multiple narrow peaks centered around a pKa of 7. Along with the potentiometric titrations, a spectrophotometric titration method was developed using a peristaltic pump to eliminate the need for aliquots of the solution to be placed in a room temperature cuvette. This allows for all measurements to made at a consistent temperature. The calculated stability constants agreed with values determined in another study for the Nd-DMA complexes. Both the potentiometric and spectrophotometric titrations can be applied to more ligands.

Chapter 6
Summary and Conclusions

This dissertation presents the development and validation of several analytical methods for the analysis of U bearing materials. These methods could be utilized to aid in the determination of attributes of samples along the nuclear fuel cycle. This data could then be utilized to determine either original location of the sample or processing history of the sample. Information such as this can be vital in the analysis of nuclear material that has been discovered outside of regulatory control. The analysis of this material can be of the upmost importance as the use of nuclear material continues to rise.

The first projected presented involved the development and validation of a method for the determination of P, S, Br, and I content in U bearing materials. The optimization of this method demonstrated that samples could be analyzed by TQ ICP – MS in a U matrix with little to no impact on transmission. This method demonstrated that O_2 gas was best used as a reaction gas for each of these analytes. Optimization of this method also demonstrated little run to run or day to day variation in the method. This method was able to show reliable results for I which can be especially difficult due to volatility. Once the method was optimized, it was validated using the certified reference material CUP-2. The TQ ICP – MS was able to determine P and S concentrations that agree with the certified value, and Br data was reported for CUP-2 for the first time.

Once the TQ ICP – MS method was developed and validated, the second project looked at the application of this method on UOC samples for the determination of both P and S content. The successful implementation of the method on solid UOC samples was first confirmed by analysis of three UOC certified reference materials. All three showed the TQ ICP – MS results agreed with the certified value. For the analysis of S, the obtained

were results were also compared to results obtained by analysis of the same samples using pyrohydrolysis method. The TQ method demonstrated higher concentrations as well as lower uncertainties for most samples. Given the agreement with the certified values, it is likely that the results obtained by TQ ICP – MS are more reliable than that of the pyrhydrolysis method. Conclusions about the process history for certain samples could be drawn from the S data. Determinations of phase content of the UOC could also be made based on the data obtained. The uncertainties were also analyzed for each case and it was determined that the calibration was the largest contributor to the overall uncertainty. The reliability of these results and the ability to make determinations about the samples based on P and S content suggest this method could be used on other U bearing samples to aid in the analysis of nuclear material found outside regulatory control.

The third project involved the development and optimization of a separation method for the Hf-Lu, Rb-Sr, and Nd-Sm isotopic systems as well as Pb and excess U. These separations were performed at significant excess U to simulate nuclear material sample. This method allowed for clean fractions to be obtained as well as column recoveries near 100% for all analytes but Rb and Sr. All recoveries were high enough to be reasonable for the determinations of isotope ratios. The advantages of this method are first the ability to also analyze the Pb isotope ratio systems as well as the other systems. In addition to this, the ability to remove large amounts of U is vital in nuclear material as the U will be in extreme excess to the other analytes. Also, the use of mainly HCl allows for limiting the number of acid switches. This method is also able to avoid the use of more complex acids such as ascorbic acid. Future work for this developed method could be the

application on real nuclear material samples. This would require the use of a multi collector ICP – MS to aid in the determination of isotope ratios.

The fourth project described in this dissertation was the development of titration methods for the determination of pKa distributions for ligands, as well as the determination of stability constants of a Nd-ligand complex. The potentiometric titration methods utilized and auto titrator and was validated using a citric acid titration with NaOH. This method was then applied to a carboxy-HOPO ligand as well as an Octyl-HOPO ligand. These pKa distributions demonstrated the utility of the ligands for rare earth element extractions. The auto titrator allowed for accurate pKa distributions as upwards of 400 data points could be collected during the titration. The spectrophotometric method was developed and validated using a previously studied titration of Nd in $BMIM^{+}$ NTF_2^{-} with the ligand DMA. The stability constants were determined using the software HypSpec and the calculated constants showed agreement with previously reported values. These titration methods can be utilized to identify ideal ligands for the extraction of rare earth elements. The potentiometric titration method is of particular interest as the autotitrator allows for accurate pKa distributions with little lab work required. Several titrations could be carried out in one day.

Bibliography

(1) Mayer, K.; Wallenius, M.; Fanghanel, T. Nuclear forensic science - From cradle to maturity. *Journal of Alloys and Compounds* **2007**, *444*, 50-56. DOI: 10.1016/j.jallcom.2007.01.164.

(2) Moody, K. J.; Grant, P. M.; Hutcheon, I. D. *Nuclear Forensic Analysis*; CRC Press Taylor & Francis Group 2015.

(3) Mayer, K.; Wallenius, M.; Varga, Z. Sample characteristics and nuclear forensic signatures. In *The New Nuclear Forensics Analysis of Nuclear Materials for Security Purposes* Fedchenko, V. Ed.; Oxford University Press, 2015; pp 93-127.

(4) Schutt, S. M.; Jacob, N. P.; Asme. THE NUCLEAR FUEL SERVICES, INC. PROGRAM TO SUPPORT DISPOSITION OF ENRICHED URANIUM-BEARING MATERIALS. *Icem2007: Proceedings of the 11th International Conference on Environmental Remediation and Radioactive Waste Management, Pts a and B* **2009**, 1419-1422, Proceedings Paper.

(5) Wallenius, M.; Morgenstern, A.; Apostolidis, C.; Mayer, K. Determination of the age of highly enriched uranium. *Analytical and Bioanalytical Chemistry* **2002**, *374* (3), 379-384, Article. DOI: 10.1007/s00216-002-1555-9.

(6) Stanley, F. E. A beginner's guide to uranium chronometry in nuclear forensics and safeguards. *Journal of Analytical Atomic Spectrometry* **2012**, *27* (11), 1821-1830, Review. DOI: 10.1039/c2ja30182b.

(7) Heumann, K. G.; Vanhaecke, F. Isotope ratios in analytical chemistry. *Analytical and Bioanalytical Chemistry* **2008**, *390* (2), 433-435, Editorial Material. DOI: 10.1007/s00216-007-1728-7.

(8) Hansmann, W.; Koppel, V. Lead-isotopes as tracers of pollutants in soils. *Chemical Geology* **2000**, *171* (1-2), 123-144, Article. DOI: 10.1016/s0009-2541(00)00230-8.

(9) Gulson, B. L. URANIUM-LEAD AND LEAD-LEAD INVESTIGATIONS OF MINERALS FROM THE BROKEN HILL LODES AND MINE SEQUENCE ROCKS. *Economic Geology* **1984**, *79* (3), 476-490. DOI: 10.2113/gsecongeo.79.3.476.

(10) Gulson, B. L.; Mizon, K. J.; Dickson, B. L.; Korsch, M. J. The effect of exposure to employees from mining and milling operations in a uranium mine on lead isotopes - a pilot study. *Science of the Total Environment* **2005**, *339* (1-3), 267-272. DOI: 10.1016/j.scitotenv.2004.11.006.

(11) Karpas, Z. *Analytical Chemistry of Uranium: Environmental, Forensic, Nuclear, and Toxicological Applications*, 1 ed.; Taylor & Francis Group, 2014.

(12) Sheldon, S.; Hadian, S.; Zik, O. Beyond carbon: Quantifying environmental externalities as energy for hydroelectric and nuclear power. *Energy* **2015**, *84*, 36-44, Article. DOI: 10.1016/j.energy.2015.01.116.

(13) Na, B. C.; Sartori, E. Organization for Economic Cooperation and Development/Nuclear Energy Agency international benchmark on the VENUS-2 MOX core measurements. *Nuclear Science and Engineering* **2002**, *142* (1), 37-47. DOI: 10.13182/nse02-a2285.

(14) Mayer, K.; Wallenius, M.; Lutzenkirchen, K.; Galy, J.; Varga, Z.; Erdmann, N.; Buda, R.; Kratz, J. V.; Trautmann, N.; Fifield, K.; et al. Nuclear Forensics: A Methodology Applicable to Nuclear Security and to Non-Proliferation. In *International Nuclear Physics Conference (INPC)*, TRIUMF, Canadian Natl Lab Particle & Nucl Phys, Vancouver, CANADA, Jul 04-09, 2010; Iop Publishing Ltd: BRISTOL, 2011; Vol. 312. DOI: 10.1088/1742-6596/312/6/062003.

(15) Stanley, F. E.; Stalcup, A. M.; Spitz, H. B. A brief introduction to analytical methods in nuclear forensics. *Journal of Radioanalytical and Nuclear Chemistry* **2013**, *295* (2), 1385-1393, Article. DOI: 10.1007/s10967-012-1927-3.

(16) Stanley, F. E.; Mathew, K. J.; Byerly, B. L.; Keller, R.; Spencer, K. J.; Thomas, M. R. Pursuing standards strategies in nuclear forensics: investigating extraction of progeny uranium in CRM-126a as a quality control material in Pu-U chronometry. *Journal of Radioanalytical and Nuclear Chemistry* **2017**, *311* (3), 1819-1824, Article. DOI: 10.1007/s10967-016-5133-6.

(17) Aggarwal, S. K. Nuclear forensics: what, why and how? *Current Science* **2016**, *110* (5), 782-791, Review.

(18) Wilson, P. D. *The nuclear fuel cycle from ore to wastes*; Vol. 28; Oxford University Press, 1996.

(19) Carvalho, F. P. Mining industry and sustainable development: time for change. *Food and Energy Security* **2017**, *6* (2), 61-77, Review. DOI: 10.1002/fes3.109.

(20) Ewing, R. C. The nuclear fuel cycle: A role for mineralogy and geochemistry. *Elements* **2006**, *2* (6), 331-334, Article. DOI: 10.2113/gselements.2.6.331.

(21) Nuclear Fuel Cycle Science and Engineering. *Nuclear Fuel Cycle Science and Engineering* **2012**, (37), 1-626, Book. DOI: 10.1533/9780857096388.

(22) Brown, N. R.; Worrall, A.; Todosow, M. Impact of thermal spectrum small modular reactors on performance of once-through nuclear fuel cycles with low-enriched uranium. *Annals of Nuclear Energy* **2017**, *101*, 166-173, Article. DOI: 10.1016/j.anucene.2016.11.003.

(23) Eichholz, G. G. NUCLEAR-REACTOR MATERIALS AND APPLICATIONS - MA,BM. *American Scientist* **1983**, *71* (6), 661-661, Book Review.

(24) Park, B. H.; Gao, F.; Kwon, E. H.; Ko, W. I. Comparative study of different nuclear fuel cycle options: Quantitative analysis on material flow. *Energy Policy* **2011**, *39* (11), 6916-6924, Article. DOI: 10.1016/j.enpol.2011.03.083.

(25) McNamara, B.; Scheele, R.; Kozelisky, A.; Edwards, M. Thermal reactions of uranium metal, UO2, U3O8, UF4, and UO2F2 with NF3 to produce UF6. *Journal of Nuclear Materials* **2009**, *394* (2-3), 166-173, Article. DOI: 10.1016/j.jnucmat.2009.09.004.

(26) Sirven, J. B.; Pailloux, A.; M'Baye, Y.; Coulon, N.; Alpettaz, T.; Gosse, S. Towards the determination of the geographical origin of yellow cake samples by laser-induced breakdown spectroscopy and chemometrics. *Journal of Analytical Atomic Spectrometry* **2009**, *24* (4), 451-459, Article. DOI: 10.1039/b821405k.

(27) Nash, J. T.; Granger, H. C.; Adams, S. S. Geology and Concepts of Genesis of Important Types of Uranium. In *Economic Geology*, Vol. Seventy Fifth Aniversary; Economic Geology, 1981.

(28) Roshani, M.; Mirjalili, K. Studies on the leaching of an arsenic-uranium ore. *Hydrometallurgy* **2009**, *98* (3-4), 304-307, Article. DOI: 10.1016/j.hydromet.2009.04.019.

(29) Spano, T. L.; Simonetti, A.; Balboni, E.; Dorais, C.; Burns, P. C. Trace element and U isotope analysis of uraninite and ore concentrate: Applications for nuclear forensic investigations. *Applied Geochemistry* **2017**, *84*, 277-285, Article. DOI: 10.1016/j.apgeochem.2017.07.003.

(30) Klipsch, S.; Herwartz, D.; Staubwasser, M. Optimizing sulfate pyrolysis triple oxygen isotope analysis for samples from desert environments. *Rapid Communications in Mass Spectrometry* **2021**, *35* (14). DOI: 10.1002/rcm.9102.

(31) Fletcher, N. D.; Manard, B. T.; Bostick, D. A.; Bostick, W. D.; Metzger, S. C.; Ticknor, B. W.; Rogers, K. T.; Hexel, C. R. Determination of phosphorus and sulfur in uranium ore concentrates by triple quadrupole inductively coupled plasma mass spectrometry. *Talanta* **2021**, *221*. DOI: 10.1016/j.talanta.2020.121573.

(32) Varga, Z.; Wallenius, M.; Mayer, K. Origin assessment of uranium ore concentrates based on their rare-earth elemental impurity pattern. *Radiochimica Acta* **2010**, *98* (12), 771-778, Article. DOI: 10.1524/ract.2010.1777.

(33) Khawassek, Y. M.; Taha, M. H.; Eliwa, A. A. Kinetics of Leaching Process Using Sulfuric Acid for Sella Uranium Ore Material, South Eastern Desert, Egypt. *International Journal of Nuclear Energy Science and Engineering* **2016**, *6*, 62-73. DOI: 10.14355/ijnese.2016.06.006.

(34) Lottering, M. J.; Lorenzen, L.; Phala, N. S.; Smit, J. T.; Schalkwyk, G. A. C. Mineralogy and uranium leaching response of low grade South African ores. *Minerals Engineering* **2008**, *21* (1), 16-22. DOI: 10.1016/j.mineng.2007.06.006.

(35) Munoz, J. A.; Gonzalez, F.; Blazquez, M. L.; Ballester, A. A STUDY OF THE BIOLEACHING OF A SPANISH URANIUM ORE .1. A REVIEW OF THE BACTERIAL LEACHING IN THE TREATMENT OF URANIUM ORES. *Hydrometallurgy* **1995**, *38* (1), 39-57, Article. DOI: 10.1016/0304-386x(94)00039-6.

(36) Badaut, V.; Wallenius, M.; Mayer, K. Anion analysis in uranium ore concentrates by ion chromatography. *Journal of Radioanalytical and Nuclear Chemistry* **2009**, *280* (1), 57-61, Article. DOI: 10.1007/s10967-008-7404-3.

(37) Keegan, E.; Wallenius, M.; Mayer, K.; Varga, Z.; Rasmussen, G. Attribution of uranium ore concentrates using elemental and anionic data. *Applied Geochemistry* **2012**, *27* (8), 1600-1609, Article. DOI: 10.1016/j.apgeochem.2012.05.009.

(38) Houk, R. S.; Fassel, V. A.; Flesch, G. D.; Svec, H. J.; Gray, A. L.; Taylor, C. E. INDUCTIVELY COUPLED ARGON PLASMA AS AN ION-SOURCE FOR MASS-SPECTROMETRIC DETERMINATION OF TRACE-ELEMENTS. *Analytical Chemistry* **1980**, *52* (14), 2283-2289. DOI: 10.1021/ac50064a012.

(39) Beltrami, D.; Calestani, D.; Maffini, M.; Suman, M.; Melegari, B.; Zappettini, A.; Zanotti, L.; Casellato, U.; Careri, M.; Mangia, A. Development of a combined SEM and ICP-MS approach for the qualitative and quantitative analyses of metal microparticles and sub-microparticles in food products. *Analytical and Bioanalytical Chemistry* **2011**, *401* (4), 1401-1409, Article. DOI: 10.1007/s00216-011-5149-2.

(40) Ek, K. H.; Morrison, G. M.; Lindberg, P.; Rauch, S. Comparative tissue distribution of metals in birds in Sweden using ICP-MS and laser ablation ICP-MS. *Archives of Environmental Contamination and Toxicology* **2004**, *47* (2), 259-269, Article. DOI: 10.1007/s00244-004-3138-6.

(41) Moor, C.; Lymberopoulou, T.; Dietrich, V. J. Determination of heavy metals in soils, sediments and geological materials by ICP-AES and ICP-MS. *Mikrochimica Acta* **2001**, *136* (3-4), 123-128, Article; Proceedings Paper. DOI: 10.1007/s006040170041.

(42) Michalski, R.; Jablonska, M.; Szopa, S.; Lyko, A. Application of Ion Chromatography with ICP-MS or MS Detection to the Determination of Selected Halides and Metal/Metalloids Species. *Critical Reviews in Analytical Chemistry* **2011**, *41* (2), 133-150, Review. DOI: 10.1080/10408347.2011.559438.

(43) Thomas, R. *Practical Guide to ICP-MS A Tutorial for Beginners*; CRC Press Taylor & Francis Group, 2013.

(44) Burger, S.; Riciputi, L. R. A rapid isotope ratio analysis protocol for nuclear solid materials using nano-second laser-ablation time-of-flight ICP-MS. *Journal of Environmental Radioactivity* **2009**, *100* (11), 970-976, Article. DOI: 10.1016/j.jenvrad.2009.07.009.

(45) Rodushkin, I.; Axelsson, M. D. Application of double focusing sector field ICP-MS for multielemental characterization of human hair and nails. Part I. Analytical methodology. *Science of the Total Environment* **2000**, *250* (1-3), 83-100, Article. DOI: 10.1016/s0048-9697(00)00369-7.

(46) Zhu, G. X.; Browner, R. F. INVESTIGATION OF EXPERIMENTAL PARAMETERS WITH A QUADRUPOLE ICP MS. *Applied Spectroscopy* **1987**, *41* (3), 349-359, Article. DOI: 10.1366/0003702874448869.

(47) Lee, M. *Mass Spectrometry Handbook*; Wiley Series on Pharmeceutical Science and Biotechnology: Practices, Applications and Methods, Vol. 7; John Wiley & Sons, 2012.

(48) Medhe, S. Mass Spectrometry: Detectors Review. Science Publishing Group: 2018; Vol. 3, pp 51-58.

(49) Inagaki, K.; Fujii, S.; Takatsu, A.; Chiba, K. High performance concentric nebulizer for low-flow rate liquid sample introduction to ICP-MS. *Journal of Analytical Atomic Spectrometry* **2011**, *26* (3), 623-630, Article. DOI: 10.1039/c0ja00128g.

(50) Lin, F. H.; Miyashita, S.; Inagaki, K.; Liu, Y. H.; Hsu, I. H. Evaluation of three different sample introduction systems for single-particle inductively coupled plasma mass spectrometry (spICP-MS) applications. *Journal of Analytical Atomic Spectrometry* **2019**, *34* (2), 401-406, Article. DOI: 10.1039/c8ja00295a.

(51) Kawabata, K.; Kishi, Y.; Thomas, R. The benefits of dynamic reaction cell ICP-MS technology to determine ultratrace metal contamination levels in high-purity phosphoric and sulfuric acid. *Spectroscopy* **2003**, *18* (1), 16-+, Article.

(52) Beres, S. A.; Bruckner, P. H.; Denoyer, E. R. PERFORMANCE EVALUATION OF A CYCLONIC SPRAY CHAMBER FOR ICP-MS. *Atomic Spectroscopy* **1994**, *15* (2), 96-99, Article.

(53) Boss, C. B.; Fredeen, K. J. *Concepts, Instrumentation and Techniques in Inductively Coupled Plasma Optical Emission Spectrometry*; Perkin-Elmer Corporation, 1997.

(54) Hoffman, E.; Vincent, S. *Mass Spectrometry principles and applications*; John Wiley and Sons, 2007.

(55) Paul, W.; Steinwedel, H. A New Mass Spectrometer Without A Magnetic Field. Zeitschrift für Naturforschung: 1953; Vol. a8.

(56) Adams, F.; Gijbels, R.; Van Grieken, R. *Inorganic Mass Spectrometry*; U.S. Department of Energy Office of Scientific and Technical Information, 1988.

(57) Du, Z. H.; Olney, T. N.; Douglas, D. J. Inductively coupled plasma mass spectrometry with a quadrupole mass filter operated in the third stability region. *Journal of the American Society for Mass Spectrometry* **1997**, *8* (12), 1230-1236, Article. DOI: 10.1016/s1044-0305(97)00220-1.

(58) Harris, D. C. *Exploring Chemical Analysis*; W. H. Freeman and Company, 2013.

(59) Fletcher, N. D.; Manard, B. T.; Metzger, S. C.; Ticknor, B. W.; Bostick, D. A.; Hexel, C. R. Determining P, S, Br, and I content in uranium by triple quadrupole inductively coupled plasma mass spectrometry. *Journal of Radioanalytical and Nuclear Chemistry* **2020**, *324* (1), 395-402, Article. DOI: 10.1007/s10967-020-07057-0.

(60) Ari, B.; Bakirdere, S. A primary reference method for the characterization of Cd, Cr, Cu, Ni, Pb and Zn in a candidate certified reference seawater material: TEA/Mg(OH)(2) assisted (IDMS)-M-3 by triple quadrupole ICP-MS/MS. *Analytica Chimica Acta* **2020**, *1140*, 178-189, Article. DOI: 10.1016/j.aca.2020.10.004.

(61) Jackson, S. L.; Spence, J.; Janssen, D. J.; Ross, A. R. S.; Cullen, J. T. Determination of Mn, Fe, Ni, Cu, Zn, Cd and Pb in seawater using offline extraction and triple

quadrupole ICP-MS/MS. *Journal of Analytical Atomic Spectrometry* **2018**, *33* (2), 304-313, Article. DOI: 10.1039/c7ja00237h.

(62) Khatri, N.; Gupta, A.; Taneja, R.; Bilandi, A.; P, B. Review on Mass Spectrometry detectors. IRJP: Vol. 3, pp 33-42.

(63) Dietz, L. A. BASIC PROPERTIES OF ELECTRON MULTIPLIER ION DETECTION AND PULSE COUNTING METHODS IN MASS SPECTROMETRY. *Review of Scientific Instruments* **1965**, *36* (12), 1763-+, Article. DOI: 10.1063/1.1719460.

(64) Allen, J. S. The detection of single positive ions, electrons and photons by a secondary electron multiplier. *Physical Review* **1939**, *55* (10), 0966-0971, Article. DOI: 10.1103/PhysRev.55.966.

(65) Collins, R. D. The use of electron multipliers in mass spectrometry *Vacuum* **1969**, *19*, 105-111. DOI: 10.1016.

(66) International Union of Pure and Applied Chemistry (IUPAC): Nomenclature of Inorganic Chemistry *Definition Rules 1970. London, Butterworths* **1971**.

(67) Golloch, A.; Stosch, H.-G.; Hu, B.; He, M.; Jakubowski, N.; Meinhardt, J.; Meyer, M.; Niederstraber, J.; Schramm, R.; Sindern, S. Handbook of Rare Earth Elements Walter de Gruyter GmbH: 2017; p 420.

(68) Staudigel, H.; Zindler, A.; Hart, S. R.; Leslie, T.; Chen, C. Y.; Clague, D. THE ISOTOPE SYSTEMATICS OF A JUVENILE INTRAPLATE VOLCANO - PB, ND, AND SR ISOTOPE RATIOS OF BASALTS FROM LOIHI SEAMOUNT, HAWAII.

Earth and Planetary Science Letters **1984**, *69* (1), 13-29, Article. DOI: 10.1016/0012-821x(84)90071-2.

(69) Negrel, P.; Allegre, C. J.; Dupre, B.; Lewin, E. EROSION SOURCES DETERMINED BY INVERSION OF MAJOR AND TRACE-ELEMENT RATIOS AND STRONTIUM ISOTOPIC-RATIOS IN RIVER WATER - THE CONGO BASIN CASE. *Earth and Planetary Science Letters* **1993**, *120* (1-2), 59-76, Article. DOI: 10.1016/0012-821x(93)90023-3.

(70) Kagami, H.; Iizumi, S.; Tainosho, Y.; Owada, M. SPATIAL VARIATIONS OF SR AND ND ISOTOPE RATIOS OF CRETACEOUS-PALEOGENE GRANITOID ROCKS, SOUTHWEST JAPAN ARC. *Contributions to Mineralogy and Petrology* **1992**, *112* (2-3), 165-177, Article. DOI: 10.1007/bf00310452.

(71) Vanhaecke, F.; Balcaen, L.; Malinovsky, D. Use of single-collector and multi-collector ICP-mass spectrometry for isotopic analysis. *Journal of Analytical Atomic Spectrometry* **2009**, *24* (7), 863-886, Article; Proceedings Paper. DOI: 10.1039/b903887f.

(72) Rehkamper, M.; Schonbachler, M.; Stirling, C. H. Multiple collector ICP-MS: Introduction to instrumentation, measurement techniques and analytical capabilities. *Geostandards Newsletter-the Journal of Geostandards and Geoanalysis* **2001**, *25* (1), 23-40, Review. DOI: 10.1111/j.1751-908X.2001.tb00785.x.

(73) Vanhaecke, F.; Degryse, P. *Isotopic Analysis*; Wiley VCH Verlag and Co. KGaA, 2012.

(74) Weis, D.; Kieffer, B.; Hanano, D.; Silva, I. N.; Barling, J.; Pretorius, W.; Maerschalk, C.; Mattielli, N. Hf isotope compositions of US Geological Survey reference

materials. *Geochemistry Geophysics Geosystems* **2007**, *8*, 15, Article. DOI: 10.1029/2006gc001473.

(75) Chu, N. C.; Taylor, R. N.; Chavagnac, V.; Nesbitt, R. W.; Boella, R. M.; Milton, J. A.; German, C. R.; Bayon, G.; Burton, K. Hf isotope ratio analysis using multi-collector inductively coupled plasma mass spectrometry: an evaluation of isobaric interference corrections. *Journal of Analytical Atomic Spectrometry* **2002**, *17* (12), 1567-1574. DOI: 10.1039/b206707b.

(76) Bizzarro, M.; Baker, J. A.; Ulfbeck, D. A new digestion and chemical separation technique for rapid and highly reproducible determination of Lu/Hf and Hf isotope ratios in geological materials by MC-ICP-MS. *Geostand. Newsl.* **2003**, *27* (2), 133-145. DOI: 10.1111/j.1751-908X.2003.tb00641.x.

(77) Saji, N. S.; Wielandt, D.; Paton, C.; Bizzarro, M. Ultra-high-precision Nd-isotope measurements of geological materials by MC-ICPMS. *Journal of Analytical Atomic Spectrometry* **2016**, *31* (7), 1490-1504, Article. DOI: 10.1039/c6ja00064a.

(78) Li, C. F.; Li, X. H.; Li, Q. L.; Guo, J. H.; Yang, Y. H. Rapid and precise determination of Sr and Nd isotopic ratios in geological samples from the same filament loading by thermal ionization mass spectrometry employing a single-step separation scheme. *Analytica Chimica Acta* **2012**, *727*, 54-60, Article. DOI: 10.1016/j.aca.2012.03.040.

(79) Badarau, E.; Giurgea, M.; Giurgea, G. H.; Trutia, T. H. Spectrochim. Acta: 1956; Vol. 11.

(80) Greenfield, S.; Berry, C. T.; Jones, I. L. HIGH-PRESSURE PLASMAS AS SPECTROSCOPIC EMISSION SOURCES. *Analyst* **1964**, *89* (106), 713-&, Article. DOI: 10.1039/an9648900713.

(81) Balaram, V. Recent advances in the determination of elemental impurities in pharmaceuticals - Status, challenges and moving frontiers. *Trac-Trends in Analytical Chemistry* **2016**, *80*, 83-95. DOI: 10.1016/j.trac.2016.02.001.

(82) Khan, N.; Jeong, I. S.; Hwang, I. M.; Kim, J. S.; Choi, S. H.; Nho, E. Y.; Choi, J. Y.; Kwak, B. M.; Ahn, J. H.; Yoon, T.; et al. Method validation for simultaneous determination of chromium, molybdenum and selenium in infant formulas by ICP-OES and ICP-MS. *Food Chemistry* **2013**, *141* (4), 3566-3570. DOI: 10.1016/j.foodchem.2013.06.034.

(83) Lienemann, C. P.; Dreyfus, S.; Pecheyran, C.; Donard, O. F. X. Trace metal analysis in petroleum products: Sample introduction evaluation in ICP-OES and comparison with an ICP-MS approach. *Oil & Gas Science and Technology-Revue D Ifp Energies Nouvelles* **2007**, *62* (1), 69-77. DOI: 10.2516/ogst:2007006.

(84) Khan, S. R.; Sharma, B.; Chawla, P. A.; Bhatia, R. Inductively Coupled Plasma Optical Emission Spectrometry (ICP-OES): a Powerful Analytical Technique for Elemental Analysis. *Food Analytical Methods* **2022**, *15* (3), 666-688. DOI: 10.1007/s12161-021-02148-4.

(85) Silva, N. D.; Gregoire, D. C. Inductively coupled plasma optical emission and mass spectrometry. In *Instrumental Multi-Element Chemical Analysis*, Alfassi, Z. B. Ed.; Kluwer Academic Publishers, 1998; p 493.

(86) Reed, T. B. INDUCTION-COUPLED PLASMA TORCH. *Journal of Applied Physics* **1961**, *32* (5), 821-&, Article. DOI: 10.1063/1.1736112.

(87) Mermet, J. M.; Poussel, E. 10 ed.; Applied Spectroscopy: 1995; Vol. 49, pp 12A-18A.

(88) Olesik, J. W.; Hartshorne, J. A.; Casey, N.; Linard, E.; Dettman, J. R. Further insight into analyte transport processes and water vapor, aerosol loading in ICP-OES and ICP-MS. *Spectrochimica Acta Part B-Atomic Spectroscopy* **2021**, *176*, 10, Article. DOI: 10.1016/j.sab.2020.106038.

(89) Olesik, J. W. ELEMENTAL ANALYSIS USING ICP-OES AND ICP MS - AN EVALUATION AND ASSESSMENT OF REMAINING PROBLEMS. *Analytical Chemistry* **1991**, *63* (1), A12-A21, Article. DOI: 10.1021/ac00001a001.

(90) Janesick, J. Charge coupled CMOS and hybrid detector arrays. In *Conference on Focal Plane Arrays for Space Telescopes*, san francisco, CA, Aug 04-06, 2003; Spie-Int Soc Optical Engineering: BELLINGHAM, 2003; Vol. 5167, pp 1-18.

(91) Sweedler, J. V.; Jalkian, R. D.; Denton, M. B. A LINEAR CHARGE-COUPLED DEVICE DETECTOR SYSTEM FOR SPECTROSCOPY. *Applied Spectroscopy* **1989**, *43* (6), 953-962, Article. DOI: 10.1366/0003702894203976.

(92) Harnly, J. M. The future of atomic absorption spectrometry: a continuum source with a charge coupled array detector. *Journal of Analytical Atomic Spectrometry* **1999**, *14* (2), 137-146, Article; Proceedings Paper. DOI: 10.1039/a807586g.

(93) MacFarlane, D.; Kar, M.; Pringle, J.; MacFarlane, D. *Fundamentals of Ionic Liquids: From Chemistry to Applications*; John Wiley & Sons, 2017.

(94) Salvi, P. P.; Mandhare, A. M.; Sartape, A. S.; Pawar, D. K.; Han, S. H.; Kolekar, S. S. Bronsted acidic ionic liquids promoted cyclocondensation reaction: Synthesis of 1,8-dioxo-octahydroxanthene. *Comptes Rendus Chimie* **2011**, *14* (10), 883-886, Article. DOI: 10.1016/j.crci.2011.04.008.

(95) Liu, W. W.; Zhao, T. Y.; Zhang, Y. M.; Wang, H. P.; Yu, M. F. The physical properties of aqueous solutions of the ionic liquid BMIM BF4. *Journal of Solution Chemistry* **2006**, *35* (10), 1337-1346, Article. DOI: 10.1007/s10953-006-9064-7.

(96) de Azevedo, R. G.; Esperanca, J.; Szydlowski, J.; Visak, Z. P.; Pires, P. F.; Guedes, H. J. R.; Rebelo, L. P. N. Thermophysical and thermodynamic properties of ionic liquids over an extended pressure range: bmim NTf2 and hmim NTf2. *Journal of Chemical Thermodynamics* **2005**, *37* (9), 888-899, Article. DOI: 10.1016/j.jct.2005.04.018.

(97) Kirchner, B. *Ionic Liquids*, 1 ed.; Kirchner, B., Ed.; Topics in Current Chemistry; Springer Berlin, Heidelberg, 2010.

(98) Zhou, F.; Liang, Y. M.; Liu, W. M. Ionic liquid lubricants: designed chemistry for engineering applications. *Chemical Society Reviews* **2009**, *38* (9), 2590-2599, Review. DOI: 10.1039/b817899m.

(99) Vidal, L.; Riekkola, M. L.; Canals, A. Ionic liquid-modified materials for solid-phase extraction and separation: A review. *Analytica Chimica Acta* **2012**, *715*, 19-41, Review. DOI: 10.1016/j.aca.2011.11.050.

(100) Liu, B. Y.; Jin, N. X. The Applications of Ionic Liquid as Functional Material: A Review. *Current Organic Chemistry* **2016**, *20* (20), 2109-2116, Review. DOI: 10.2174/1385272820666160527101844.

(101) Armand, M.; Endres, F.; MacFarlane, D. R.; Ohno, H.; Scrosati, B. Ionic-liquid materials for the electrochemical challenges of the future. *Nature Materials* **2009**, *8* (8), 621-629, Review. DOI: 10.1038/nmat2448.

(102) Moniruzzaman, M.; Goto, M. Ionic Liquids: Future Solvents and Reagents for Pharmaceuticals. *Journal of Chemical Engineering of Japan* **2011**, *44* (6), 370-381, Review.

(103) Hough, W. L.; Smiglak, M.; Rodriguez, H.; Swatloski, R. P.; Spear, S. K.; Daly, D. T.; Pernak, J.; Grisel, J. E.; Carliss, R. D.; Soutullo, M. D.; et al. The third evolution of ionic liquids: active pharmaceutical ingredients. *New Journal of Chemistry* **2007**, *31* (8), 1429-1436, Article. DOI: 10.1039/b706677p.

(104) Freitas, R. G.; Santanna, M. A.; Pereira, E. C. Preparation and Characterization of TiO2 Nanotube Arrays in Ionic Liquid for Water Splitting. *Electrochimica Acta* **2014**, *136*, 404-411, Article. DOI: 10.1016/j.electacta.2014.05.097.

(105) Cognigni, A.; Palvogyi, A. M.; Schroder, C.; Peterlik, H.; Mullner, A. R. M.; Zirbs, R.; Weil, M.; Bica, K. Surface-Active Ionic Liquids in Catalytic Water Splitting. *Australian Journal of Chemistry* **2019**, *72* (1-2), 34-41, Article. DOI: 10.1071/ch18104.

(106) Qiu, B.; Lin, B. C.; Yan, F. Ionic liquid/poly(ionic liquid)-based electrolytes for energy devices. *Polymer International* **2013**, *62* (3), 335-337, Article. DOI: 10.1002/pi.4454.

(107) Arbizzani, C.; Biso, M.; Cericola, D.; Lazzari, M.; Soavi, F.; Mastragostino, M. Safe, high-energy supercapacitors based on solvent-free ionic liquid electrolytes. *Journal*

of Power Sources **2008**, *185* (2), 1575-1579, Article. DOI: 10.1016/j.jpowsour.2008.09.016.

(108) Wang, Y.; Gong, S.; Wang, S. J.; Simon, G. P.; Cheng, W. L. Volume-invariant ionic liquid microbands as highly durable wearable biomedical sensors. *Materials Horizons* **2016**, *3* (3), 208-213, Article. DOI: 10.1039/c5mh00284b.

(109) Galpothdeniy, W. I. S.; McCarter, K. S.; De Rooy, S. L.; Regmi, B. P.; Das, S.; Hasan, F.; Tagge, A.; Warner, I. M. Ionic liquid-based optoelectronic sensor arrays for chemical detection. *Rsc Advances* **2014**, *4* (14), 7225-7234, Article. DOI: 10.1039/c3ra47518b.

(110) Chernyshov, D. V.; Shuedene, N. V.; Antipova, E. R.; Pletnev, I. V. Ionic liquid-based miniature electrochemical sensors for the voltammetric determination of catecholamines. *Analytica Chimica Acta* **2008**, *621* (2), 178-184, Article. DOI: 10.1016/j.aca.2008.05.042.

(111) Wei, G. T.; Yang, Z. S.; Chen, C. J. Room temperature ionic liquid as a novel medium for liquid/liquid extraction of metal ions. *Analytica Chimica Acta* **2003**, *488* (2), 183-192, Article. DOI: 10.1016/s0003-2670(03)00660-3.

(112) Sas, O. G.; Dominguez, I.; Gonzalez, B.; Dominguez, A. Liquid-liquid extraction of phenolic compounds from water using ionic liquids: Literature review and new experimental data using C(2)mim FSI. *Journal of Environmental Management* **2018**, *228*, 475-482, Review. DOI: 10.1016/j.jenvman.2018.09.042.

(113) Marsousi, S.; Karimi-Sabet, J.; Moosavian, M. A.; Amini, Y. Liquid-liquid extraction of calcium using ionic liquids in spiral microfluidics. *Chemical Engineering Journal* **2019**, *356*, 492-505, Article. DOI: 10.1016/j.cej.2018.09.030.

(114) Baba, Y.; Kubota, F.; Kamiya, N.; Goto, M. Recent Advances in Extraction and Separation of Rare-Earth Metals Using Ionic Liquids. *Journal of Chemical Engineering of Japan* **2011**, *44* (10), 679-685, Review. DOI: 10.1252/jcej.10we279.

(115) Bourbos, E.; Giannopoulou, I.; Karantonis, A.; Paspaliaris, I.; Panias, D. Reduction of Light Rare Earths and a Proposed Process for Nd Electrorecovery Based on Ionic Liquids. *Journal of Sustainable Metallurgy* **2018**, *4* (3), 395-406, Article. DOI: 10.1007/s40831-018-0186-0.

(116) Dong, Y. M.; Sun, X. Q.; Wang, Y. L.; Huang, C.; Zhao, Z. Y. The Sustainable and Efficient Ionic Liquid-Type Saponification Strategy for Rare Earth Separation Processing. *Acs Sustainable Chemistry & Engineering* **2016**, *4* (3), 1573-1580, Article. DOI: 10.1021/acssuschemeng.5b01499.

(117) Rout, A.; Binnemans, K. Influence of the ionic liquid cation on the solvent extraction of trivalent rare-earth ions by mixtures of Cyanex 923 and ionic liquids. *Dalton Transactions* **2015**, *44* (3), 1379-1387, Article. DOI: 10.1039/c4dt02766c.

(118) Perkampus, H. H. *UV-VIS Spectroscopy and its Applications*, 1 ed.; Lab, S., Ed.; Springer-Verlag, 1992.

(119) Kenkel, J. *Analytical Chemistry Refresher Manual*; CRC Press, 1992.

(120) Biyada, S.; Merzouki, M.; Elkarrach, K.; Benlemlih, M. Spectroscopic characterization of organic matter transformation during composting of textile solid waste

using UV-Visible spectroscopy, Infrared spectroscopy and X-ray diffraction (XRD). *Microchemical Journal* **2020**, *159*, 10, Article. DOI: 10.1016/j.microc.2020.105314.

(121) Desai, R.; Mankad, V.; Gupta, S. K.; Jha, P. K. Size Distribution of Silver Nanoparticles: UV-Visible Spectroscopic Assessment. *Nanoscience and Nanotechnology Letters* **2012**, *4* (1), 30-34, Article. DOI: 10.1166/nnl.2012.1278.

(122) Zawisza, B.; Pytlakowska, K.; Feist, B.; Polowniak, M.; Kita, A.; Sitko, R. Determination of rare earth elements by spectroscopic techniques: a review. *Journal of Analytical Atomic Spectrometry* **2011**, *26* (12), 2373-2390, Review. DOI: 10.1039/c1ja10140d.

(123) Ocean Optics USB200+ Fiber Optic Spectrometer Installation and Operation Manual. Ocean Optics Denedin, FL, 2010; p 21.

(124) Loewen, E.; Popov, E. Diffraction Gratings and Applications. Taylor & Francis Group: Boca Raton, 2017; p 630.

(125) Kneubuhl, F. Diffraction Grating Spectroscopy. OPTICA Publishing Group: 1969; Vol. 8, pp 505-519.

(126) Rodriguez-Penalonga, L.; Soria, B. Y. M. A Review of the Nuclear Fuel Cycle Strategies and the Spent Nuclear Fuel Management Technologies. *Energies* **2017**, *10* (8), 16, Review. DOI: 10.3390/en10081235.

(127) Benn, T. M.; Westerhoff, P. Nanoparticle silver released into water from commercially available sock fabrics. *Environmental Science & Technology* **2008**, *42* (11), 4133-4139. DOI: 10.1021/es7032718.

(128) Fichet, P.; Tabarant, M.; Salle, B.; Gautier, C. Comparisons between LIBS and ICP/OES. *Analytical and Bioanalytical Chemistry* **2006**, *385* (2), 338-344, Article. DOI: 10.1007/s00216-006-0384-7.

(129) Chu, S.; Majumdar, A. Opportunities and challenges for a sustainable energy future. *Nature* **2012**, *488* (7411), 294-303, Review. DOI: 10.1038/nature11475.

(130) Keegan, E.; Richter, S.; Kelly, I.; Wong, H.; Gadd, P.; Kuehn, H.; Alonso-Munoz, A. The provenance of Australian uranium ore concentrates by elemental and isotopic analysis. *Appl. Geochem.* **2008**, *23* (4), 765-777, Article. DOI: 10.1016/j.apgeochem.2007.12.004.

(131) Lin, M.; Zhao, Y. G.; Zhao, L. F.; Li, L. L.; Wang, F.; Zhu, L. C.; Hu, X. N.; Ning, W. Tracing origins of uranium ore concentrates (UOCs) by multidimensional statistical analysis of rare-earth impurities. *J. Anal. At. Spectrom.* **2015**, *30* (2), 396-402, Article. DOI: 10.1039/c4ja00354c.

(132) Svedkauskaite-LeGore, J.; Rasmussen, G.; Abousahl, S.; van Belle, P. Investigation of the sample characteristics needed for the determination of the origin of uranium-bearing materials. *Journal of Radioanalytical and Nuclear Chemistry* **2008**, *278* (1), 201-209, Article. DOI: 10.1007/s10967-007-7215-y.

(133) *Significance of Mineralogy in the Developments of Flowsheets flow sheets for Processing Uranium Ores*; International Atomic Energy Agency, Vienna, 1980.

(134) Kristo, M. J.; Gaffney, A. M.; Marks, N.; Knight, K.; Cassata, W. S.; Hutcheon, I. D. Nuclear Forensic Science: Analysis of Nuclear Material Out of Regulatory Control. In *Annual Review of Earth and Planetary Sciences, Vol 44*, Jeanloz, R., Freeman, K. H.

Eds.; Annual Review of Earth and Planetary Sciences, Vol. 44; Annual Reviews, 2016; pp 555-579.

(135) Su, Y. F.; Tonkyn, R. G.; Sweet, L. E.; Corbey, J. F.; Bryan, S. A.; Johnson, T. J. Characterization of Uranium Ore Concentrate Chemical Composition via Raman Spectroscopy. In *19th Meeting of the Chemical, Biological, Radiological, Nuclear, and Explosives (CBRNE) Sensing as part of the SPIE Defense and Commercial Sensing (DCS) Symposium*, Orlando, FL, Apr 16-18, 2018; Spie-Int Soc Optical Engineering: BELLINGHAM, 2018; Vol. 10629. DOI: 10.1117/12.2304304. Pointurier, F.; Marie, O. Use of micro-Raman spectrometry coupled with scanning electron microscopy to determine the chemical form of uranium compounds in micrometer-size particles. *J. Raman Spectrosc.* **2013**, *44* (12), 1753-1759, Article. DOI: 10.1002/jrs.4392. Lin, D. H. M.; Manara, D.; Varga, Z.; Berlizov, A.; Fanghanel, T.; Mayer, K. Applicability of Raman spectroscopy as a tool in nuclear forensics for analysis of uranium ore concentrates. *Radiochim. Acta* **2013**, *101* (12), 779-784, Article. DOI: 10.1524/ract.2013.2110.

(136) Varga, Z.; Ozturk, B.; Meppen, M.; Mayer, K.; Wallenius, M.; Apostolidis, C. Characterization and classification of uranium ore concentrates (yellow cakes) using infrared spectrometry. *Radiochim. Acta* **2011**, *99* (12), 807-813, Article. DOI: 10.1524/ract.2011.1886.

(137) Burger, S.; Boulyga, S. F.; Penkin, M. V.; Bostick, D.; Jovanovic, S.; Lindvall, R.; Rasmussen, G.; Riciputi, L. Quantifying multiple trace elements in uranium ore concentrates: an interlaboratory comparison. *Journal of Radioanalytical and Nuclear*

Chemistry **2014**, *301* (3), 711-729, Article; Proceedings Paper. DOI: 10.1007/s10967-014-3224-9.

(138) Rogers, K. T.; Giaquinto, J.; Essex, R. M.; Metzger, S. C.; Ticknor, B. W.; Hexel, C. R. Trace impurity analysis in uranium oxide via hybrid quantification techniques-gravimetric standard addition and isotope dilution mass spectrometry. *Journal of Radioanalytical and Nuclear Chemistry* **2018**, *318* (1), 685-694. DOI: 10.1007/s10967-018-6106-8.

(139) Manard, B. T.; Metzger, S. C.; Quarles, C. D.; Rogers, K. T.; Ticknor, B. W.; Bostick, D. A.; McBay, E. H.; Hexel, C. R. Evaluation and Specifications for In-Line Uranium Separations Using Inductively Coupled Plasma Optical Emission Spectroscopy (ICP-OES) Detection for Trace Elemental Analysis. *Applied Spectroscopy* **2019**, *73* (8), 927-935, Article. DOI: 10.1177/0003702819837650.

(140) Wylie, E. M.; Manard, B. T.; Quarles, C. D.; Meyers, L. A.; Xu, N. An automated micro-separation system for the chromatographic removal of uranium matrix for trace element analysis by ICP-OES. *Talanta* **2018**, *189*, 24-30, Article. DOI: 10.1016/j.talanta.2018.06.063.

(141) Khumalo, N.; Mathuthu, M. Determination of trace elements and lanthanide (REE) signatures in uranium mine products in South Africa by means of inductively coupled plasma mass spectrometry. *J. Geochem. Explor.* **2018**, *186*, 235-242, Article. DOI: 10.1016/j.gexplo.2017.12.012.

(142) Boulyga, S. F.; Cunningham, J. A.; Macsik, Z.; Hiess, J.; Penkin, M. V.; Walsh, S. J. Development, validation and verification of an ICP-MS procedure for a multi-element

analysis of uranium ore concentrates. *Journal of Analytical Atomic Spectrometry* **2017**, *32* (11), 2226-2237, Article. DOI: 10.1039/c7ja00180k. Varga, Z.; Katona, R.; Stefanka, Z.; Wallenius, M.; Mayer, K.; Nicholl, A. Determination of rare-earth elements in uranium-bearing materials by inductively coupled plasma mass spectrometry. *Talanta* **2010**, *80* (5), 1744-1749, Article. DOI: 10.1016/j.talanta.2009.10.018.

(143) Balcone-Boissard, H.; Michel, A.; Villemant, B. Simultaneous Determination of Fluorine, Chlorine, Bromine and Iodine in Six Geochemical Reference Materials Using Pyrohydrolysis, Ion Chromatography and Inductively Coupled Plasma-Mass Spectrometry. *Geostandards and Geoanalytical Research* **2009**, *33* (4), 477-485. DOI: 10.1111/j.1751-908X.2009.00018.x.

(144) Jeyakumar, S.; Mishra, V. G.; Das, M. K.; Raut, V. V.; Sawant, R. M.; Ramakumar, K. L. Study on the identification of organic and common anions in the pyrohydrolysis distillate of mixed uranium-plutonium carbide for the interference free determination of chlorine and fluorine by ion chromatography. *Radiochim. Acta* **2014**, *102* (4), 291-302, Article. DOI: 10.1515/ract-2013-2131.

(145) Shimizu, K.; Suzuki, K.; Saitoh, M.; Konno, U.; Kawagucci, S.; Ueno, Y. Simultaneous determinations of fluorine, chlorine, and sulfur in rock samples by ion chromatography combined with pyrohydrolysis. *Geochem. J.* **2015**, *49* (1), 113-124, Article. DOI: 10.2343/geochemj.2.0338.

(146) Chai, J. Y.; Muramatsu, Y. Determination of bromine and iodine in twenty-three geochemical reference materials by ICP-MS. *Geostand. Geoanal. Res.* **2007**, *31* (2), 143-150, Article. DOI: 10.1111/j.1751-908X.2007.00856.x.

(147) Oliveira, A. A.; Trevizan, L. C.; Nobrega, J. A. REVIEW: Iodine Determination by Inductively Coupled Plasma Spectrometry. *Appl. Spectrosc. Rev.* **2010**, *45* (6), 447-473, Review. DOI: 10.1080/05704928.2010.502207.

(148) Tanner, S. D.; Baranov, V. I.; Bandura, D. R. Reaction cells and collision cells for ICP-MS: a tutorial review. *Spectroc. Acta Pt. B-Atom. Spectr.* **2002**, *57* (9), 1361-1452, Review. DOI: 10.1016/s0584-8547(02)00069-1.

(149) Balcaen, L.; Bolea-Fernandez, E.; Resano, M.; Vanhaecke, F. Inductively coupled plasma - Tandem mass spectrometry (ICP-MS/MS): A powerful and universal tool for the interference-free determination of (ultra) trace elements - A tutorial review. *Analytica Chimica Acta* **2015**, *894*, 7-19, Review. DOI: 10.1016/j.aca.2015.08.053.

(150) Haldimann, M.; Eastgate, A.; Zimmerli, B. Improved measurement of iodine in food samples using inductively coupled plasma isotope dilution mass spectrometry. *Analyst* **2000**, *125* (11), 1977-1982, Article. DOI: 10.1039/b005879n.

(151) Todorov, T. I.; Gray, P. J. Analysis of iodine in food samples by inductively coupled plasma-mass spectrometry. *Food Addit. Contam. Part A-Chem.* **2016**, *33* (2), 282-290, Article. DOI: 10.1080/19440049.2015.1131337.

(152) Schnetger, B.; Muramatsu, Y.; Yoshida, S. Iodine (and other halogens) in twenty six geological reference materials by ICP-MS and ion chromatography. *Geostand. Newsl.* **1998**, *22* (2), 181-186, Article. DOI: 10.1111/j.1751-908X.1998.tb00690.x.

(153) Fecher, P. A.; Goldmann, I.; Nagengast, A. Determination of iodine in food samples by inductively coupled plasma mass spectrometry after alkaline extraction. *J. Anal. At. Spectrom.* **1998**, *13* (9), 977-982, Article; Proceedings Paper. DOI:

10.1039/a801671b. Shah, M.; Wuilloud, R. G.; Kannamkumaratha, S. S.; Caruso, J. A. Iodine speciation studies in commercially available seaweed by coupling different chromatographic techniques with UV and ICP-MS detection. *J. Anal. At. Spectrom.* **2005**, *20* (3), 176-182, Article. DOI: 10.1039/b415756g.

(154) Krajko, J.; Varga, Z.; Wallenius, M.; Mayer, K.; Konings, R. Investigation of sulphur isotope variation due to different processes applied during uranium ore concentrate production. *Journal of Radioanalytical and Nuclear Chemistry* **2016**, *309* (3), 1113-1121, Article. DOI: 10.1007/s10967-016-4733-5.

(155) Lerch, R. E.; Norman, R. E. NUCLEAR-FUEL CONVERSION AND FABRICATION CHEMISTRY. *Radiochimica Acta* **1984**, *36* (1-2), 75-88, Article. Lunt, D.; Boshoff, P.; Boylettt, M.; El-Ansary, Z. Uranium extraction: the key process drivers. *Journal of the South African Institute of Mining and Metallurgy* **2007**, *107* (7), 419-426.

(156) Dhara, S.; Misra, N. L.; Aggarwal, S. K. Determination of sulphur in uranium matrix by total reflection X-ray fluorescence spectrometry. *Spectrochimica Acta Part B-Atomic Spectroscopy* **2008**, *63* (12), 1395-1398. DOI: 10.1016/j.sab.2008.10.033.

(157) Crewe, M. T. I.; Lopes, P. C.; Moura, S. C.; Sampaio, J. A. G.; Bustillos, O. V. *Characterization of Hydrogen, Nitrogen, Oxygen, Carbon and Sulfur in Nuclear Fuel (UO_2) and Cladding Nuclear Rod Materials*; Instituto de Pesquisas Energeticas e Nucleares, 05508-000 Sao Paulo, SP.

(158) Kinman, W. S.; Borg, L. E.; Kaye, P.; Mayer, K.; Varga, Z.; Wallenius, M. S. *Interlaboratory Report on the Analysis Results and Metadata for the Springfields Uranium Ore Concentrate Sample Collection*; LA-UR-16-24131.

(159) Jeyakumar, S.; Raut, V. V.; Ramakumar, K. L. Simultaneous determination of trace amounts of borate, chloride and fluoride in nuclear fuels employing ion chromatography (IC) after their extraction by pyrohydrolysis. *Talanta* **2008**, *76* (5), 1246-1251, Article. DOI: 10.1016/j.talanta.2008.05.039.

(160) Golik, V. M.; Golik, S. V.; Trepachev, S. A.; Kuz'mina, N. V. Determination of B, Si, P, S, Cl, and Br in uranium materials by inductively coupled plasma mass spectrometry. *Journal of Analytical Chemistry* **2010**, *65* (14), 1511-1516, Article. DOI: 10.1134/s106193481014011x.

(161) Fletcher, N.; Manard, B.; Metzger, S.; Ticknor, B.; Bostick, D.; Hexel, C. Determining P, S, Br, and I content in uranium by triple quadrupole inductively coupled plasma mass spectrometry. Manuscript in review, 2019.

(162) Han, S.-H.; Varga, Z.; Krajko, J.; Wallenius, M.; Song, K.; Mayer, K. Measurement of the Sulphur isotope ratio (^{34}S / ^{32}S) in uranium ore concentrates (yellow cakes) for origin assessment. *Journal of Analytical Atomic Spectrometry* **2013**, *28*, 1919-1925. DOI: 10.1039/C3JA50231G.

(163) Schaefer, B. *Radiogenic Isotope Geochemistry: A Guide for Industry Professionals*; University Printing House, 2016.

(164) Schmitz, M. D.; Kuiper, K. F. High-Precision Geochronology. *Elements* **2013**, *9* (1), 25-30, Article. DOI: 10.2113/gselements.9.1.25.

(165) Boudin, A.; Deutsch, S. Geochronology: Recent Development in the Lutetium-176/Hafnium-176 Dating Method. *Science* **1970**, *168* (3936), 1219-1220. Riley, G. H.; Compston, W. THEORETICAL AND TECHNICAL ASPECTS OF RB-SR

GEOCHRONOLOGY. *Geochim. Cosmochim. Acta* **1962**, *26* (DEC), 1255-1281, Article. DOI: 10.1016/0016-7037(62)90055-8. Lugmair, G. W.; Scheinin, N. B.; Marti, K. Sm-Nd age and history of Apollo 17 basalt 75075: Evidence for early differentiation of the lunar exterior Proc Lunar Sci: United States of America, 1975; Vol. 6, pp 1419-1429.

(166) Allegre, C. *Isotope Geology*; Cambridge University Press, 2008.

(167) Nebel-Jacobsen, Y.; Scherer, E. E.; Munker, C.; Mezger, K. Separation of U, Pb, Lu, and Hf from single zircons for combined U-Pb dating and Hf isotope measurements by TIMS and MC-ICPMS. *Chemical Geology* **2005**, *220* (1-2), 105-120. DOI: 10.1016/j.chemgeo.2005.03.009.

(168) Krajko, J.; Varga, Z.; Wallenius, M.; Mayer, K. Development of a versatile sample preparation method and its application for rare-earth pattern and Nd isotope ratio analysis in nuclear forensics. *J. Radioanal. Nucl. Chem.* **2015**, *304* (1), 177-181. DOI: 10.1007/s10967-014-3505-3.

(169) Shollenberger, Q. R.; Borg, L. E.; Ramon, E. C.; Sharp, M. A.; Brennecka, G. A. Samarium isotope compositions of uranium ore concentrates: A novel nuclear forensic signature. *Talanta* **2021**, *221*. DOI: 10.1016/j.talanta.2020.121431.

(170) White, W. M.; Albarede, F.; Telouk, P. High-precision analysis of Pb isotope ratios by multi-collector ICP-MS. *Chemical Geology* **2000**, *167* (3-4), 257-270, Article. DOI: 10.1016/s0009-2541(99)00182-5.

(171) Varga, Z.; Wallenius, M.; Mayer, K.; Keegan, E.; Millett, S. Application of Lead and Strontium Isotope Ratio Measurements for the Origin Assessment of Uranium Ore Concentrates. *Anal. Chem.* **2009**, *81* (20), 8327-8334. DOI: 10.1021/ac901100e.

(172) Aggarwal, J.; Habicht-Mauche, J.; Juarez, C. Application of heavy stable isotopes in forensic isotope geochemistry: A review. *Appl. Geochem.* **2008**, *23* (9), 2658-2666. DOI: 10.1016/j.apgeochem.2008.05.016.

(173) Kleinhanns, I. C.; Kreissig, K.; Kamber, B. S.; Meisel, T.; Nagler, T. F.; Kramers, J. D. Combined chemical separation of Lu, Hf, Sm, Nd, and REEs from a single rock digest: Precise and accurate isotope Determinations of Lu-Hf and Sm-Nd using multicollector-ICPMS. *Anal. Chem.* **2002**, *74* (1), 67-73. DOI: 10.1021/ac010705z.

(174) Chernyshev, I. V.; Chugaev, A. V.; Shatagin, K. N. High-precision Pb isotope analysis by multicollector-ICP-mass-spectrometry using Tl-205/Tl-203 normalization: Optimization and calibration of the method for the studies of Pb isotope variations. *Geochemistry International* **2007**, *45* (11), 1065-1076. DOI: 10.1134/s0016702907110018.

(175) Manard, B. T.; Bostick, D. A.; Metzger, S. C.; Ticknor, B. W.; Zirakparvar, N. A.; Rogers, K. T.; Hexel, C. R. Rapid and automated separation of uranium ore concentrates for trace element analysis by inductively coupled plasma - optical emission spectroscopy/triple quadrupole mass spectrometry. *Spectroc. Acta Pt. B-Atom. Spectr.* **2021**, *179*. DOI: 10.1016/j.sab.2021.106097.

(176) BlichertToft, J.; Chauvel, C.; Albarede, F. Separation of Hf and Lu for high-precision isotope analysis of rock samples by magnetic sector multiple collector ICP-MS. *Contributions to Mineralogy and Petrology* **1997**, *127* (3), 248-260. DOI: 10.1007/s004100050278.

(177) Li, C. F.; Guo, J. H.; Yang, Y. H.; Chu, Z. Y.; Wang, X. C. Single-step separation scheme and high-precision isotopic ratios analysis of Sr-Nd-Hf in silicate materials. *J. Anal. At. Spectrom.* **2014**, *29* (8), 1467-1476. DOI: 10.1039/c3ja50384d.

(178) Pin, C.; Gannoun, A. Integrated Extraction Chromatographic Separation of the Lithophile Elements Involved in Long-Lived Radiogenic Isotope Systems (Rb-Sr, U-Th-Pb, Sm-Nd, La-Ce, and Lu-Hf) Useful in Geochemical and Environmental Sciences. *Anal. Chem.* **2017**, *89* (4), 2411-2417. DOI: 10.1021/acs.analchem.6b04289.

(179) Yang, Y. H.; Zhang, H. F.; Chu, Z. Y.; Xie, L. W.; Wu, F. Y. Combined chemical separation of Lu, Hf, Rb, Sr, Sm and Nd from a single rock digest and precise and accurate isotope determinations of Lu-Hf, Rb-Sr and Sm-Nd isotope systems using Multi-Collector ICP-MS and TIMS. *International Journal of Mass Spectrometry* **2010**, *290* (2-3), 120-126. DOI: 10.1016/j.ijms.2009.12.011.

(180) Kinman, W. S.; Borg, L. E.; Kaye, P.; Mayer, K.; Varga, Z.; Wallenius, M. S. *Interlaboratory Report on the Analysis Results and Metadata for the Springfields Uranium Ore Concentrate Sample Collection*; LA-UR-16-24131; Los Alamos National Laboratory, Los Alamos National Laboratory, 2016.

(181) Eichrom. *Ln Resins*. Eichrom, (accessed 2020.

(182) Voncken, J. H. L. *The Rare Earth Elements an Introduction*, 1 ed.; Springer Briefs in Earth Sciences; Springer Cham, 2016.

(183) Atwood, D. A. *The Rare Earth Elements: Fundamentals and Applications*, 2 ed.; Atwood, D. A., Ed.; EIC Bks; John Wiley & Sons Incorporated, 2012.

(184) Maton, C.; De Vos, N.; Stevens, C. V. Ionic liquid thermal stabilities: decomposition mechanisms and analysis tools. *Chemical Society Reviews* **2013**, *42* (13), 5963-5977, Review. DOI: 10.1039/c3cs60071h.

(185) Ruiz-Angel, M. J.; Carda-Broch, S. Recent Advances on Ionic Liquid Uses in Separation Techniques. *Separations* **2022**, *9* (4), 4, Editorial Material. DOI: 10.3390/separations9040096.

(186) Ventura, S. P. M.; Silva, F. A. E.; Quental, M. V.; Mondal, D.; Freire, M. G.; Coutinho, J. A. P. Ionic-Liquid-Mediated Extraction and Separation Processes for Bioactive Compounds: Past, Present, and Future Trends. *Chemical Reviews* **2017**, *117* (10), 6984-7052, Review. DOI: 10.1021/acs.chemrev.6b00550.

(187) Joseph, B.; Venkatesan, K. A.; Nagarajan, K.; Rao, P. R. V. Electrowinning of UO2 from Ionic Liquid Medium. *Separation Science and Technology* **2013**, *48* (16), 2506-2511, Article; Proceedings Paper. DOI: 10.1080/01496395.2013.807834.

(188) Karimi-Maleh, H.; Fakude, C. T.; Mabuba, N.; Peleyeju, G. M.; Arotiba, O. A. The determination of 2-phenylphenol in the presence of 4-chlorophenol using nano-Fe3O4/ionic liquid paste electrode as an electrochemical sensor. *Journal of Colloid and Interface Science* **2019**, *554*, 603-610, Article. DOI: 10.1016/j.jcis.2019.07.047.

(189) Sorour, N.; Zhang, W.; Gabra, G.; Ghali, E.; Houlachi, G. Electrochemical studies of ionic liquid additives during the zinc electrowinning process. *Hydrometallurgy* **2015**, *157*, 261-269, Article. DOI: 10.1016/j.hydromet.2015.09.003.

(190) Yang, X. F.; Wang, Y. S.; Qing, X. L. A Flexible Capacitive Pressure Sensor Based on Ionic Liquid. *Sensors* **2018**, *18* (7), 10, Article. DOI: 10.3390/s18072395.

(191) Plechkova, N.; Seddon, K. Applications of ionic liquids in the chemical industry. Royal Society of Chemistry: 2008; Vol. 37, pp 123-150.

(192) Sambasivarao, S. V.; Acevedo, O. Development of OPLS-AA Force Field Parameters for 68 Unique Ionic Liquids. *Journal of Chemical Theory and Computation* **2009**, *5* (4), 1038-1050, Review. DOI: 10.1021/ct900009a.

(193) Abbott, A. P.; Capper, G.; Davies, D. L.; Rasheed, R. K.; Shikotra, P. Selective extraction of metals from mixed oxide matrixes using choline-based ionic liquids. *Inorganic Chemistry* **2005**, *44* (19), 6497-6499, Article. DOI: 10.1021/ic0505450.

(194) de los Rios, A. P.; Hernandez-Fernandez, F. J.; Lozano, L. J.; Sanchez, S.; Moreno, J. I.; Godinez, C. Removal of Metal Ions from Aqueous Solutions by Extraction with Ionic Liquids. *Journal of Chemical and Engineering Data* **2010**, *55* (2), 605-608, Article; Proceedings Paper. DOI: 10.1021/je9005008.

(195) Lertlapwasin, R.; Bhawawet, N.; Imyim, A.; Fuangswasdi, S. Ionic liquid extraction of heavy metal ions by 2-aminothiophenol in 1-butyl-3-methylimidazolium hexafluorophosphate and their association constants. *Separation and Purification Technology* **2010**, *72* (1), 70-76, Article. DOI: 10.1016/j.seppur.2010.01.004.

(196) Visser, A.; Swatlozki, R.; Griffen, S.; Hartman, D.; Rogers, R. Liquid/Liquid Extraction of Metal Ions in Room Temperature Ionic Liquids. Separation Science and Technology: 2007; Vol. 36.

(197) Wasserscheid, P.; van Hal, R.; Bosmann, A. 1-n-Butyl-3-methylimidazolium (bmim) octylsulfate - an even 'greener' ionic liquid. *Green Chemistry* **2002**, *4* (4), 400-404, Article. DOI: 10.1039/b205425f.

(198) Sun, X. Q.; Luo, H. M.; Dai, S. Ionic Liquids-Based Extraction: A Promising Strategy for the Advanced Nuclear Fuel Cycle. *Chemical Reviews* **2012**, *112* (4), 2100-2128, Review. DOI: 10.1021/cr200193x.

(199) Nockemann, P.; Thijs, B.; Pittois, S.; Thoen, J.; Glorieux, C.; Van Hecke, K.; Van Meervelt, L.; Kirchner, B.; Binnemans, K. Task-specific ionic liquid for solubilizing metal oxides. *Journal of Physical Chemistry B* **2006**, *110* (42), 20978-20992, Article. DOI: 10.1021/jp0642995.

(200) Wang, K. Y.; Adidharma, H.; Radosz, M.; Wan, P. Y.; Xu, X.; Russell, C. K.; Tian, H. J.; Fan, M. H.; Yu, J. Recovery of rare earth elements with ionic liquids. *Green Chemistry* **2017**, *19* (19), 4469-4493, Review. DOI: 10.1039/c7gc02141k.

(201) Matsumiya, M.; Nomizu, D.; Tsuchida, Y.; Sasaki, Y. Separation of rare earth elements by synergistic solvent extraction with phosphonium-based ionic liquids using a beta-diketone extractant and a neutral ligand. *Solvent Extraction and Ion Exchange* **2021**, *39* (7), 764-784, Article. DOI: 10.1080/07366299.2021.1889761.

(202) Onghena, B.; Jacobs, J.; Van Meervelt, L.; Binnemans, K. Homogeneous liquid-liquid extraction of neodymium(III) by choline hexafluoroacetylacetonate in the ionic liquid choline bis(trifluoromethylsulfonyl)imide. *Dalton Transactions* **2014**, *43* (30), 11566-11578, Article. DOI: 10.1039/c4dt01340a.

(203) Riano, S.; Foltova, S. S.; Binnemans, K. Separation of neodymium and dysprosium by solvent extraction using ionic liquids combined with neutral extractants: batch and mixer-settler experiments. *Rsc Advances* **2020**, *10* (1), 307-316, Article. DOI: 10.1039/c9ra08996a.

(204) Wang, J. P.; Zhao, J. Y.; Feng, D.; Kang, X. C.; Sun, Y. Y.; Zhao, L. L.; Liang, H. Z. Enhancing extraction ability by rational design of phosphoryl functionalized ionic liquids and mechanistic investigation on neodymium (III) extraction. *Journal of Rare Earths* **2016**, *34* (1), 83-90, Article. DOI: 10.1016/s1002-0721(14)60579-2.

(205) Zarrougui, R.; Mdimagh, R.; Raouafi, N. Highly efficient and eco-friendly extraction of neodymium using, undiluted and non-fluorinated ionic liquids. Direct electrochemical metal separation. *Separation and Purification Technology* **2017**, *175*, 87-98, Article. DOI: 10.1016/j.seppur.2016.11.017.

(206) Freiderich, J. W.; Stankovich, J. J.; Luo, H. M.; Dai, S.; Moyer, B. A. Dissolution of the Rare-Earth Mineral Bastnaesite by Acidic Amide Ionic Liquid for Recovery of Critical Materials. *European Journal of Inorganic Chemistry* **2015**, (26), 4354-4361, Article. DOI: 10.1002/ejic.201500509.

(207) Okamura, H.; Hirayama, N. Recent Progress in Ionic Liquid Extraction for the Separation of Rare Earth Elements. *Analytical Sciences* **2021**, *37* (1), 119-130, Review. DOI: 10.2116/analsci.20SAR11.

(208) Yang, F.; Kubota, F.; Baba, Y.; Kamiya, N.; Goto, M. Selective extraction and recovery of rare earth metals from phosphor powders in waste fluorescent lamps using an ionic liquid system. *Journal of Hazardous Materials* **2013**, *254*, 79-88, Article. DOI: 10.1016/j.jhazmat.2013.03.026.

(209) Dimmock, P. W.; Warwick, P.; Robbins, R. A. APPROACHES TO PREDICTING STABILITY-CONSTANTS. *Analyst* **1995**, *120* (8), 2159-2170, Review. DOI: 10.1039/an9952002159.

(210) Singh, J.; Srivastav, A.; Singh, N.; Singh, A. Stability Constants of Metal Complexes in Solution. In *Stability and Applications of Coordination Compounds*, 1 ed.; Srivastva, N., Ed.; IntechOpen, 2019.

(211) Witter, A. E.; Hutchins, D. A.; Butler, A.; Luther, G. W. Determination of conditional stability constants and kinetic constants for strong model Fe-binding ligands in seawater. *Marine Chemistry* **2000**, *69* (1-2), 1-17, Article. DOI: 10.1016/s0304-4203(99)00087-0.

(212) Ansari, S. A.; Gujar, R. B.; Mohapatra, P. K. Complexation of tetraalkyl diglycolamides with trivalent f-cations in a room temperature ionic liquid: extraction and spectroscopic investigations. *Dalton Transactions* **2017**, *46* (23), 7584-7593, Article. DOI: 10.1039/c7dt01090g.

(213) Abbaspour, A.; Kamyabi, M. A. Characterization and determination of stability constants of copper(II)-L-histidine complexation system by using multivariate curve resolution method of visible spectra and two hard modeling methods in aqueous solutions. *Analytica Chimica Acta* **2004**, *512* (2), 257-269, Article. DOI: 10.1016/j.aca.2004.02.056.

(214) Quang, N.; Han, P.; Nhung, N.; Tat, P. Calculation of Stability Constant of Metal-thiosemicarbazone Complexes using MLR, PCR, and ANN. Indian Journal of Science and Technology: 2019; Vol. 12.

(215) Schwoebel, S. D.; Hohlich, D.; Mehner, T.; Lampke, T. Stabilization of the Computation of Stability Constants and Species Distributions from Titration Curves. *Computation* **2021**, *9* (5), 25, Article. DOI: 10.3390/computation9050055.

(216) Van Den Berg, C. M. G. DETERMINATION OF THE COMPLEXING CAPACITY AND CONDITIONAL STABILITY-CONSTANTS OF COMPLEXES OF COPPER(II) WITH NATURAL ORGANIC-LIGANDS IN SEAWATER BY CATHODIC STRIPPING VOLTAMMETRY OF COPPER CATECHOL COMPLEX-IONS. *Marine Chemistry* **1984**, *15* (1), 1-18, Article.

(217) Hubin, T. J.; Alcock, N. W.; Clase, H. J.; Busch, D. H. Potentiometric titrations and nickel(II) complexes of four topologically constrained tetraazamacrocycles. *Supramolecular Chemistry* **2001**, *13* (2), 261-276, Article. DOI: 10.1080/10610270108027481.

(218) Lahsasni, S. A.; Ammar, R. A.; Amin, M. F.; Shoukry, E. M. Mixed-Ligand Complex Formation of Cu(II) with 1,2-Diphenylethylenediamine as Primary Ligand and Amino Acids as Secondary Ligands. *International Journal of Electrochemical Science* **2012**, *7* (8), 7699-7711, Article.

(219) Jagiello, J.; Bandosz, T. J.; Putyera, K.; Schwarz, J. A. DETERMINATION OF PROTON AFFINITY DISTRIBUTIONS FOR CHEMICAL-SYSTEMS IN AQUEOUS ENVIRONMENTS USING A STABLE NUMERICAL-SOLUTION OF THE ADSORPTION INTEGRAL-EQUATION. *Journal of Colloid and Interface Science* **1995**, *172* (2), 341-346, Article. DOI: 10.1006/jcis.1995.1262.

(220) Eyal, A. M.; Canari, R. PH-DEPENDENCE OF CARBOXYLIC AND MINERAL ACID-EXTRACTION BY AMINE-BASED EXTRACTANTS - EFFECTS OF PK(A), AMINE BASICITY, AND DILUENT PROPERTIES. *Industrial & Engineering Chemistry Research* **1995**, *34* (5), 1789-1798, Article. DOI: 10.1021/ie00044a030.

(221) Huddleston, J. G.; Willauer, H. D.; Swatloski, R. P.; Visser, A. E.; Rogers, R. D. Room temperature ionic liquids as novel media for 'clean' liquid-liquid extraction. *Chemical Communications* **1998**, (16), 1765-1766, Article. DOI: 10.1039/a803999b.

(222) Kislik, V. S. Solvent Extraction: Classical and Novel Approaches. *Solvent Extraction: Classical and Novel Approaches* **2012**, 1-555, Book.

(223) Contescu, C.; Jagiello, J.; Schwarz, J. A. HETEROGENEITY OF PROTON BINDING-SITES AT THE OXIDE SOLUTION INTERFACE. *Langmuir* **1993**, *9* (7), 1754-1765, Article. DOI: 10.1021/la00031a024.

(224) Gans, P.; Sabatini, A.; Vacca, A. Investigation of equilibria in solution. Determination of equilibrium constants with the HYPERQUAD suite of programs. *Talanta* **1996**, *43* (10), 1739-1753, Article. DOI: 10.1016/0039-9140(96)01958-3.

Appendix



Figure 1 Image of the quadrupoles and detector used in the TQ ICP – MS



Figure 2 Images of the Ln resin (left) and AG resin (right) in use.

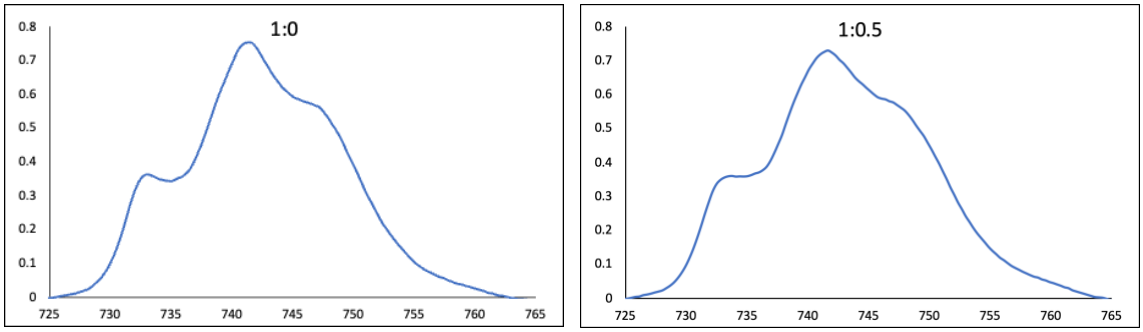


Figure 3 UV-Vis spectra that were collected during the spectrophotometric titration of Nd in $BMIM^{+}NTf_2^{-}$ with DMA

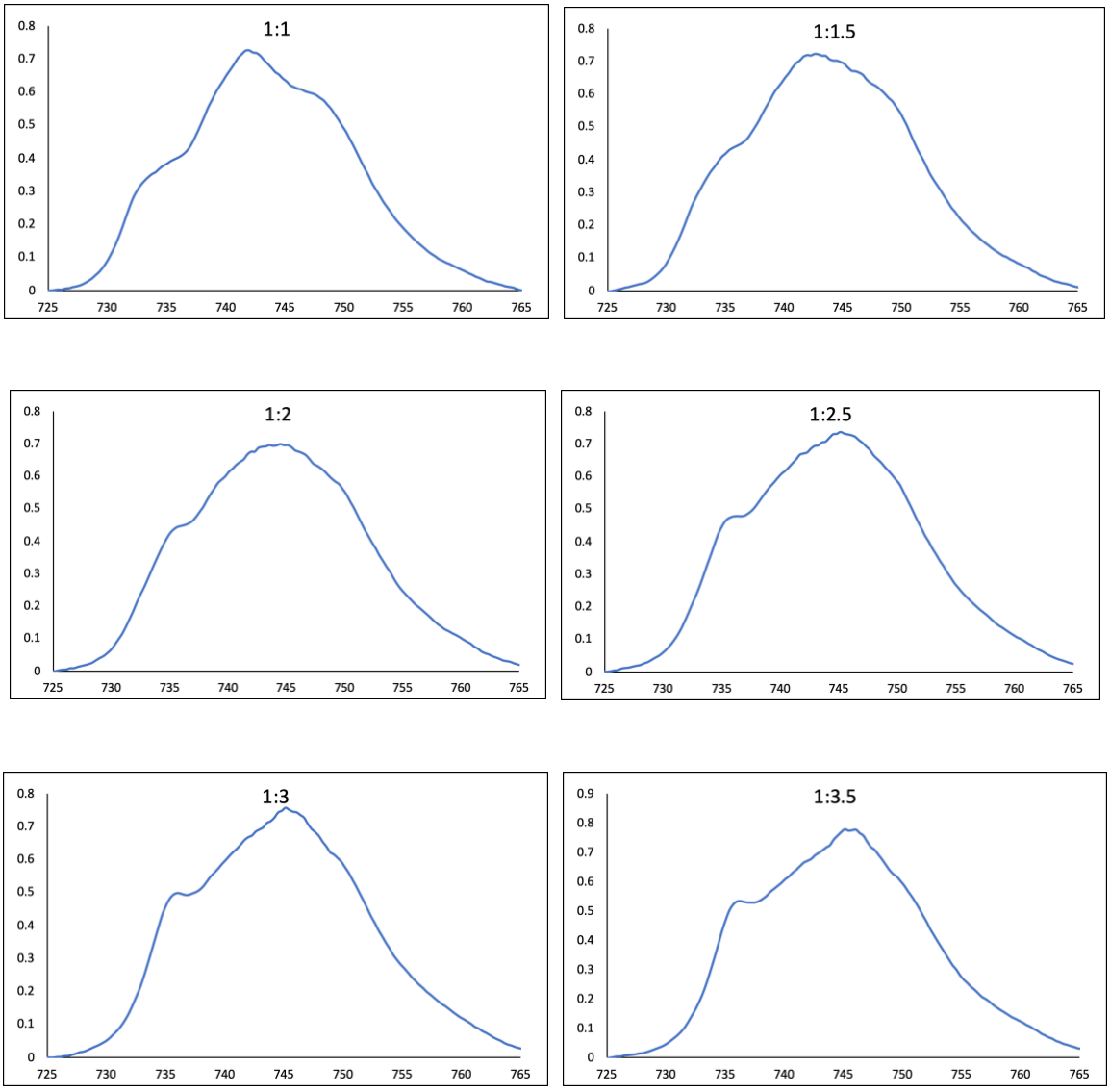


Figure 3 Continued

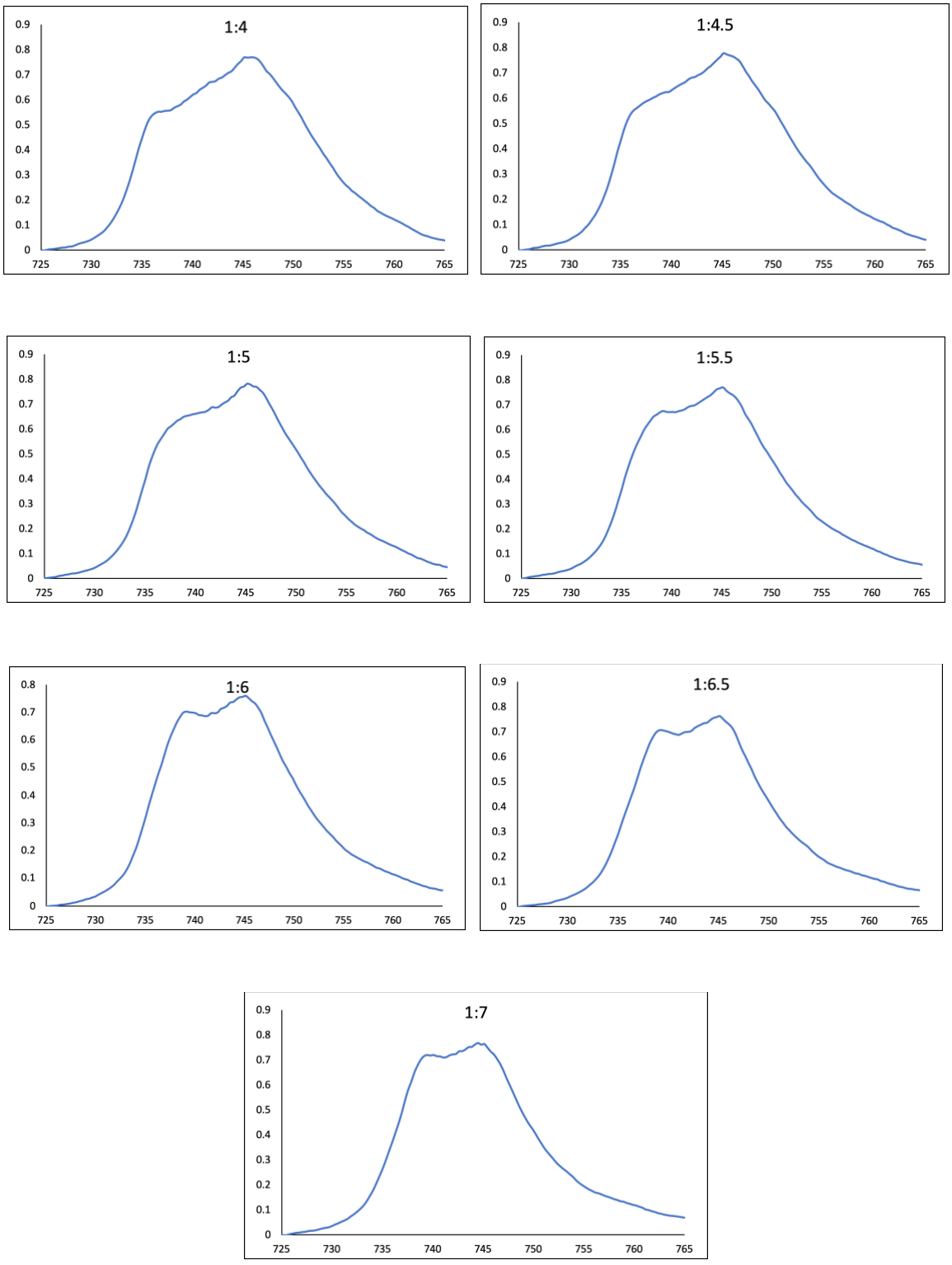


Figure 3 Continued

Vita

Nathaniel Fletcher first began working in chemistry labs at the age of 16 during the summers at the Savannah River Ecology lab. In 2017, he received his Bachelors of Science degree in chemistry of the College of Charleston. While there he participated in undergraduate research and discovered an interest in analytical chemistry. After graduation, Nathaniel spent one year in an analytical chemistry lab at Oak Ridge National Lab. He then joined the Dr. Sheng Dai lab at the University of Tennessee as a Ph.D. student in the chemistry program. While there he helped develop several analytical methods for the analysis of nuclear material. Nathaniel obtained a Ph.D. from the University of Tennessee in December of 2022.